Volume 1, Issue 1 2010

Heat Pipe Science and Technology

An International Journal

JAY M. OCHTERBECK
LEONARD L. VASILIEV
EDITORS-IN-CHIEF

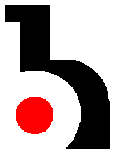

begell house, inc.
publishers

HEAT PIPE SCIENCE AND TECHNOLOGY
AN INTERNATIONAL JOURNAL

EDITORS-IN-CHIEF

Editorial Board Members

AIMS and SCOPE

Heat Pipe Science and Technology, An International Journal is encompassed on publishing i) fundamental studies of heat and mass transfer in heat pipes and two-phase thermosyphons, ii) new streams of technology development, iii) industrial innovation in electronic thermal control, air conditioning, heating and cooling, aerospace thermal control, and associated fields which are related to the journals major topic. The main objective of *Heat Pipe Science and Technology* is to provide a greater understanding of the fundamentals, principles and technologies associated with the design and operation of heat pipes and thermosyphons and their optimal connection to active systems such as heat pumps, coolers, refrigerators, power sources, space components and future thermal applications. Applied and fundamental research in energy systems and environment are the priority framework of the Journal that will include the following:

- review articles on heat pipes and thermosyphons fundamental and technologies
- heat pipes for space and ground application
- mini- and micro scale heat transfer at phase changes – fundamentals, experiments
- electronic cooling
- two-phase heat exchangers for refrigeration and air-conditioning systems
  * heat transfer in micro and nano-porous structures; nano-fluids; nano-technologies
  * heat pipe thermal management in fuel cells and ancillary systems
  * development of new materials for heat pipes and heat exchangers
  * computational simulation of two-phase components and heat pipes
  * heat pipe modelling and integration
  * thermal simulation of system integrated heat pipes and thermosyphons innovative heat pipes (pulsating/"oscillating" heat pipe, conducting heat pipe, new materials for heat pipes)
  * heat pipe/thermosyphons implementation in industrial components, such as molds, lab-on-chip, cold and hot plates, food homogenizers, distillation columns, etc.).

COMPOSITES: HEAT PIPE SCIENCE AND TECHNOLOGY,

An International Journal

VOLUME 1 / ISSUE 1 2010

Heat Pipe Science and Technology, An International Journal 1(1) 1–18 (2010)

DEPLOYABLE RADIATOR QUALIFICATION

K. Goncharov[*]*, O. Golovin, M. Balykin, & A. Kochetkov*

TAIS (Thermal Aggregates and Systems) Ltd., Russia

[*]Address all correspondence to K. Goncharov
E-mail: tais@heatpipe.ru

In 2004–2006 the engineering model of a deployable radiator based on a loop heat pipe (LHP) was developed. It was designed for qualification tests.

Application of ammonia as the LHP working fluid is attributable to its high thermal physical properties. However, the freezing temperature of ammonia is minus 77°C. This fact impedes the application of ammonia when the operating temperatures of the LHP radiator are lower than this value. Application of other working fluids with lower freezing temperatures (propylene, for example) leads to a rather substantial decrease in the heat power transferred or increase in the LHP dimensions and mass, which is not acceptable in many cases.

An important problem to be solved for ammonia LHP application is the recovery of the LHP operating capacity after the freezing of a working fluid in a radiator-condenser. To recover the working fluid circulation in an LHP, it is necessary to defreeze the entire LHP. During multiple freezing/melting cycles of the LHP working fluid, the LHP depressurization may occur. This paper is devoted to solving some aspects of the recovery of the radiator operating capacity after freezing.

The aspects of passive temperature control of the LHP evaporator using a pressure regulator and the aspects of the LHP active temperature control using heaters and Peltier elements mounted in the compensation chamber are also considered in this paper.

The development of new key components made it possible to design a deployable radiator with a specific mass of less than 10 kg/kW. The deployable radiator parameters are described in the paper.

KEY WORDS: *loop heat pipe (LHP), deployable radiator (DR), two-phase technology, thermal key, flexible section*

1. INTRODUCTION

Since space vehicles require a great amount of power, the area of the radiator needs to be increased to ensure the sink of heat. The spacecraft surface may not suffice for to site radiators. The application of deployable radiators (DR) based on loop heat pipes (LHP) after 1997, when they gained public recognition, has become the commonly used and classic solution of the problem. First DRs for a space platform were designed with TAIS participation in the European project Atleed in Bradford Engeneering [1]. The DRs based on LHPs found their first real application in space vehicles in the USA. Designed by Hughes, Dynatherm Company, and supported by TAIS, the DRs have been successfully used on powerful telecommunicational platforms for 10 years [2]. The DRs based on LHPs have higher mass-power characteristics in comparison with the radiators based on traditional heat pipes or liquid loops. The possibility of using small-diameter tubes, different control systems of evaporator temperature makes the LHP-based DRs very attractive for the designers of thermal control systems used in space vehicles. The DR designed by us at the request of the Alenia company offers its evident advantages [3].

In the radiators mentioned above ammonia is used as the working fluid. Ammonia is used in LHP due to its high thermophysical properties, but the freezing temperature of ammonia is minus 78^{o}C, and this makes the use of ammonia difficult when the radiator operating temperatures are below minus 78^{o}C. The relatively high freezing temperature of ammonia imposes significant limitations on the thermal-control system of spacecraft.

Use of lower-temperature working fluids (propylene with the freezing temperature of minus 189^{o}C) partially solves this problem. We used propylene in a series of space vehicles to avoid working fluid freezing [4–6]. Propylene was also successfully used in the Glass spacecraft [7]. However, the thermophysical properties of propylene, like the thermophysical properties of other low-temperature working fluids, are considerably worse [8]. The application of these working fluids makes the mass and overall dimensions characteristics of radiators significantly worse. The diameters of the transport lines and condensers abruptly increased. The increase in the LHP internal volumes leads to an increase in the dimensions and mass of the compensation chamber.

Therefore, an important engineering problem is to recover the LHP operating capacity after the freezing of the working fluid in the condenser. The possibility of occurrence of a multiple freezing–melting cycle of the working fluid in the condenser is the most critical point in the LHP operation for its reliability. As a result of the

change in the phase of the working fluid density there is a probability of loop leakage. In this paper, the authors are trying to find the solutions of the temperature control problems and the means of recovering the LHP operation recovery after the working fluid freezing.

2. DESIGN OF A DEPLOYABLE RADIATOR AND ITS CHARACTERISTICS

A deployable radiator (DR) is a heat transfer device based on an LHP with a condenser as a part of a radiation heat exchanger that deploys after the spacecraft orbiting.

Designed at the request of China Academy of Space Technology (CAST), the DR must have high mass-power characteristics:

- The specifications requirements of the DR were defined taking into account the typical needs of scientific and telecommunication satellites and a maximum possibility of the up-to-date two-phase technology. The driving parameters are the following. Heat transfer and rejection capability are from 10 to 600 W.
- The evaporator temperature at a minimum and maximum heat loads is not allowed to exceed the range from minus 10 to 50^{o}C. The thermal resistance of the LHP at a maximum heat power is 0.015 K/W in orbit and 0.018 K/W on the ground in a vertical position (the evaporator above the condenser).
- The deployable radiator assembly is able to withstand typical natural and induced environmental conditions during integration, ground testing, and launch phases.
- The deployment mechanism provides the necessary torque at the mobile panel interface, and with a latch engaged when in a fully deployed position. Manual resetting for the on-ground tests is foreseen.

To fulfil the above challenging requirements, a wide range of technical alternatives were the object of trade-off to obtain an appropriate design. Most of the DR key components have been improved as against the previous projects [9, 10].

The DR consists of two honeycomb panels attached to each other with deployable and locking mechanisms (Fig. 1).

The parts of the DR are:

- a deployable panel with an LHP;
- an internal panel;
- a deployable mechanism;
- a locking mechanism;
- a service frame for tests and transportation.

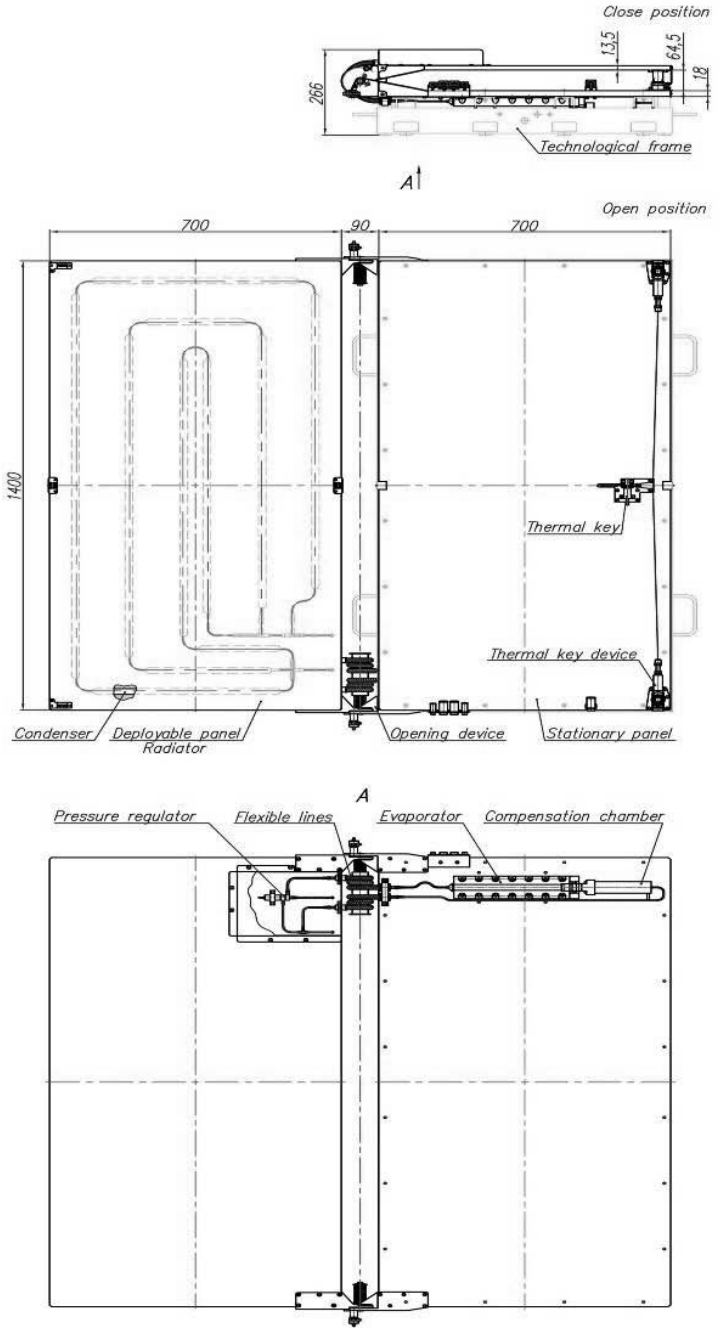

FIG. 1: DR overall drawing

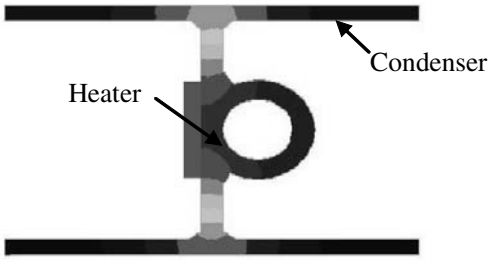

FIG. 2: Condenser profile

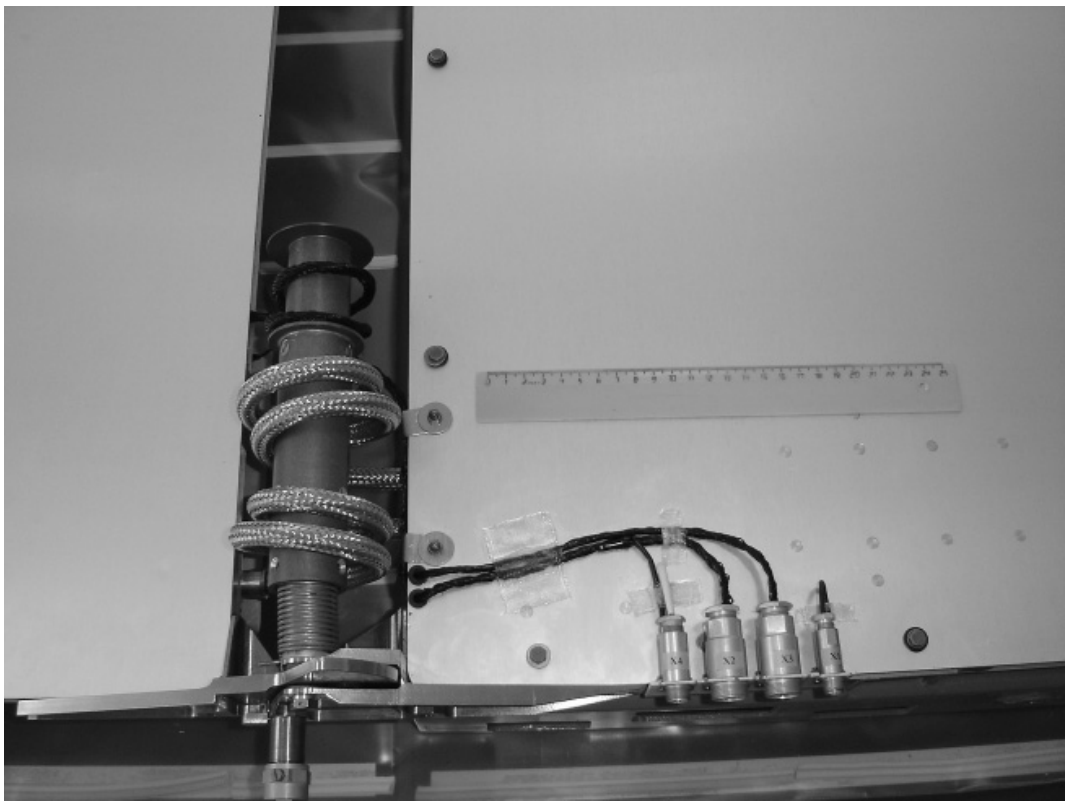

FIG. 3: Flexible sections

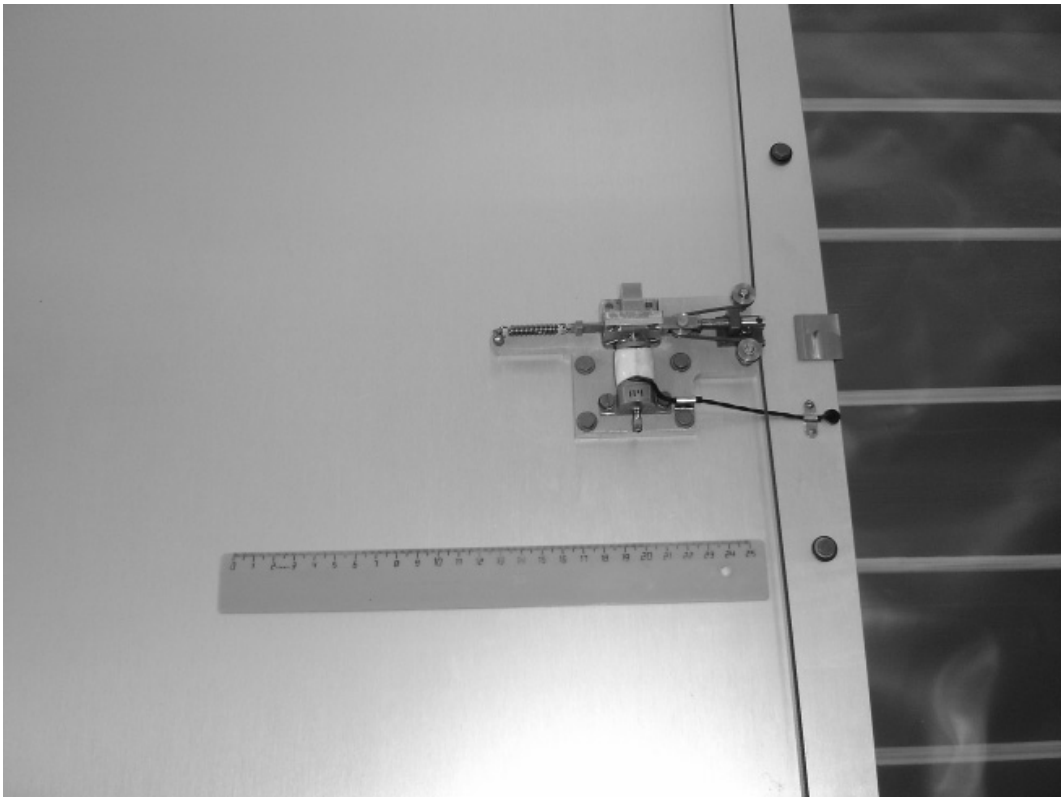

FIG. 4: Thermal key

The deployable part of the DR assembly consists of a honeycomb panel (14-mm thick) with an embedded LHP condenser. The LHP condenser sections are formed by an array of embedded aluminum profile with an internal diameter of 3 mm. The condenser profiles were developed to combine thermal performances (the heat is rejected from both sides of radiator) and mechanical characteristics in order to withstand the freezing of the working fluid.

The LHP condenser consists of 3 parallel sections connected through capillary isolators.

The recovery after freezing is attained by means of the heaters allowing initial thawing in one section; progressively the entire panel returns to operating conditions. On the internal panel there is an LHP evaporator connected to the condenser through transport lines (vapor line and condenser line) which have flexible sections thus allowing the external deployable panel to open. The transport lines are made of thin-

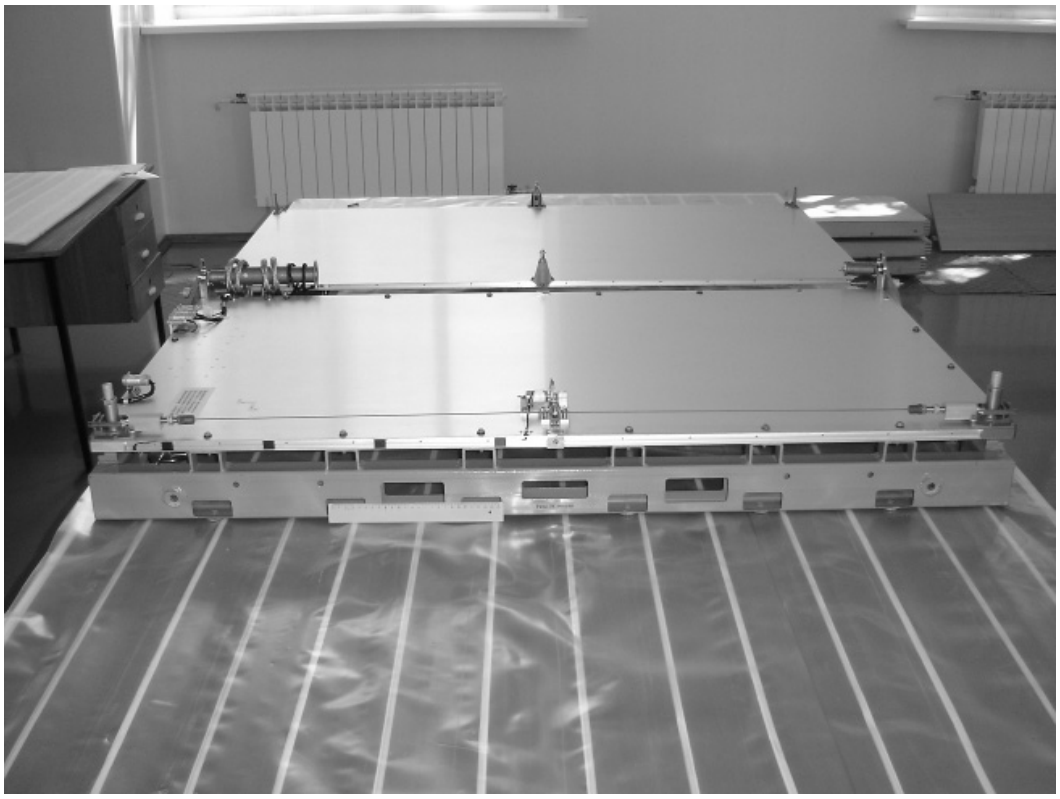

FIG. 5: Deployable radiator

walled tubes with an outer diameter of 3 and 4 mm. The fixed part of the DR assembly (corresponding to the traditional spacecraft wall) consists of a honeycomb panel (18-mm thick).

The heat loading is applied by heated plates mounted with the aid of bolts on the LHP evaporator. To minimize the thermal resistance at the interface between the heater and LHP evaporator, the latter is mounted on a "window" of the panel. A thermal filler (graphite foil) is located between the LHP evaporator and heated plates.

Thermohydraulic connection between the locking and deployment LHP elements is provided by stainless-steel flexible hoses, to allow the 180^{o} rotation of the hinge during the deployment.

The deployment actuator (spring loaded) is able to perform its function also on the ground, with the DR in a vertical position, without the help of anti-gravity compensation mechanisms.

FIG. 6: LHP evaporator

The DR in a stowed state is prevented from deployment by an electrically operated blocking device. It consists of a "thermal key" (Fig. 4) which is filled with a special fluid with a high temperature to volume expansion ratio. The "thermal key" has been designed specially for the deployable radiator and provides significant advantages over alternative systems (pyro devices, fusible elements, etc.).

It has small dimensions, low weight, no safety hazards, can be operated with a low power (few watts), allows multiple activations on the ground, and is self-redundant in the DR installation: in case the thermal key electrical heating is not available (that prevents deployment), the heat load on the fixed panel is not rejected efficiently, and the temperature of the panel increases until the thermal key (mounted on it) is heated by thermal conductivity up to its activation temperature. At that point the deployment takes place and the nominal conditions are recovered. The activation temperature can be changed at the design stage by chosen PCM materials.

The passive temperature control is achieved with a great effectiveness by using a pressure regulator with the bypass line. A heater on the LHP compensation chamber serves as a temperature control. The latter task can also be accomplished by using Peltier elements connected to the evaporator body and to the compensation chamber as an alternative to the heater.

3. LHP CONDENSER LINE

One of the main goals of this work was to investigate the process of the working fluid freezing/unfreezing in the condenser lines. The LHP condenser was made from a 6063 aluminum alloy. The cross section of the condenser profile was selected due to the hypothesis that the working fluid undergoes compression while the material of the condenser is left in the zone of elastic deformation, i.e., the pressure of the melting working fluid does not exceed the ultimate strength of the condenser material. A preliminary analysis of the strength had been made and afterwards an experiment was carried out.

A piece of the condenser aluminum profile (880-mm long) was selected as an object of testing. The compensation chamber was welded to one end of the profile. A simulator of the LHP condenser was charged with ammonia. The LHP condenser sample was connected to the 1-mm thick aluminum sheet of size 800 × 300 mm that simulated the radiator.

The tests of the LHP condenser model were carried out in a vacuum chamber. The tests proceeded as follows.

The LHP condenser model was cooled down using a nitrogen screen 10–20^{o}C lower than the temperature of ammonia freezing with subsequent heating by a simu-

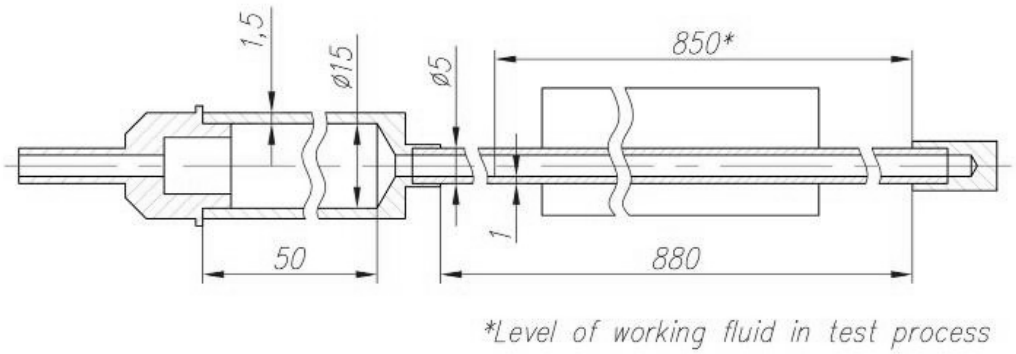

FIG. 7: LHP condenser model

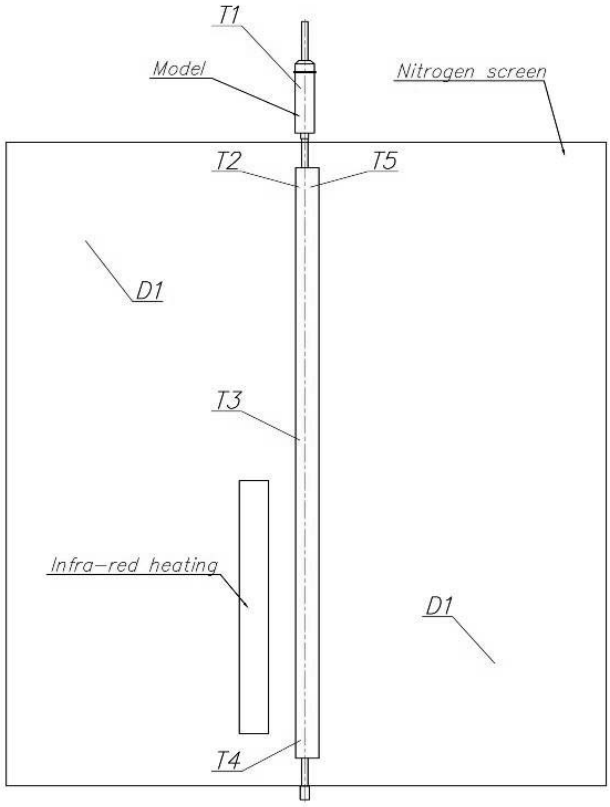

FIG. 8: LHP condenser model testing layout

lator of solar radiation. The heat flux power during heating was 1500 W/m^2. The sample was placed in the chamber inclined relative to the vertical position by 20 degrees, with a compensation chamber placed above. This position ensured complete filling of the profile with the liquid phase of the freezing working fluid. Cooling and heating of the LHP condenser model was arranged in such a way that the freezing and melting of ammonia started from the lower blind edge. After completion of the freezing cycle under these conditions the ammonia solid phase filled the condenser profile uniformly. During ammonia melting the top part of the profile was blocked by ice, and the melting ammonia was unable to emerge and enter the compensation chamber until its complete melting. The ammonia liquid phase was blocked in the lower part of the profile and this created the most critical situation for the LHP condenser model. The testing layout is presented in Fig. 8.

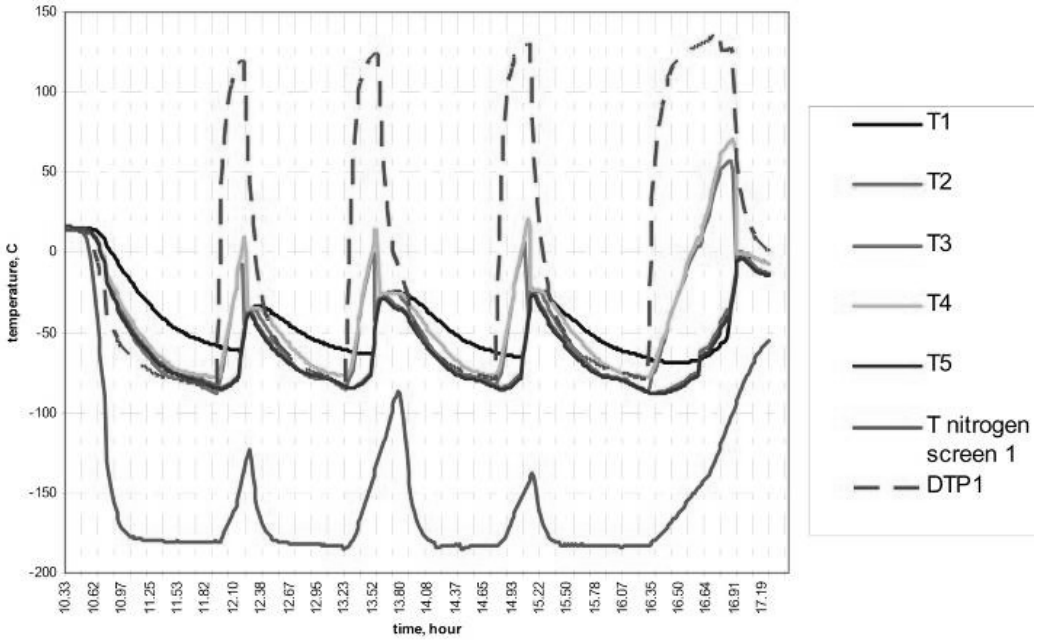

FIG. 9: LHP condenser model test results

Ten freezing/unfreezing cycles were carried out for the sample within the temperature range from minus 85 to 0°C. The environment was approximated as close as possible to the real space conditions. The sample sustained the tests without changing its dimensions and integrity. The test results are presented in Fig. 9.

These test results as well as the previous experience on the DR design for the Alenia company were taken into consideration while developing this DR [3]. The parameters of the DR presented are not worse than those of the modern DRs designed in Europe and in the USA [11, 12].

4. LHP CONDENSER DEFROSTING SYSTEM

Let us assume that we have managed to design the condenser profile that can sustain multiple cycles of freezing and melting. But this does not as yet solve the problem of developing the real condenser of an LHP that would make it possible to recover

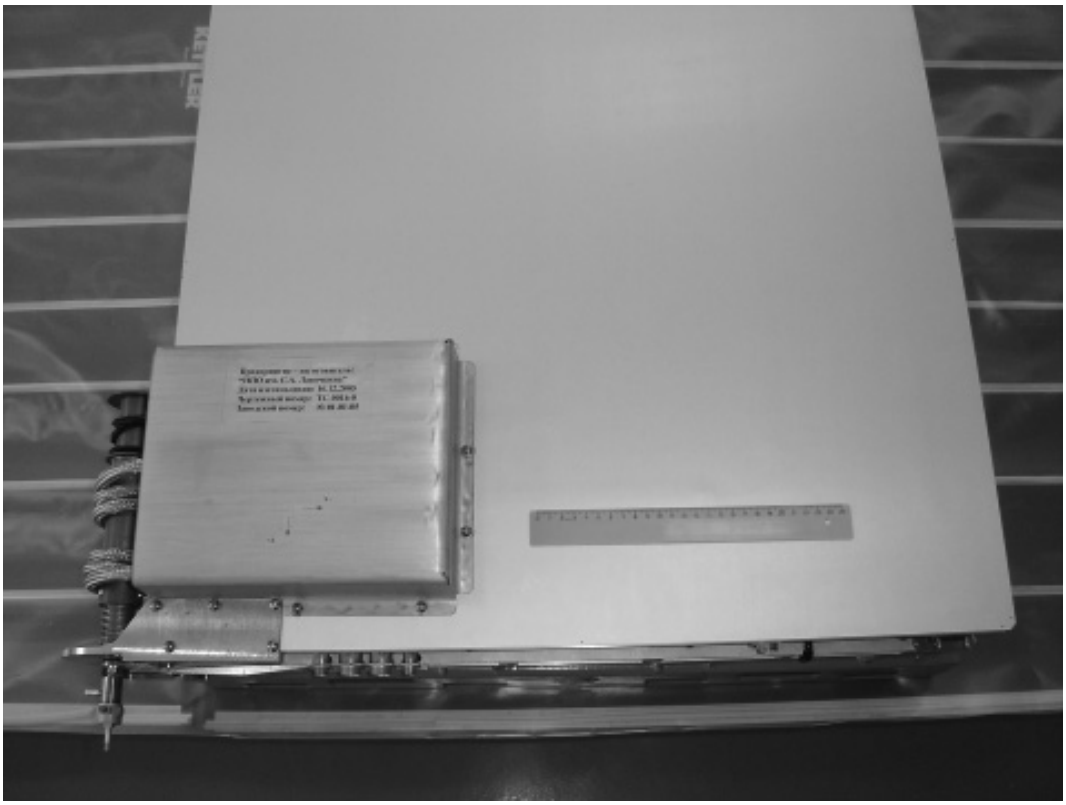

FIG. 10: Flexible lines and special shell

the radiator operation capacity after the working fluid was frozen. There are two more problems to be solved when developing the real radiator:

In the joints of the condenser profile with the LHP liquid and vapor lines the welding joints were usually used that do not withstand the pressure of melting ammonia. Their strength is much lower than that of the main profile. We intended to avoid the working fluid freezing in the transport lines, flexible sections, bypass line and in the pressure regulator. For this purpose, the part of the deployable radiator with a pressure regulator, bypass line, and the working fluid inlet/outlet from the panel was covered with a special shell, and three film heaters were glued to the panel surface. These heaters are switched on when the temperature of either the transport lines or valve-regulator approaches to minus 70^{o}C. So the working fluid circulation was maintained in the bypass line and the LHP flexible sections were pre-

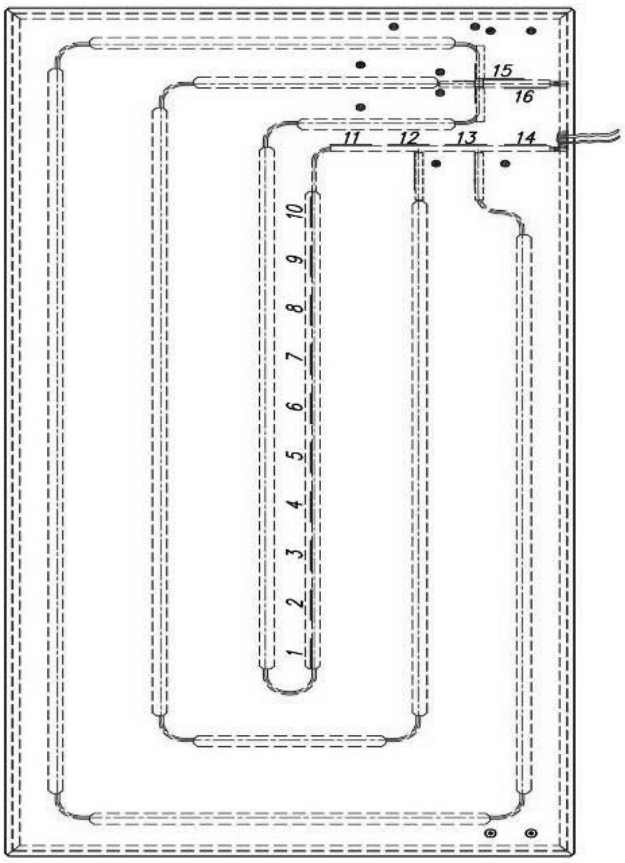

FIG. 11: Layout of defrosting heaters

vented from freezing. After the freezing of the working fluid in all parallel sections of the condenser, the working fluid circulation in them is stopped.

If the heat power applied to the LHP evaporator increases, the working fluid in the radiator cannot be melted as the circulation in it is absent. The evaporator heating without a heat sink will be continued up to the moment of its destruction. In this situation it is necessary to heat at least one section of the condenser by external heat sources to start the working fluid circulation in the condenser.

This heating can be done by electric heaters located on the radiator panel. This is the simplest method. In the DR designed the heaters were glued inside the radiator panel on the profile of the "small" section of the condenser (Fig. 11).

As soon as the heaters are switched on, the "small" section of the condenser starts to be heated and the working fluid in it starts melting. After the renewing of the circulation in the "small" section of the condenser, the temperature in the part of the radiator increases, and the working fluid in other radiator sections undergoes defrosting by thermal conductivity through the radiator skins. The design provides gradual switching on of all sections of the condenser when an increasing power is applied to the LHP evaporator. The selected layout of the heaters allows reducing the electric power and time required for radiator unfreezing.

To minimize the hazard of loop leakage, it is necessary to create a directed front of the working fluid melting inside the condenser profile so that the closed volumes of the working fluid liquid phase during melting would not be created. This requirement was taken into consideration when selecting the layout of the heaters and their operating modes. Step and unit capacity of separate film heaters were chosen to provide the initial melting of the working fluid in the zones of the condenser sections and liquid/vapor lines joining. Close to the joints, the spacing between the heaters was minimal and the unit power was maximum. At a distance from the joints the specific heat generation of the heaters decreased according to the linear law.

5. DR TEST RESULTS

Tests of the DR in atmospheric conditions were carried out in horizontal and vertical positions. The startup power was 10 W and a maximum transferred heat power was 600 W. The tests verified the possibility of the LHP active control by means of the compensation chamber heater and thermal electrical microcooler (TEMC). The LHP thermal resistance at a power of 600 W in a horizontal position was 0.0187 K/W and in a vertical position — 0.0195 K/W.

During thermal vacuum tests the following modes were maintained:

- Permanent heat transfer (includes the determination of the LHP thermal resistance at a maximum heat power, the capacity of the valve-regulator, compensation chamber heater and TEMC for temperature control of the LHP evaporator and operation of the DR when simulating the external heat flux).
- Freezing/unfreezing of the LHP condenser.

The results of thermal-vacuum tests are as follows:

- The heat power transferred by the LHP was within 30–550 W.
- The maximum thermal resistance of the DR at a maximum heat power Q_{max} = 550 W and maximum temperature of evaporator without temperature control was 0.025 K/W.

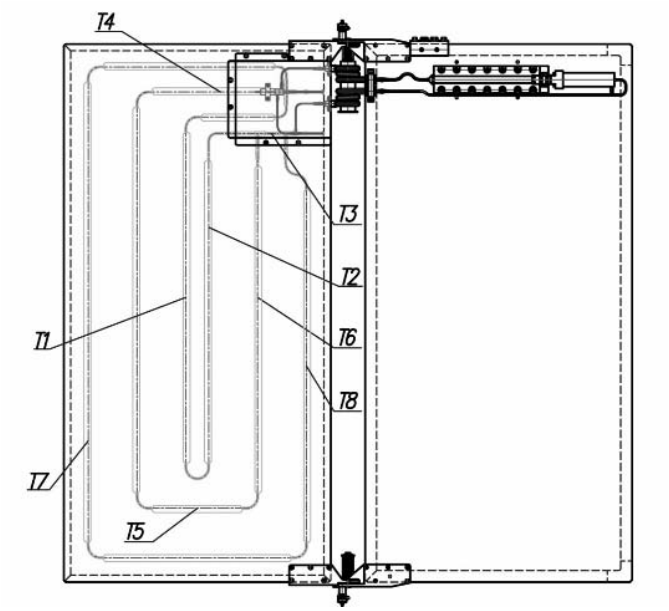

FIG. 12: Layout of the location of thermocouples

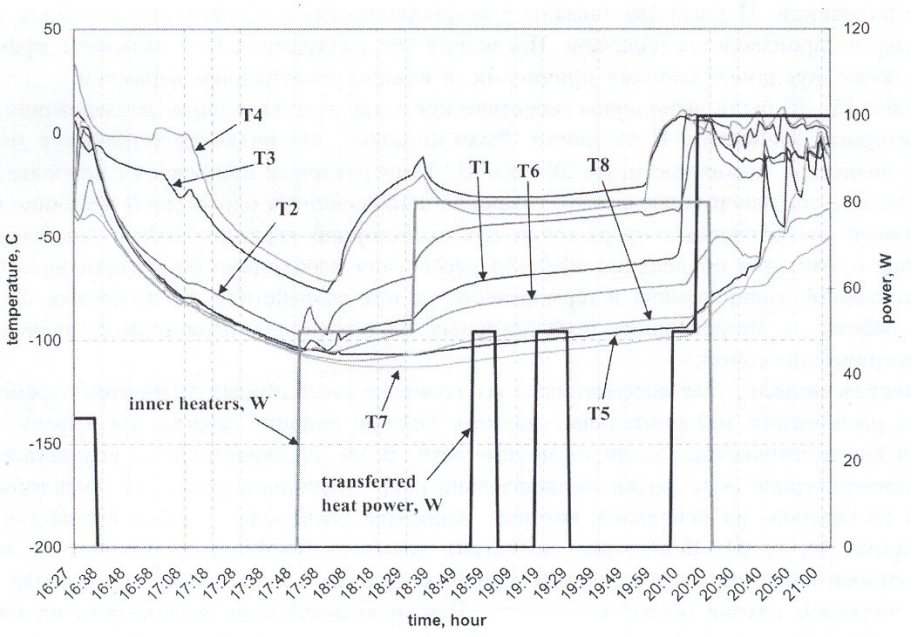

FIG. 13: Complete freezing of the radiator

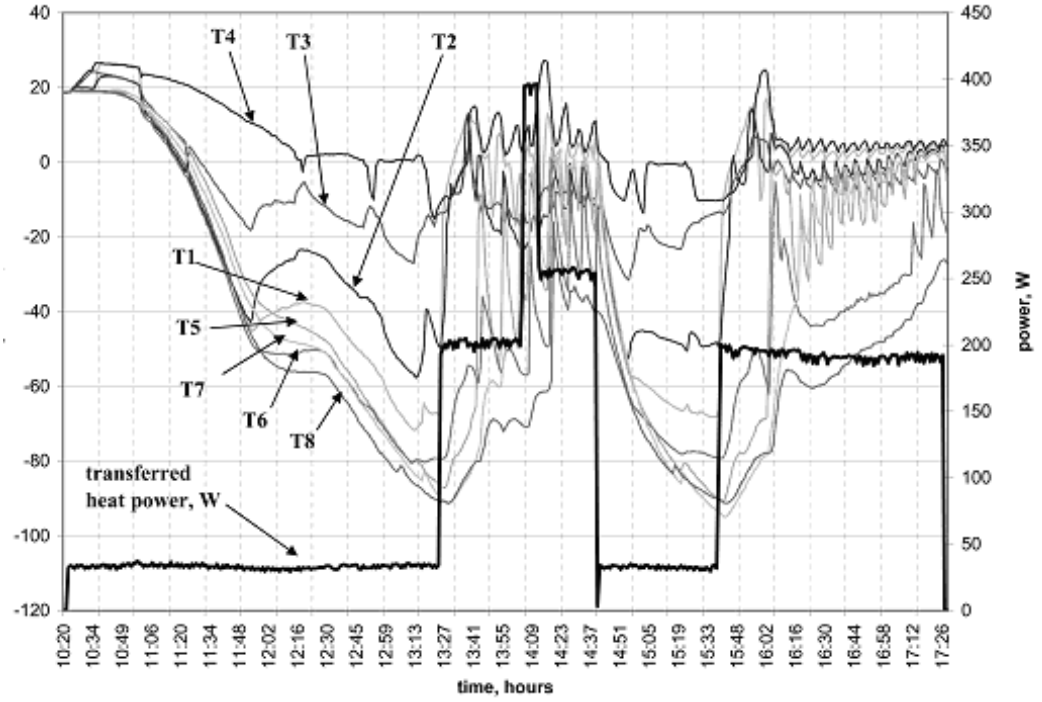

FIG. 14: Radiator freezing without a "small" line

– The valve-regulator provides the evaporator temperature $T_{evap} > 5^{o}C$.
– The compensation chamber heater and TEMC provide active control of the LHP operation.

Two freezing/unfreezing cycles of the deployable panel (LHP condenser) were carried out (Fig. 13).

After the heating up to the operating temperature, the LHP functioned properly. Leakage of the working fluid and any changes in the LHP dimensions and mass have not been detected. On freezing of the radiator, the evaporator temperature remained above $0^{o}C$. The experiment was repeated three times.

Experiments with partial freezing of the working fluid in the condenser were carried out too. The two lines of the condenser were frozen during these cycles. On freezing of the radiator, the evaporator temperature remained above $0^{o}C$.

In the third ("small") line circulation of the working fluid was maintained. The temperature of the "small" line was maintained higher than the freezing temperature of the working fluid with the aid of the heaters embedded inside the panel. During freezing the temperature of the panel was minus 112°C (Fig. 14). The temperature of the pressure-regulator, transport lines, bypass line, and flexible sections of the DR was not lower than minus 63°C due to the use of the heaters glued onto the panel.

6. CONCLUSIONS

1. The concept of a deployable radiator on the basis of an LHP has been developed. All DR components were designed, built, and successfully passed qualification tests.
2. The task of the development of the DR condenser that would withstand multiple (complete or partial) freezing of the working fluid was solved.
3. A system of forced condenser defreezing that provides reliable recovery of the working fluid circulation in an LHP has been developed.

REFERENCES

1. Goncharov, K. A., Smirnov, G. F., and Buz, V. N., Investigation of the issue of loop heat pipes long condensers with direct condensation, *'CPL 96' Int. Workshop*, ESTEC, Noordwijk, May 8–10, 1996, WPP-112.
2. Goncharov, K. A., Golovin, O. A., Kolesnikov, V. A., and Orlov, A. A., Experience in field of loop heat pipes development and application in spacecraft designs, *Int. Workshop on Non Compression Refrigeration Cooling*, Odessa, Ukraine, June 7–11, 1999, p. 72.
3. Goncharov, K., Orlov, A., Tarabrin, A., Gottero, M., Perotto, V., Taverra, S., and Zoppo, G. P., 1500 W deployable radiator with LHP, *ICES30*, Tolouse, France, July 10–13, 2000, 01ICES-68.
4. Goncharov, K., Maidani,k Yu., and Fershtater, Yu., Capillary pumped loop for the systems of thermal regulation of spacecraft, *ICES 4th*, Florence, Italy, October 21–24, 1991, p. 17.
5. Goncharov, K., Nikitkin, M., Golovin, O., Maidanik, Yu., Fershtater, Yu., and Piukov, S., Loop heat pipes in thermal control systems for "OBZOR" spacecraft, *25th ICES*, San Diego, California, July 10–13, 1995, #951555.
6. Goncharov, K. A., Buz, V., Elchin, A., Prochorov, Yu., and Surguchev, O., Development of loop heat pipes for thermal control system of nickel-hydrogen batteries of "Yamal" satellite, *13th Int. Heat Pipe Conf. (13th IHPC)*, Shanghai, China, September 21–25, 2004, p. 622.
7. Baker, C., Geoscience laser altimetry system (GLAS) on-orbit flight report on the propylene loop heat pipe, *Two-Phase 2003 Workshop*, Noordwijk, the Netherlands, September 15–17, 2003.
8. Goncharov, K., Kolesnikov, V., and Buz, V., Characteristic features of the development of a propylene LHP for spacecraft thermal control system, *Two-Phase 2003 Workshop*, Noordwijk, the Netherlands, September 15–17, 2003.
9. Russian patent "Control method of LHP thermal resistance", RU 2015483 C1.

10. France patent No. 9613274.
11. Galouye, A. S., Tjiptahardja, T., Van Oost, S., Bekaert, G., and Supper, W., Delphrad: Lightweight and high performance deployable radiator. Development program, *ICES34*, Colorado Springs, USA, July 07.
12. Andersen, W., Dussinger, P., Ernst, D., Hartenstin, J., and Sarraf, D., Design, fabrication and preliminary testing of a deployable loop heat pipe radiator, *Space Craft Thermal Workshop*, El Segundo, CA, USA, March 14–16, 2006.

Heat Pipe Science and Technology, *An International Journal* 1(1) 19–46 (2010)

DEVELOPMENT OF PROPYLENE LHP FOR EUROPEAN MARS ROVER APPLICATIONS

Donatas Mishkinis, [*] ***Carmen Gregori, Francisco Romera, & Alejandro Torres***

IberEspacio Technologia Aerospacial c/Fuencarral, 123, Madrid, 28010, Spain

[*]Address all correspondence to D. Mishkinis
E-mail: dmg@iberespacio.es

This paper presents the results of modeling and experimental investigation of a Passive Variable Thermal-Conductance Device for Mars Rover applications. The device is composed of a Loop Heat Pipe (LHP) and a pressure regulating valve. Both function as a heat switch and temperature control element. Propylene was selected as a working fluid due to challenging Mars environmental conditions. Excellent agreement between the EcosimPro model and test data was found. Special investigation with design optimization was conducted to demonstrate LHP functionality in any arrangement with respect to the gravity vector, including the worst possible orientation and environmental operating scenarios. High robustness and effectiveness of LHP with a pressure regulating valve as a heat switch for Mars Rover thermal control applications were fully validated through an extensive test campaign.

KEY WORDS: *loop heat pipe, pressure regulating valve, heat switch, passive variable thermal-conductance device, EcosimPro, thermal control, Mars Rover, secondary wick*

1. INTRODUCTION

The main objective of a thermal control system is to maintain some components within some appropriate temperature limits. This objective usually implies only the need of thermal power removal to prevent electronics from an excess of a maximum upper temperature limit. But for some applications where the operation modes of heat dissipating units and/or the external environmental conditions vary in a wide range,

2151-7995/10/$35.00

ACRONYMS

CC	Compensation Chamber	PVTCD	Passive Variable Thermal-Conductance Device
Cond	Condenser	SS	Stainless Steel
CPL	Capillary Pumped Loop	SW	Secondary Wick
ESA	European Space Agency	T	Temperature, Thermocouple
Evap	Evaporator	TRP	Technological Research Program
HB	Heater Block	TCS	Thermal Control System
HP	Heat Pipe	VL	Vapor Line
LL	Liquid Line		

there is also the need, for some periods, of introducing thermal power in the system to keep it above a lower temperature boundary. A constantly running heat power pumping system will require much more heat power injection in the situations where there is no need to remove heat. For space applications, the availability of power is limited. In such circumstances, a kind of heat or thermal "switch", in which the pumping capacity of the thermal control system may be turned ON/OFF, is of great interest for power (and mass) optimization.

A clear example of such applications is the thermal control system for a Mars Rover. During the Martian day, the environment is relatively hot (~10^{o}C) and the on-board instruments are usually in operation; heat power must be dissipated. In night time, the ambient conditions are well below –100^{o}C and the payload units are normally off; heat power must be applied to counterbalance the heat leaks to the very cold environment.

Capillary Pumped Loops are providing a very effective thermal control solution for many current and ongoing space missions. Current thermal demands (or rather challenges) of onboard electronics are leading to very extensive use of two-phase heat transfer systems. Especially it is related to planetary exploration missions as soon as no other technology today can provide such degree of flexibility as two-phase capillary pumped loops do taking into account a high ratio of their heat transfer capacity to mass, energy-independence, and self-regulation.

Within the frame of its Exploration Program, ESA is promoting and carrying out a number of activities to support and prepare future robotic and human missions to the Moon and Mars. The Technological Research Program (TRP) "Passive Variable

Thermal-Conductance Device (PVTCD) for Mars Rover Applications" is one of such activities. The objective of the TRP work is the development and experimental validation of a PVTCD (or Heat Switch) for passively controlling the temperature of a dissipating unit. An industrial team on the strength of IberEspacio and Carlo Gavazzi Space was established for the development, design, manufacturing, and testing of this Heat Switch, to demonstrate its performance at a breadboard model level.

ESA has specified the following governing requirements for the Mars Rover Heat Switch:

- A variable thermal conductance link with:
  - global thermal conductance (defined between the evaporator and the radiator) in ON conditions ("closed" switch): >0.75 W/K;
  - global thermal conductance in OFF conditions ("open" switch): <0.015 W/K;
  - transition between ON and OFF conditions: <20 K;
  - transition temperature set point: TBD, in the range from –40 to +40^{o}C;
- Maximum/minimum operating temperatures (evaporator side) +50/–40^{o}C;
- Maximum/minimum nonoperating temperatures (evaporator side) +60/–50^{o}C;
- Maximum heat transfer capacity: ~40 W;
- Passive and self-regulating;
- Minimum mass and volume;
- The design aim shall be the correct operation of the device in any orientation under 1 g. Design features, which preclude reaching this aim, shall be fully justified and subject to ESA approval.

To address the thermal control system issue, a passive thermal switch is proposed. It is based on a conventional loop heat pipe (LHP) coupled with a valve which can bypass the condenser when there is no need of pumping heat. An analogous thermal scheme was successfully implemented in a number of satellites [1–4] as a temperature control system and it was tested and qualified in Lavochkin Association/TAIS for MARS96 mission [5].

2. HEAT SWITCH THERMOMECHANICAL DESIGN

After extensive trade-off of available technologies (mainly Phase-Change Material and Two-Phase systems were analyzed [6]) the design based on the LHP technology was preferred. A pressure regulating valve was selected as a heat flow controlling element because this solution is totally passive and self-regulating. The selected working fluid

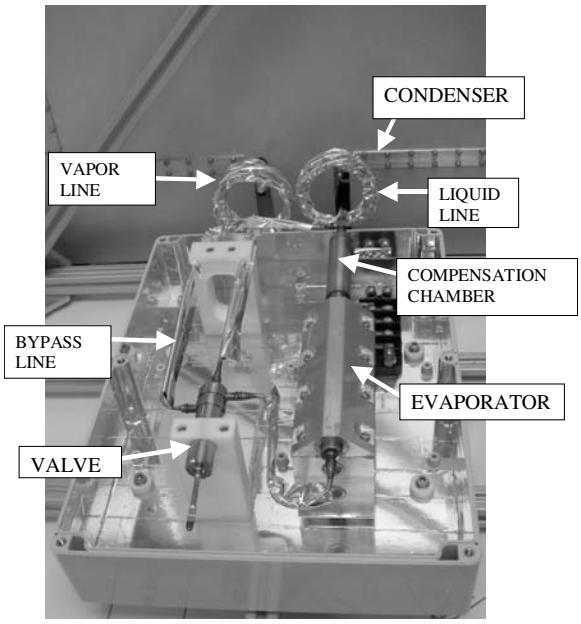

FIG. 1: General view of the Heat Switch (Model-I evaporator)

is propylene to avoid the freezing problem in the condenser during Mars night time cold temperatures.

A general view of the Heat Switch is shown in Fig. 1.

The main characteristics of the design are:

- Condenser line: 2.3 m, ∅2 mm;
- Vapor line: 0.5 m, ∅3 mm;
- Liquid line: 0.8 m, ∅2 mm;
- Evaporator: 120 mm, ∅12 mm;
- Sintered nickel primary wick with a 1.4-μm pore diameter, 60% porosity;
- Compensation chamber: 65 mm, ∅17 mm;
- Radiator: aluminum honeycomb panel 0.65 m × 0.6 m × 5.9 mm;
- Condenser tube attached to the radiator with aluminum saddles;
- Propylene charge: 9.5 g;
- LHP mass without radiator or saddles: 254 g;
- LHP mass with radiator and saddles: 2259 g.

The "switch" capacity of the LHP is provided by the valve. It is a 3-way valve, actuated by the pressure difference between the working fluid and an argon gas res-

FIG. 2: Model-I evaporator LHP with a technological condenser

ervoir which is sealed into a bellow. The valve passively splits the evaporator flow to the bypass line or the condenser in accordance with the working fluid pressure. This pressure is directly related to the working fluid saturation temperature given by the saturation line dependency. For low temperatures, the flow is completely diverted to the bypass line (OFF mode). When the temperature reaches a given set point, the flow starts going first partially to the condenser (regulation mode). For further temperature increase, there is another characteristic temperature (called regulation point) above which the flow goes totally to the condenser and the bypassed flow becomes zero (ON mode).

The valve set point is established, in accordance with the application requirements, by an adjustable back pressure in the valve. This backpressure is obtained by argon gas charging. For this application, a $8^{o}C$ set point has been established, with a corresponding argon pressure (at room temperature) of around 11 bar. The transition temperature range from OFF to ON modes is $8^{o}C$–$17^{o}C$.

Due to the great variety of design cases combining possible rover orientations and environmental scenarios a second LHP evaporator (Model II) was manufactured to optimize the design of the secondary wick (SW).

A general view of Model-I evaporator with a technological condenser is presented in Fig. 2.

The second LHP have the following characteristics:

- Condenser line: 1.1 m, ∅2 mm;
- Vapor line: 1.2 m, ∅3 mm;
- Liquid line: 0.55 m, ∅2 mm;
- Evaporator: 120 mm, ∅12 mm;
- Sintered nickel primary wick with a 1.4-μm pore diameter, 60% porosity;
- Propylene charge: 9.2 g.

3. PASSIVE TEMPERATURE REGULATION CAPABILITIES

Besides the valve capabilities to totally prevent the fluid from reaching the condenser (OFF mode) or to send all the fluid to the condenser (ON mode), the valve provides also a "temperature regulation" capacity when it allows the flow to be distributed between the bypass line and the condenser (intermediate ON/OFF or regulation mode).

The valve piston is subjected to the argon pressure, the working fluid pressure, and the bellows spring force. For a low working fluid pressure, the valve position is to fully close the condenser (see Fig. 3); all the flow, if any, goes to the bypass line. When the pressure increases, there is a pressure (set point) at which the condenser path starts to be open. With a further increase in pressure, another characteristic pressure is found (called regulation point) when the condenser is finally completely open and therefore the bypass line is totally closed. This situation keeps unchanged for higher pressures and the LHP behaves as a typical LHP without a valve. The pressure difference between these two points is a feature of each particular valve and it depends only on the valve stroke and the bellows spring coefficient (not on the argon pressure). It is usually in the range from 1.5 to 2 bar.

For a given valve, the pressure difference between the set point and the regulation point is fixed. But the temperature difference between these two points depends on the selected set point. Effectively, the pressure difference translates into temperature difference in accordance with the working fluid saturation line. For low set points,

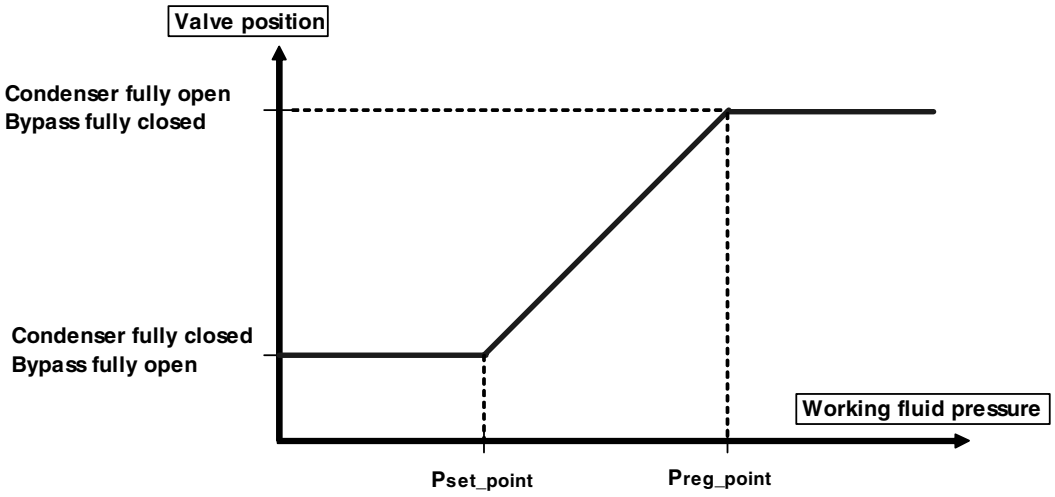

FIG. 3: Valve position versus working fluid pressure

the *dP*/*dT* is small and large temperature differences are obtained. For high set points, there is an opposite situation. This temperature difference is often referred to as the transition range.

The question now is to what extent the condenser path could open. The answer is clear if we take into account that the thermal load shall be removed in the condenser. This power removal is mainly performed by condensation. If the most part of the vapor is not sent to the condenser, the power still to be rejected after vapor condensation would require a very high liquid sub-cooling that could not be produced by the existing sink conditions. Therefore, the actual valve operating conditions is with the condenser almost totally open and just a small bypassed vapor flow. The resulting evaporator temperature is then very close to the regulation point (hence the origin of this name). However, for low thermal powers and high sink temperatures (where the bypass line can provide some cooling capacity) or in the presence of the gravity assistance effect (thermosyphon configuration), the operating point can sometimes drift towards the set point.

4. EXPERIMENTAL PROGRAM

4.1 Test Approach

Two LHP prototypes were manufactured and tested. The first prototype (Model-I Evaporator) with a standard evaporator was the breadboard model of Heat Switch (see Fig. 4). This model was investigated in ambient and vacuum environment ac-

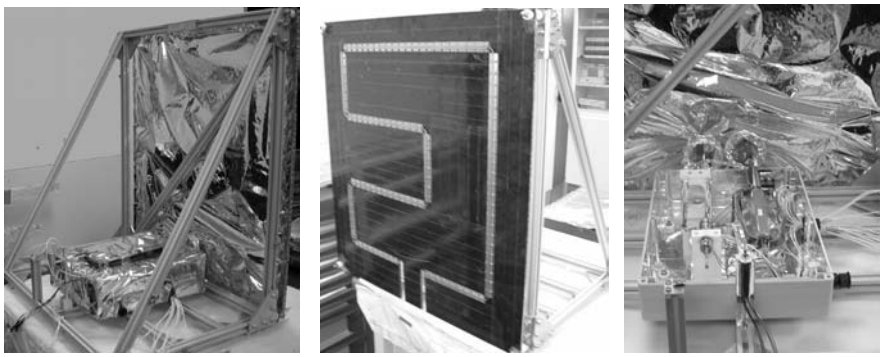

FIG. 4: Views of the Heat Switch assembly for testing in the vacuum chamber: a) test setup; b) radiator; c) LHP evaporator and valve layout

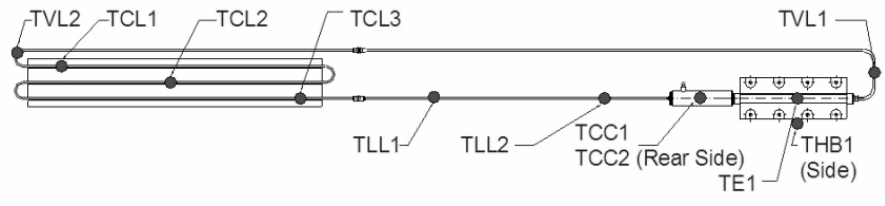

FIG. 5: Thermocouple layout of the Model-II evaporator LHP

cording to the prepared test program within the frame of ESA TRP. The objective was to perform a detailed characterization of the unit as a Heat Switch.

An extensive 2-months test campaign has been accomplished to demonstrate heat switch design compliance with the requirements. The test campaign has been performed mainly in vacuum conditions. A specific test plan has been prepared to test the following features:

- Minimum start-up power for several controlled LHP initial conditions;
- Thermal power capability;
- Thermal cycling to check regulating valve actuation;
- LHP response under sharp thermal power variations;
- LHP characteristics for adverse orientations under 1 g;
- Conductance in ON and OFF modes;
- Behavior for a Mars sol representative cycle (in terms of thermal power and ambient conditions);
- Heat Switch behavior with a very cold sink (–120^{o}C) obtained with LN2, performed in ambient conditions.

The second prototype (Model-II Evaporator) had optimized the design of SW for LHP operation in any possible orientation in the gravity field. The Internal IberEspacio test plan was developed and issued to verify LHP performance at different tilts and stressful transient regimes (when SW properties are critical for the proper operation of LHP). The LHP was well thermally insulated and all tests were conducted in ambient. The thermocouple layout is shown in Fig. 5.

4.2 Model-I Evaporator Experimental Investigation

The Heat Switch tests were conducted by Carlo Gavazzi Space with IberEspacio support. The general conclusion is that the "performance of the Heat Switch exceeds the requirements and shows excellent conductance values and heat transport capabilities":

- Global thermal conductance in ON conditions: 5 W/K versus 0.75 W/K required;
- Global thermal conductance in OFF conditions: 0.009 W/K versus 0.015 W/K required;
- Transition between ON and OFF conditions: ~9 K versus <20 K required;
- Demonstrated maximum heat transfer capacity: ~55 W versus 40 W required

(the limit being constituted by reaching the maximum operating temperature for the given radiator area at a vacuum chamber cold temperature of –55°C. Therefore it is not intrinsic to the Heat Switch and heat power could be still raised if a colder sink would be provided).

The valve regulation behavior was "extremely satisfactory, preventing the system from cooling down whenever the power levels or the external temperatures bring the system below the temperature threshold".

During the tests, valve oscillations were observed between the ON and OFF positions (evaporator temperature 8°C–17°C) for certain combinations of powers and shroud temperatures. In particular, they appear for:

- power of 10 W and $T_{shroud} = -10^{o}C$;
- power of 15–20 W and T_{shroud} $-20^{o}C$.

The oscillations are related to the gravity effect in the condenser. The position of the condensation front is around the TC2 measurement point when the oscillation occurs (see Fig. 6a) and the front moves forward and backward from this point during the oscillation. This can be verified in Fig. 6b, where the temperature measured by the thermocouple in the TC2 position is shown by the orange line with the square marker and it can be seen that this temperature oscillates between the vapor and subcooled liquid. The period of the oscillations is very stable and lasts about 30 minutes.

The geometrical layout of the loop with parts of the condenser 0.6 m above the evaporator can make the gravity to assist the circulation of fluid through the loop with the assistance effect being very dependent on the position of the vapor front. Gravity assistance is maximum when the front is at TC2, while it is negligible when it is located at TC1 or TC6.

Gravity assistance is so high when the front is located at TC2 that the hydrostatic head in the condenser becomes greater than the pressure losses in the loop (we must note that the oscillations occur at low power). If this happens the pressure in the compensation chamber is greater than the pressure in the vapor outlet; in other

words, the loop can work as a thermosyphon at a low power without any capillary rise. In this situation, no bypassed hot flow exists (in fact, a back flow occurs in the bypass line) and the evaporator temperature (and pressure) decreases. In this situation, the valve closes the condenser, less flow reaches the condenser and the condensation front goes back to the TC1 position. This implies that the gravity assistance disappears, the evaporator temperature increases again, the valve start to open the condenser, and oscillation cycle resumes.

It is also interesting to point out that the situation of the condensation front depends on the power and the shroud temperature. High power and/or shroud temperature push this front towards the condenser end. We can observe that the condensation front is around the TC2 position with only 10 W when the shroud temperature is high (–10^{o}C). In order to attain the same position when the shroud is colder (< –20^{o}C), more power is needed (15–20 W).

These oscillations may be avoided in a final flight model with a more appropriate condenser design.

4.3 Model-II Evaporator Experimental Investigation

We consider two cases of LHP orientation in the gravity field in general; these cases are governed by relative positioning of:

1. LHP evaporator and condenser,
2. LHP evaporator and compensation chamber.

Very often, when the "LHP operation in any orientation" statement is clamed it is related to case No. 1. It means that the condenser can be installed anywhere around the evaporator and the primary capillary pump will be capable to overcome gravity constraints if a condenser will be underneath. In some LHP designs SW is not present at all and it is suggested that the compensation chamber will always be above the evaporator or at least at the same level.

In realization of the Heat Switch TRP program, special attention was given to orientation case No. 2. The Heat Switch Model-I has demonstrated successful start-up and operation for all cases where the angle between the evaporator axis and the horizon line (the compensation chamber below the capillary pump) does not exceed 30^{o}. An attempt to start LHP at 60^{o}-tilt was not successful. Taking into account that gravity on Mars is less than on Earth (0.38 g) the maximum angle will be higher in Martian conditions. However internal research activity was conducted by IberEspacio to overcome this operating limitation of the Heat Switch.

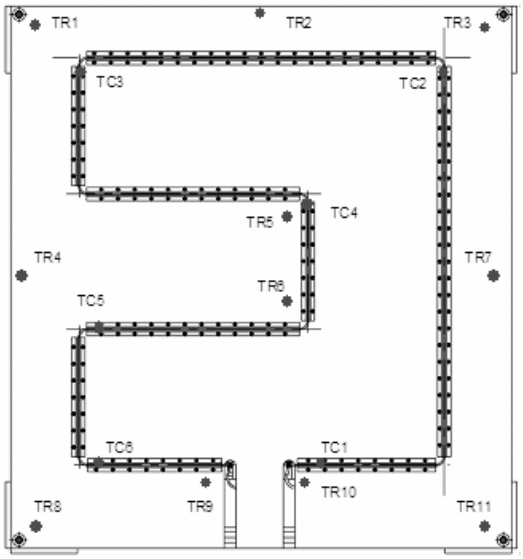

a)

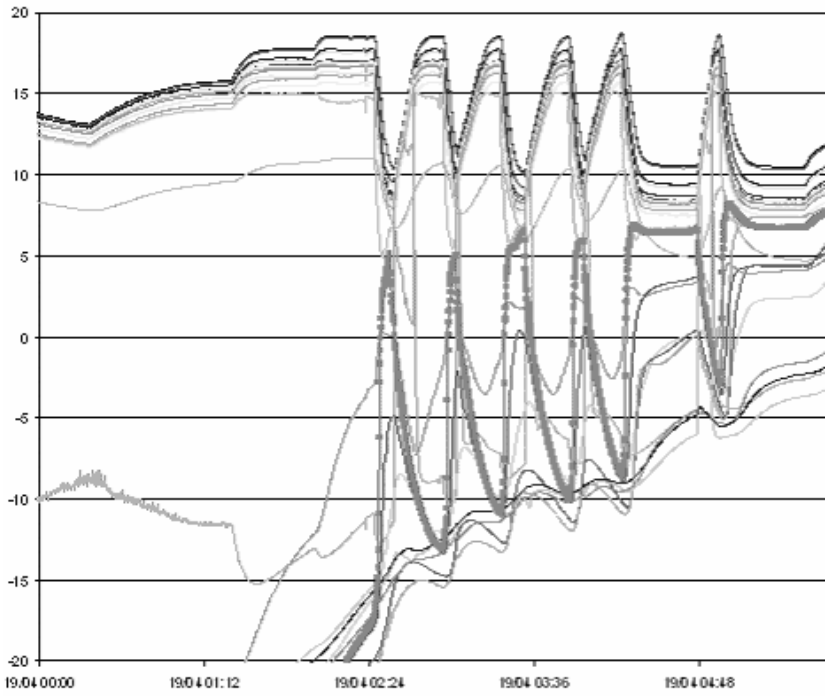

b)

FIG. 6: Temperature oscillations caused by gravity: liquid to vapor oscillations in a vertical inlet tube of the Heat Switch condenser (part TC1–TC2): a) layout of temperature sensors on a radiator; b) experimental data. TC2 — dotted line

After certain optimization of the SW design, the Model-II evaporator was manufactured and IberEspacio prepared and conducted a number of tests to demonstrate full compliance to the "operation in any orientation" requirement. This requirement is not critical as soon as the main thermal characteristics of the Heat Switch exceed the specification but it gives more flexibility for the Mars Rover system level design, Heat Switch integration, and Earth test campaign.

The SW is one of the critical elements of the LHP and often it is responsible for LHP functionality at start-up and stressful transient regimes. The main functions of the secondary wick can be bulleted as follows [7]:

- SW ensures that the primary wick is wetted before start-up;
- SW must maintain mass balance on the primary wick (operation);
- SW must replace vapor condensed in the reservoir with liquid supplied to the primary wick (vapor could be generated in the evaporator core or returned from the condenser);
- SW must compensate for differences in flow rate in the vapor line and liquid line during transients.

The test program of the Model-II evaporator was based on the analysis, which was made in [7] and comprises the following main steps:

- LHP characterization: heat transfer performance at 0^{o}-tilt;
- Worst orientation scenario: heat transfer performance at 90^{o}-tilt (the evaporator is above the compensation chamber and the compensation chamber is above the condenser);
- Worst operating scenario: sink temperature/power cycling at 0^{o}-tilt;
- Worst orientation and operating scenario: sink temperature/power cycling at tilt angles 30, 60, 90^{o}.

Heat Transfer Performance of the Model-II LHP at 0^{o}-tilt for two sink temperatures –38 and 20^{o}C is shown in Fig. 7. The thermocouple positioning in all figures of this sections corresponds to Fig. 5. LHP demonstrates a typical behavior and a maximum heat transfer capacity is around 140 W. The dry-out was reached in the case of the cold sink (Fig. 7a). At a sink temperature of 20^{o}C (Fig. 7b) the maximum power is 80 W but the test was limited by a maximal allowable evaporator temperature (~50^{o}C). The power values are significantly higher than the Heat Switch requirement of 40 W.

The results of LHP testing for the worst orientation scenario are presented in Fig. 8. No anomalies were observed at positive sink temperatures 2–9^{o}C (Fig. 8a). In

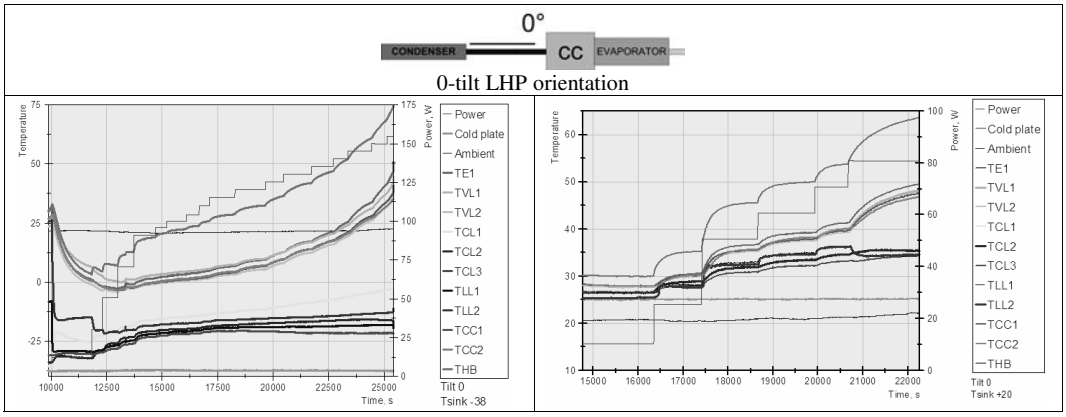

a) b)

FIG. 7: Heat transfer performance of the Model-II LHP in horizontal layout for different sink temperatures: a) sink temperature –38°C; b) sink temperature 20°C

this case, a large part of the condenser was open and the liquid level in the compensation chamber was high.

For a low sink temperature (Fig. 8b,c) the temperature oscillations were detected at 30 W. With further power increase the LHP behavior stabilized. It means that the oscillation regime is a characteristic feature of the low-power and low-temperature LHP operation. A maximum reached power before dry-out took place is 80 W. It is 40% less than the power reached in the horizontal orientation.

It is interesting to analyze the oscillating regime in detail (see Fig. 8c). When the evaporator temperature (TE1) grows up the inlet of the condenser (TCL2) is getting colder but the liquid line outlet (TLL2) is getting hotter. In the beginning of this mode, the temperature of the vapor line outlet (TVL2) goes down but in short time it returns back to rising evaporator (TE1), heater block (THB), vapor line inlet (TVL1), and compensation chamber (TCC1 and TCC2) temperatures. An opposite behavior of the described TVL2 point is demonstrated by the liquid line outlet (TLL1).

The possible explanation is as follows: at the phase of temperature increase there is no circulation in the loop. The liquid column in the liquid line disconnects from the primary wick and drops down into the condenser. Vapor is present and generated on both sides of the primary wick. Thus, vapor slugs are in the vapor and liquid lines. The central core of the evaporator is operating as an anti-gravitational heat pipe: propylene evaporates from the inner part of the primary wick and condenses in the compensation chamber. The primary wick does not dry out because the SW re-

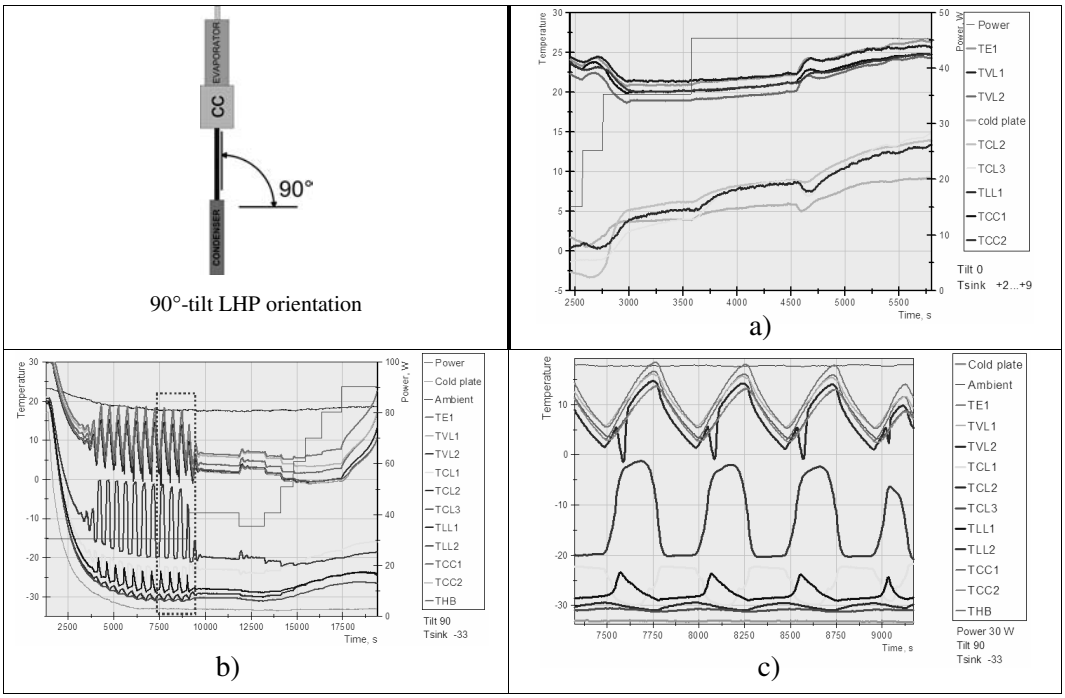

FIG. 8: Heat transfer performance of Model-II LHP in vertical layout for different sink temperatures: a) sink temperature 2–9°C; b) sink temperature –33°C; c) sink temperature –33°C, power 30 W

turns liquid back and wets the primary wick. In parallel, evaporation from the outer surface also takes place. Corresponding saturation pressures grow on both sides of the primary wick and, at a certain moment, the pressure in the vapor line is capable to push liquid out of the condenser (action against gravity) and restore circulation in the LHP. All temperatures go down (only the condenser inlet temperatures TCL1 and TCL2 are increasing, which is logical as soon as the LHP operates). However, because of a low sink temperature and a low mass flow rate, the bubbles, which are generated in the central core of the capillary pump due to the heat leak, are not evacuated into the compensation chamber. In fact, they migrate into the upper part of the wick central core (buoyancy effect). These bubbles can agglomerate and finally block liquid access from the liquid line to the primary wick. As soon as the liquid path is broken, the capillary forces are not capable to support the liquid column and the column drops down. The situation repeats.

To show that the SW really prevents the dry-out of the primary wick, a simple estimation can be performed. The time of the evaporator temperature rise is around 300 s. It means that a total amount of heat generated during the off-circulation phase is 30 W × 300 s = 9000 J. The mass of the evaporator block (evaporator and compensation chamber), including SS, Ni elements, and propylene, is around 130 g. The mass of the aluminum alloy evaporator saddle (including the heater) is 140 g. Taking into account that the temperature increase during this phase is ~12°C, the amount of energy which goes for evaporator block heating can be calculated and it is 2040 J. Therefore 9000 – 2040 = 6960 J are used for propylene evaporation (followed by condensation in different parts of the LHP). The average latent heat of propylene for the given case is 362 J/g. Consequently, the amount of the evaporated liquid is 6960/362 = 19 g. It is ~2 times higher than the total charge of the LHP and 6 times more than the amount of liquid, that can be stored in the primary capillary wick. If the SW does not provide effective wetting of the primary wick by liquid return from the compensation chamber, the dry-out will happen quickly and circulation in the LHP will never be re-established. 19 g of propylene are not a couple of drops even in the American System of Units.

To verify the stability of LHP operation in transient regimes during sharp changes of the sink temperature and power, a series of tests were conducted. Such regimes are very important for SW characterization. "Transients which are particularly problematic are rapid decreases in power and/or sink temperature that can temporarily stagnate flow in the liquid line, or rapid increases in power and/or sink temperature that can force vapor through the condenser into the reservoir" [7]. That is why rapid simultaneous up-down cycling of power (from 15 to 60 W) and sink temperature (from –33 to 10°C) was proposed as the worst operating scenario as a most stressful for the SW. It is important, that the power step up/down and sink temperature increase/decrease are applied at the same time. As is shown in Fig. 9a, the LHP demonstrates a very robust operation during cycling at 0°-tilt. From a close view of one of the step-down modes (Fig. 9b) it is clear that the compensation chamber is becoming the hottest element of the LHP in about 8 min (in time interval between 4000 and 4500 s).

Three cycles were conducted with evaporator elevation above the compensation chamber at 30°-tilt (Fig. 10). The LHP operates even though at low power, low temperature oscillations were observed. The explanation of this phenomenon has been made above. The oscillations are stable and repeatable and they disappeared as soon as the power was increased although the sink temperature is still –33°C (see the temperature stabilization in the right part of Fig. 9).

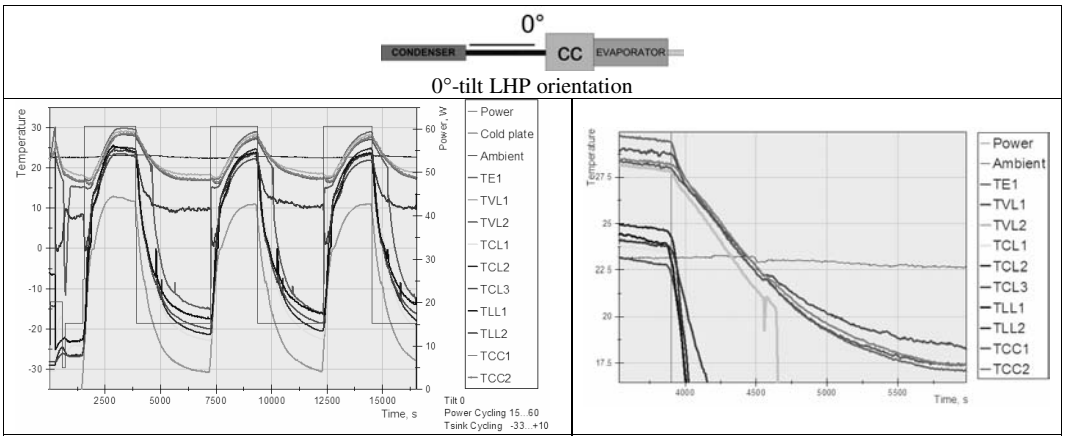

FIG. 9: Heat transfer performance of the Model-II LHP at power/sink temperature cycling (30^{o}-tilt): a) three compete cycles; b) temperature behavior in the step-down mode

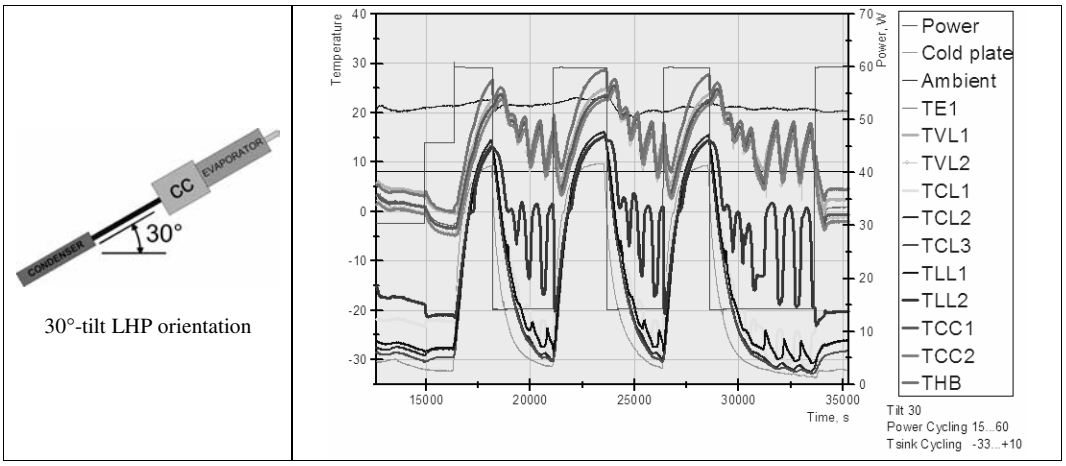

FIG. 10: Heat transfer performance of the Model-II LHP in power/sink temperature cycling (30^{o}-tilt)

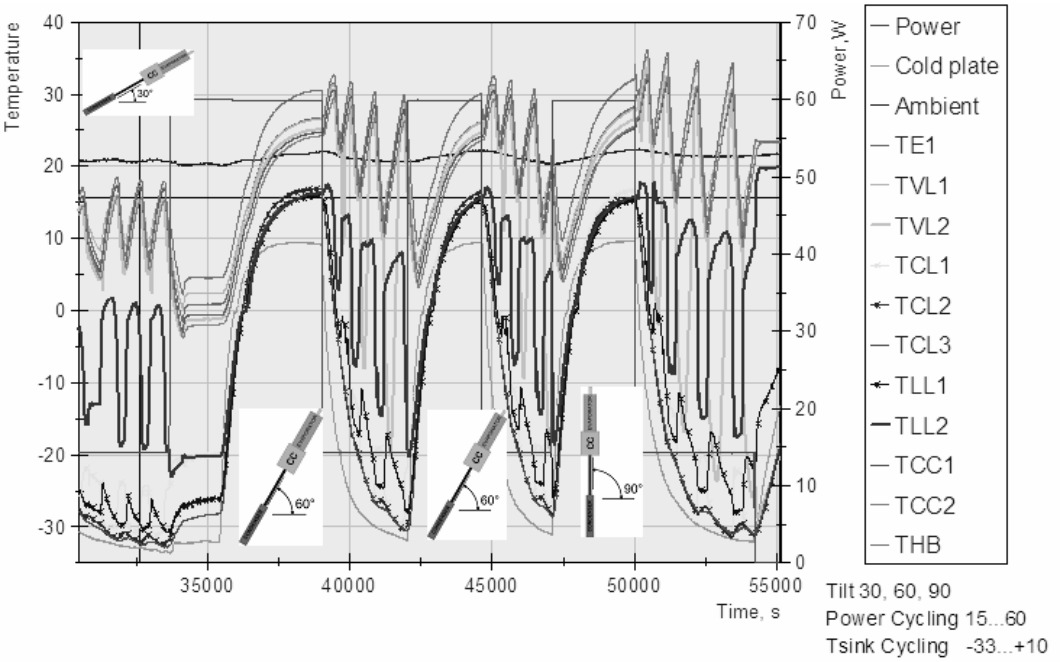

FIG. 11: Heat transfer performance of the Model-II LHP in power/sink temperature cycling (30^o-tilt, 60^o-tilt, 90^o-tilt)

The experiment was continued and orientation of the LHP was changed from 30^o-tilt to 60^o-tilt and finally to 90^o-tilt (Fig. 11). The amplitude of oscillations was increased, but the LHP was still operative and no evidence of dry-out was observed. The evaporator with an optimized design of the SW is capable to provide the operation of the Heat Switch in any orientation and position of the compensation chamber and condenser (relative to the evaporator) in the Earth/Mars gravity fields.

5. NUMERICAL MODELING

5.1 LHP Library of EcosimPro

To design the LHP and verify its performances, a model has been developed using the EcosimPro solver [8]. The mathematical model has a modular architecture. It means that the complete LHP model has been created connecting the standard LHP

components: evaporator, compensation chamber, transport lines, condenser, pressure regulator valve, etc. A modular character of the EcosimPro code allows one to quickly introduce new elements or upgrade the existing ones and to analyze complex two-phase thermal systems including multi-evaporator and multi-condenser schemes [9, 10]. The following main assumptions have been made for the modeling:

- The 1D fluid flow model is a homogeneous equilibrium model. It is considered that the two phases are in equilibrium assuming equal phase velocities, temperatures, and pressures.
- The calculated thermodynamic properties correspond to the two-phase mixture and they are obtained by interpolation using the tables built from NIST routines.
- The LHP components can exchange heat with the environment by convection and radiation, and they can exchange heat with other external components (such as saddles) by conduction.
- The fluid model is based on the one-dimensional fundamental conservation equations (mass, momentum, and energy) applied to control volumes. The fluid part of each LHP component is sub-divided into individual control volumes.
- The compressibility and transient effects are taken into account. The viscous effects are taken into account through the pressure drop calculations, which include empirical correlations for the pressure drop in porous media.
- The gravity effects due to the different orientations of the LHP have been taken into account in the formulation.

Full explanation of the general mathematical model and the main hypothesis made for the capillary pump and the LHP lines can be found in [9, 10]. A more detailed description of the valve modeling is provided below.

5.2 Pressure Regulating Valve Modeling

The mass and energy conservation equations are applied to the fluid in the valve in order to obtain the density and the internal energy at any time. To fix the valve set point, the model requires an input temperature value (T_{close}). The saturation pressure corresponding to this temperature (P_{close}) is obtained by interpolation using the tables from NIST and represents the point where the valve starts to open the bypass line. Taking into account the properties of the valve bellows, a new pressure (P_{open}) is calculated to define the point where the valve is completely open and, consequently, the radiator branch is completely closed.

The valve position is calculated depending on the relation between the fluid pressure and the values of P_{open} and P_{close} as follows:

$$
\begin{aligned}
&pos = 0 && P_{fluid} \geq P_{close} \\
&0 < pos < 1 && P_{close} > P_{fluid} > P_{open} \\
&pos = 1 && P_{fluid} \leq P_{open}
\end{aligned}
$$

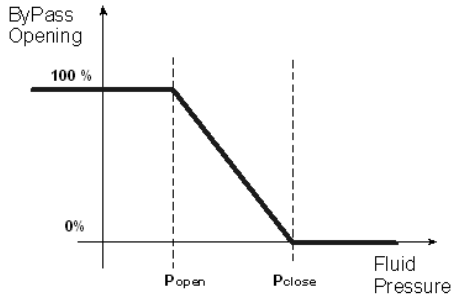

FIG. 12: Valve position vs fluid pressure

Therefore, in regulation conditions, it is assumed that the valve reaches a steady state in an intermediate position between 0 and 1 (Fig. 12).

Finally, the momentum equation is solved for each of the branches (direct and bypass) taking into account the value of the valve position.

5.3 LHP Model for the Heat Switch Design

To design the Heat Switch for Mars Rover application, an LHP model has been developed using the previous mathematical formulation and assuming the following conditions:

- The LHP components do not exchange heat with the ambient.
- The electronic unit (heat source) is a single thermal diffusion node.
- An equivalent sink temperature is considered for the thermal environment of the radiator.
- The radiator is modeled as a single thermal diffusion node.
- The radiative coupling between the radiator and the sink has been calculated taken into account a radiator efficiency of 0.89 and the following emissivities: 0.85 for the radiator and 0.49 for the chamber test.
- The valve set point has been set in accordance with the Heat Switch design. That is, a T_{close} value of 17^{o}C has been introduced in the model as input data.

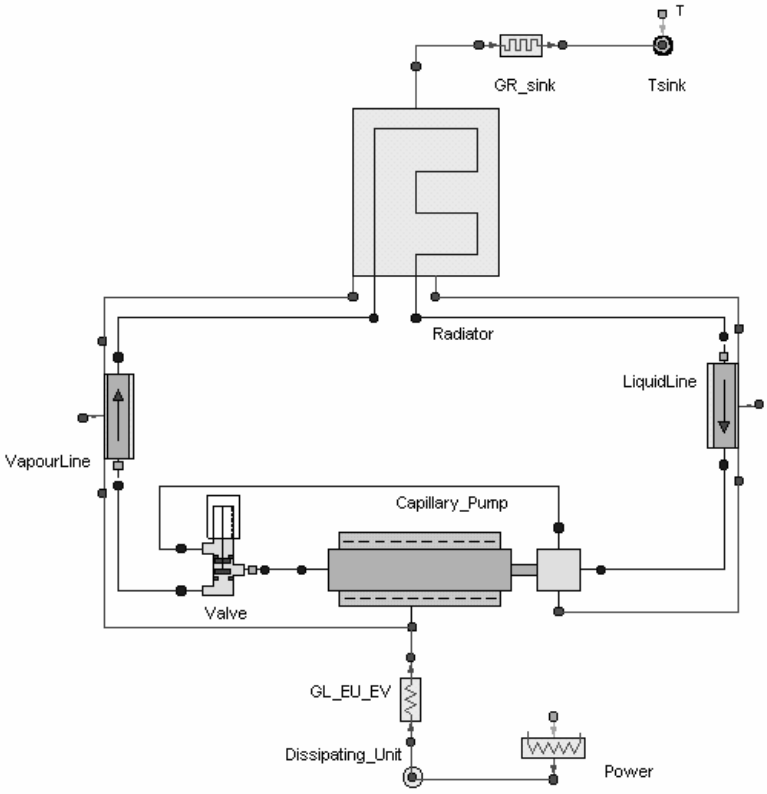

FIG. 13: LHP model schematic

The LHP model schematic is presented in Fig. 13.

6. COMPARISON OF HEAT SWITCH TEST RESULTS WITH ECOSIMPRO PREDICTIONS

Although an extensive test campaign has been carried out for this LHP, only the most representative cases are given in this paper. To show the correlation between the thermal model and the experimental results, three steady states and one transient state in horizontal conditions are discussed below.

For each of the cases, the power applied to the evaporator and the sink temperature have been introduced as boundary conditions in accordance with the experimental data.

6.1 Comparison of Steady-State Regimes of Heat Switch Operation

Three different tests have been selected to verify the agreement between the Ecosim-Pro model predictions and the test results. The set of boundary conditions of power and sink temperatures are different for each case. The calculated and experimental temperatures in steady conditions are presented in Table 1.

TABLE 1: Test and model temperatures comparison for 3 representative cases

Component	Temperature, ^{o}C								
	Case 1: power 30 W, sink temperature –30^{o}C			Case 2: power 10 W, sink temperature –37^{o}C			Case 3: power 30 W, sink temperature –6.5^{o}C		
	Test	Model	ΔT	Test	Model	ΔT	Test	Model	ΔT
Heater block	22.4	25.6	3.2	17.8	18.1	0.3	35.7	39.5	3.9
Evaporator saddle	20.8	22.9	2.1	17.2	17.2	0.0	34.1	36.8	2.8
Evaporator	19.8	22.8	3.0	16.9	17.2	0.3	33.1	36.8	3.7
VL Inlet	19.0	22.2	3.2	16.5	17.0	0.5	32.3	36.2	3.9
VL Medium	19.3	22.2	3.0	16.8	17.0	0.2	32.5	36.2	3.7
VL Outlet	18.7	22.2	3.5	16.0	16.8	0.9	32.1	36.2	4.1
Compensation chamber	18.5	22.0	3.5	16.1	16.9	0.7	31.6	35.9	4.3
Cond 1	18.7	20.2	1.5	9.0	–9.8	–18.8	31.9	34.4	2.5
Cond 2	17.7	19.6	1.9	–19.8	–16.6	3.1	30.9	34.0	3.1
Cond 3	17.6	19.1	1.4	–21.4	–16.7	4.7	30.9	33.8	2.9
Cond 4	18.4	18.2	–0.2	–17.7	–16.7	1.0	31.6	33.4	1.8
Cond 5	18.1	17.6	–0.5	–18.3	–16.7	1.6	31.3	32.9	1.6
Cond 6	17.7	17.6	–0.2	–17.8	–16.7	1.1	31.0	32.4	1.5
LL Inlet	16.2	17.6	1.4	–16.5	–16.7	–0.2	31.2	32.7	1.5
LL Outlet	15.2	17.6	2.4	–10.9	–16.3	–5.4	29.7	32.8	3.0
Radiator	16.6	17.5	0.9	–16.8	–16.7	0.1	30.0	32.3	2.3
Sink	–30.1	–30.1	0.0	–37.0	–37.0	0.0	–6.5	–6.5	0.0

Since a high power has been applied in Case 1, the valve does not regulate the temperatures. That means, that the bypass line is completely closed and all the fluid flows through the radiator and the liquid line to reach the compensation chamber.

For the model correlation, a maximum temperature difference of $\pm 5^{o}$C between the calculated and the experimental temperatures was required. As is shown, all the temperature differences are lower than the specified range for Cases 1 and 3. For these two cases, the largest temperature differences are for the components at the hot side. Additionally, the experimental relative temperature differences between the heater block and the evaporator saddle and between the evaporator saddle and the evaporator differ from the calculated ones. In fact, the experimental temperature difference between the heater block and the evaporator saddle is lower than the calculated one and the difference between the evaporator saddle and the evaporator is higher. This is because of the values of the thermal contact couplings introduced in the model. It would be possible to fit better the results by adjusting the values of these parameters. On the one hand, the thermal conductance between the heater block and the evaporator saddle can be increased since the real thermal contact conductance of the interfiller is better than the model value. On the other hand, the conduction between the evaporator saddle and the evaporator case shall be decreased if the conduction across the saddle is taken into account. Since the updating of the contact thermal conductances will not substantially affect the results and the current model fits quite well with the experimental results ($\pm 5^{o}$C), the conductance values were not updated. These values are intrinsic for the model and are not affected by the power or the sink temperature. Therefore, this comment is also applicable for all the following comparisons.

For Case 2, the power applied is relatively low as well as the sink temperature. Therefore, the valve needs to open partially the bypass line to keep the temperatures above its set point. As is shown, the vapor temperatures are about 17^{o}C. That means that the valve is in an intermediate position regulating in its upper range to reach this steady state.

According to the table, most of the calculated temperatures are within $\pm 5^{o}$C. However, there are two temperatures in Case 2, which differ more from the experimental ones. The calculated temperature at the condenser inlet is much lower than the experimental one. This is due to the fact that the thermocouple TC1 was located at the very inlet of the condenser. On the contrary, in the model this value corresponds to the temperature at the first node which is located farther from the condenser inlet. That means that in the model, the calculated value corresponds to a point which has much subcooling than experimental. The difference is so large because of the low

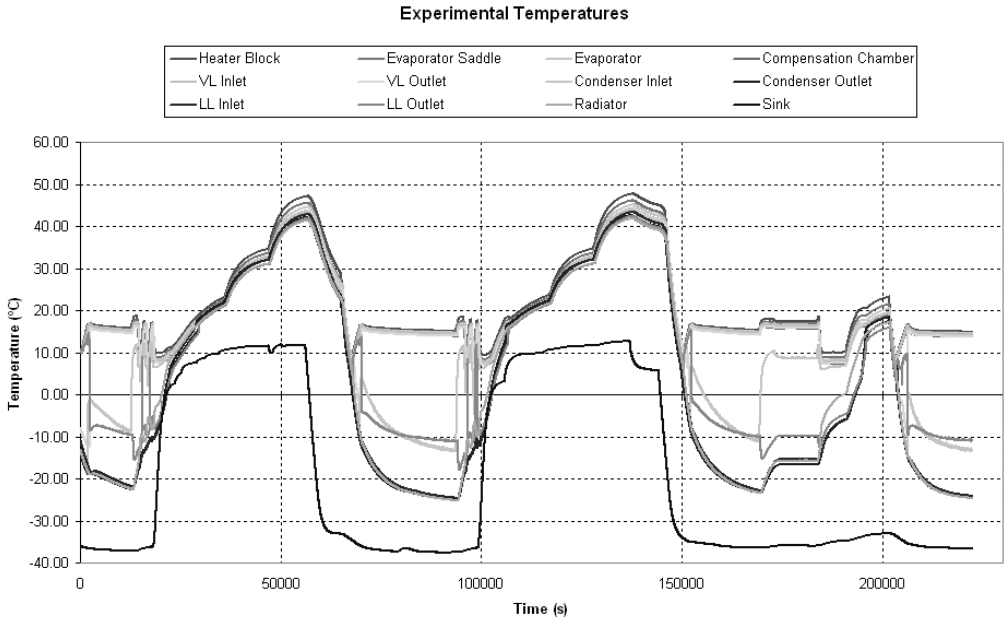

a)

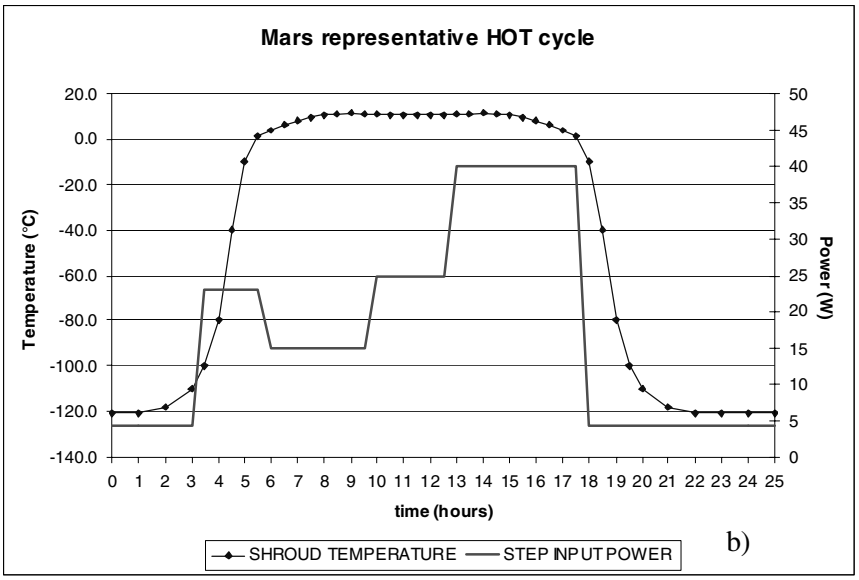

b)

FIG. 14: Mars scenario case: a) experimental temperatures; b) Mars representative hot cycle

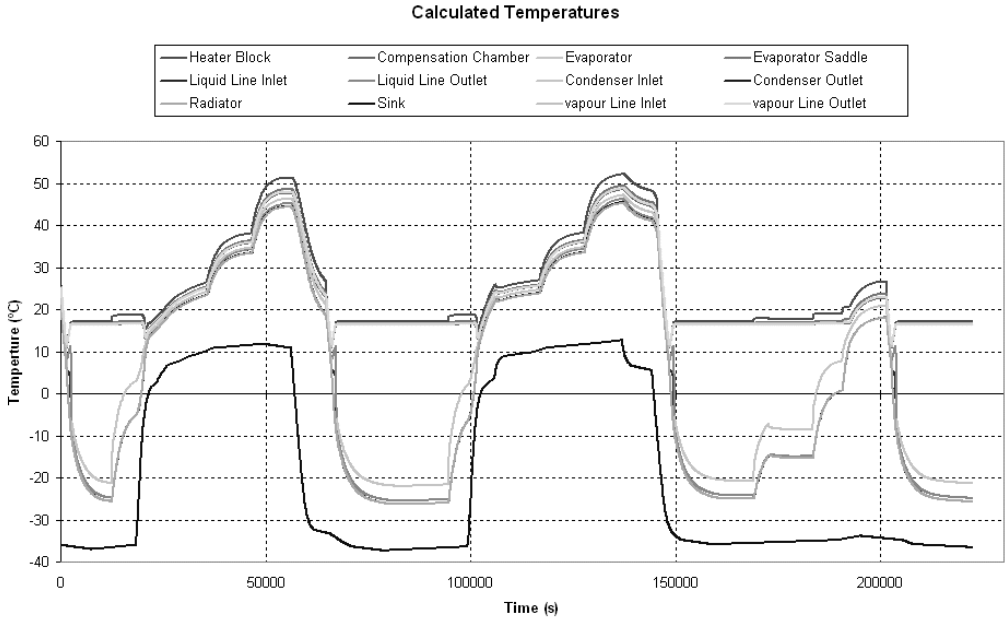

FIG. 15: Mars scenario case — calculated temperatures

power applied. Then the mass flow through the condenser is very small and the different locations of the real thermocouple and the calculated point affect the results notably. The second temperature which differs by more than 5°C from the experimental is the one calculated at the liquid line outlet. In the experiments, the thermocouple was located in front of the joint between the liquid line and the bypass line and it can be influenced by the vapor temperature in the bypass line. However, in the model, it was considered that the vapor from the valve flows directly to the compensation chamber (not to the liquid line). For this reason, the calculated value is much lower than the experimental one.

6.2 Comparison of Transient Regimes of Heat Switch Operation

In one of the tests the sink temperature and the applied power are varying continuously in order to represent the Mars scenario (Fig. 14). The temperatures obtained experimentally are presented in Fig. 14a.

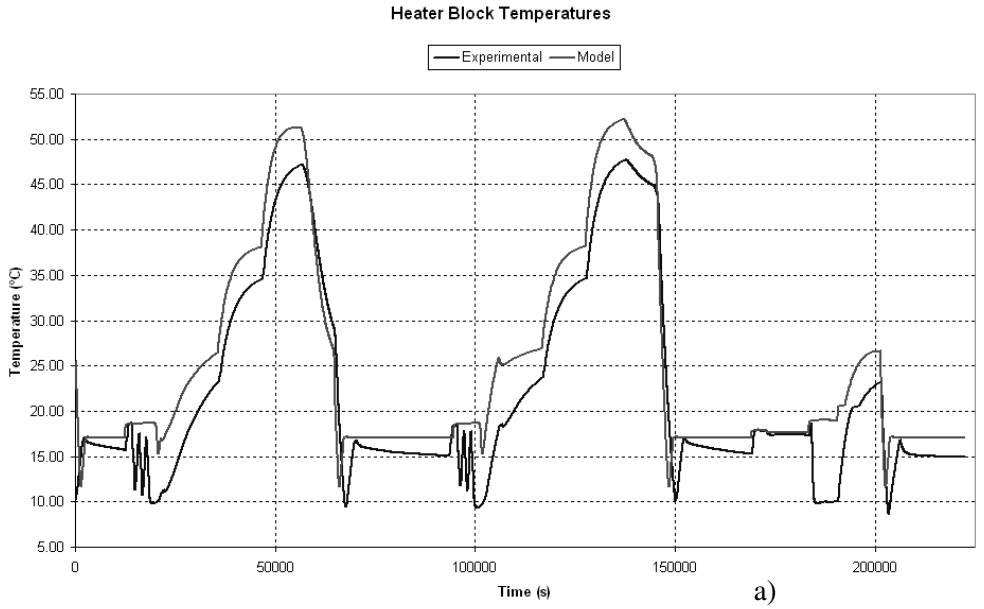

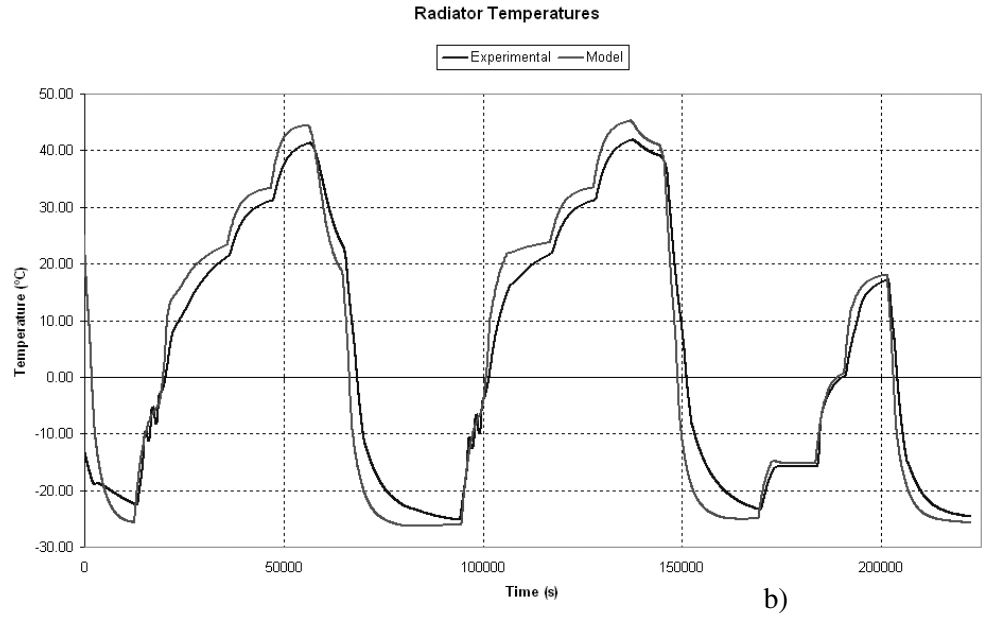

FIG. 16: Mars scenario case — comparison of temperatures of the Heat Switch elements: a) heater block temperatures; b) radiator temperatures

The sink temperature and the power have been introduced as boundary conditions in accordance with the testing values in the model. The calculated temperatures are presented in Fig. 15.

When the sink temperature is low, the valve is regulating the temperature and the LHP temperatures are decoupled. In fact, a temperature difference higher than 30°C can be found between the capillary pump temperatures and the condenser ones. On the contrary, when the sink temperature is higher, the valve is not acting, that is, the bypass line is completely closed and the relative differences between the LHP temperatures are small.

As is shown, the calculated temperatures are very close to the experimental ones even in transient conditions. For direct comparisons, the heater block and radiator temperatures are presented as examples in Fig. 16.

According to these figures, practically all the temperature differences between the calculated and experimental values are within the specified range for both components. Exceptions are the regions were the gravity-caused temperature oscillations were observed. This effect is connected with the position of the liquid front in the condenser. Then the valve is not capable to find an equilibrium position, but oscillated between the two limiting points (transition close/open valve temperature range was 8–17°C) as it was explained before. Some improvements of the model are necessary to predict this transient behavior. A homogeneous condensation model is not fully realistic and flow mapping is not precise, especially with propylene. Also the condenser is a critical item and accuracy in monitoring of the location of temperature sensors in tests with regard to the model is very important.

7. CONCLUSIONS

The Thermal Control System — the Heat Switch — for the European Mars Rover was developed on the basis of the Loop Heat Pipe technology. A passive bypass regulating valve was used as a heat flow control element.

Two models of evaporators were manufactured and tested.

The Model-I evaporator was integrated in the Heat Switch prototype with a radiator and extensively tested in ambient and vacuum conditions. The device has demonstrated an outstanding thermal performance. Corresponding thermal conductances in ON and OFF Heat Switch modes are 5 W/K (0.75 W/K ON required) and 0.009 W/K (0.015 W/K OFF required). The observed oscillations of temperatures at certain combinations of power and sink conditions are connected with the present design of the condenser (~0.5 vertical tube above the evaporator at the vapor input) and can be

avoided by different routing of LHP vapor/liquid/condenser lines. It has to be mentioned that the oscillations are very stable and lie inside the operational range. Thus, in the general case, this effect will not have impact on functionality of controlled objects.

The Model-II evaporator with an optimized secondary wick design was integrated with a representative technological condenser and has been tested in the worst orientation (the evaporator on the top of the compensation chamber and the compensation chamber on the top of the condenser) and worst operating (rapid simultaneous decrease or increase of the sink temperature and input power) conditions. The LHP have operated in all the tests. An oscillating regime of heat transfer was realized under most stressful conditions (low power and low sink temperature). A high performance of the secondary wick provides LHP functionality in any orientation in the gravity field.

The EcosimPro model of the Heat Switch was developed. The experimental results obtained from the tests have been analyzed and compared to the temperatures calculated by the thermal model. The results agree within the $\pm 5^{o}C$ range required for steady conditions. Moreover, very good agreement was achieved for the transient cases also.

ACKNOWLEDGMENT

The present work has been developed under the ESA TRP contract AO/1-4974/05/NL/SF.

REFERENCES

1. Bodendieck, F., Schlitt, R., Romberg, O., Goncharov, K., Hildebrand, U., and Buz, V., Precision temperature control with a loop heat pipe, *SAE Paper* No. 2005-01-2938, 2005.
2. Goncharov, K., Kolesnikov, V., Schlitt, R., Bodendieck, F., and Supper, W., COM2PLEX/Tatiana-3 ground and in-orbit test results, *Two-Phase 2003 Workshop*, Noordwijk, The Nederlands, September 15–17, 2003.
3. Mishkinis, D., Wang, G., Nikanpour, D., MacDonald, E., and Kaya, T., Advances in two-phase loop with capillary pump technology and space applications, *SAE Paper* No. 2005-01-2883, 2005.
4. Goncharov, K., Buz, V., Elchin, A., Prokhorov, Yu., and Surguchev, O., Development of loop heat pipes for thermal control system of nickel–hydrogen batteries of "Yamal" satellite, *Proc. 13th Int. Heat Pipe Conf.,* Shanghai, China, October 21–26, 2004, pp. 622–627.
5. Kozmin, D., Goncharov, K. A., Nikitkin, M., Maidanik, Yu. F., Fershtater, Yu. G., and Smirnov, H., Loop heat pipes for space mission Mars 96, *SAE Paper* No. 961602, 1996.
6. Molina, M., Franzoso, A., Bursi, A., Romera, F., and Barbagallo, G., A heat switch for European Mars Rover, *SAE Paper* No. 2008-01-2153, 2008.

7. Wolf, D., LHP secondary wicks: design, analysis, and test, *Spacecraft Thermal Control Workshop*, March 11–13, 2008.
8. EcosimPro Simulation Tool V3.42. http://www.ecosimpro.com/
9. Gregori, C., Torres, A., Perez, R., and Kaya, T., LHP modeling with EcosimPro and experimental validation, *SAE Paper* No. 2005-01-2934, 2005.
10. Gregori, C., Torres, A., Pérez, R., Kaya, T., Mathematical modeling of multiple evaporator/multiple condenser LHPs using EcosimPro, *Proc. 36th Conf. on Environmental Systems*, Norfolk, Virginia, USA, 2006, SAE Paper 2006-01-2174, 2006.

Heat Pipe Science and Technology, *An International Journal* 1(1) 47–57 (2010)

DEVELOPMENT AND INVESTIGATION OF A COOLER FOR ELECTRONICS ON THE BASIS OF TWO-PHASE LOOP THERMOSYPHONS

Vladimir G. Pastukhov, Yury F. Maydanik, *
& Valery I. Dmitrin

Laboratory of Heat Transfer Devices, Institute of Thermal Physics, Ural Branch of the Russian Academy of Sciences, 106 Amundsen St., Ekaterinburg 620016, Russia

*Address all correspondence to Yu. F. Maydanik
E-mail: maidanik@etel.ru

The objective of this work was to develop a device for cooling electronic elements with a heat power up to 30 W by its rejection and dissipation in the ambient by free air convection. The device specification assigned the temperature range of the ambient conditions from –40 to +105°C and the available space of 30(W) × 120(H) × 200(L) mm. As a result a hybrid scheme based on a loop thermosyphon was proposed, where the evaporator embodied the capillary structure. In such a scheme, the return working fluid flow was ensured by the combined action of the gravity and capillary forces. Several prototypes with different loop and evaporator designs were tested in laboratory conditions. Water and heptane were used as working fluids. The experiments showed that the role of the capillary structure locally placed in the evaporator can be efficiently implemented by both highly porous cellular materials and capillary grooves made on the evaporating surface. It is also shown that heptane can be effectively used as a working fluid which is appropriate for the temperature range requirements. At the same time the device has good mass-and-size characteristics and total thermal resistance under a nominal heat load of about 1.7°C/W.

KEY WORDS: *loop thermosyphon, evaporator, capillary structure, thermal resistance*

1. INTRODUCTION

The simplicity of the two-phase thermosyphons (TS) design is as a whole the main factor which has attracted to them great attention for many years. As the return of liquid from the condenser in the evaporator is realized under the gravity forces, the application of these devices is limited by the terrestrial conditions. Nevertheless, TSs allow quite a technological solution for a wide range of thermal problems and, particularly, electronics cooling problems [1]. Because of the high-dense electronics packaging in the limited space, the cooling device compact size and its convenient placement become very important. In view of this, the loop thermosyphon (LTS) design, where the evaporator is attached to the condenser by a pair of individual channels for liquid and vapor flows, has several advantages over the tubular TS. Firstly, the entrainment thermal limit typical of the tubular TS is eliminated. Secondly, the connecting channels can have a relatively small diameter, which allows their easy configuration. And, finally, the evaporator and the condenser can have different geometry and sizes corresponding to the concrete conditions of the external heat exchange.

The limitations of the LTS thermal performance first of all are connected with two basic limits. The first one is the so-called pressure losses limit, which appears when the total hydraulic losses in the loop become equal to the pressure of the highest possible hydrostatic liquid column. The second one is related to the boiling limit, which for a smooth internal surface of the evaporator and under the flooded condition is close to the values of the pool boiling limit [1].

The requirements of modern electronics with the necessity of cooling elements with heat rejection densities up to 100 W/cm^2 and more stimulated the appearance of a large number of research works concerning the heat transfer intensification in evaporators by enhancing the internal surface. The main efforts in this direction consist in the creation of a thin grooved system, porous coatings of sintered powders or fibers and porous inserts [2–7].

In this connection the effect of an enhanced surface on heat transfer during boiling on it is studied in a liquid flooded horizontal position. For these conditions, the increase of critical heat fluxes in comparison with a smooth surface may range from one and a half [1] to six [2, 5] times. The typical size of structural grooves is usually equal to 0.3–0.55 mm. The range of optimal thicknesses of sintered structures is from 0.1 to 1.5 mm at a porosity of 49–80% and at pore sizes of about 50–200 μm. The conditions of the capillary feeding of porous coating were realized in [4] where a 2–3-order increase of the heat-transfer coefficient in the range of low and moderate

heat fluxes (0.1–10 W/cm^2) was obtained. The data were obtained on a 0.3-mm-thick sintered copper coating with a porosity 50–55% and a pore size of 24.5 μm. The working fluid was R290 (propane).

The working fluids, examined in LTS for electronics cooling, is limited by the following line: water, ethanol, methanol, PF5060, and FC-72. Water is often excluded from this line because of the abnormal density during freezing. Freon R134a was successfully used for a thermoelectric refrigerator with a working temperature range from –5 to +5^{o}C [8].

The objective of this work was the development and tests of a heat transfer device which would allow heat rejection into the ambient from the electronics elements with a maximal admissible temperature of 150^{o}C and in a wide temperature range of the ambient medium from –40 to +105^{o}C. The device should conform to the specification by the dimensions and should be easily made.

2. DESIGN PROCESS

The design specification for the heat transfer device is presented in Table 1.

The LTS scheme was taken as the basic one. There the heated evaporator surface is placed vertically and its bottom is almost at the same level as the condenser bottom (Fig. 1). Such a composition was enforced by the limited height H = 120 mm. It was supposed that the effective work of such an LTS can be realized at a partial flooding of the evaporator by organizing on its hot side a capillary structure to realize the liquid feeding and evaporating cooling. Besides, it would allow decreasing the required height h_l of the driving liquid column.

TABLE 1: Design specification

Maximal heat load	30 W
Maximal admissible temperature	150^{o}C
Range of the ambient temperature	–40 +105^{o}C
Sizes of the contact area	30 × 30 mm
Available volume for the cooling device	30(W) × 120(H) × 200(L) mm
Inclination	0 ± 20^o
Means of external radiator cooling	free air convection
Mass of the device	minimum

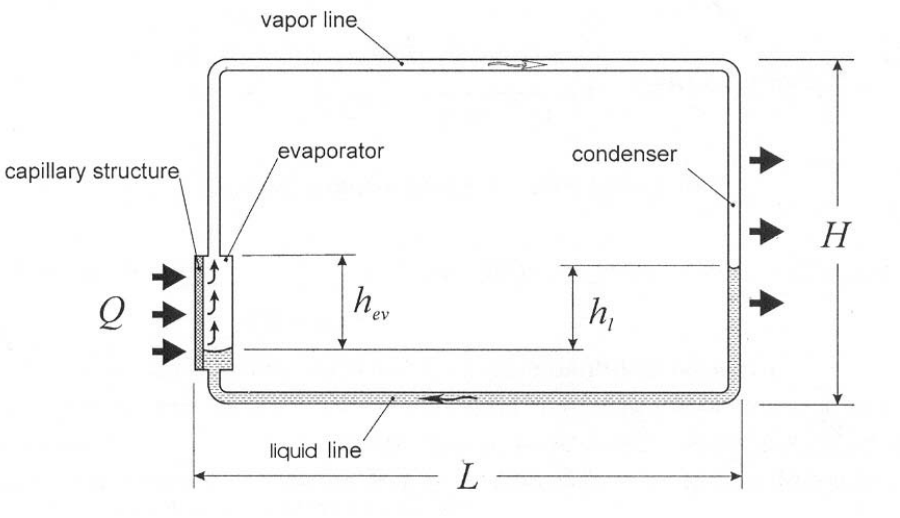

FIG. 1: Principal scheme of hybrid LTS

Then the working fluid circulation conditions can be described by the system of two equations:

$$\Delta P_g(h_l) = \Delta P_v + \Delta P_l \,, \tag{1}$$

$$\Delta P_c \geq \Delta P_l^{CS} + \Delta P_g(h_{ev}) \,. \tag{2}$$

Equation (1) describes the condition of equality of the hydrostatic pressure of the liquid column with height h_l to the sum of hydraulic losses in the vapor and liquid lines (ΔP_v and ΔP_l, respectively). Equation (2) is the capillary limitations when the maximal capillary head ΔP_c should exceed the pressure losses in filtration of liquid ΔP_l^{CS} through the wick and its lifting to height h_{ev}, $\Delta P_g(h_{ev})$.

Based on these equations, the LTS design parameters and the working fluid were selected. Besides, the working fluid selection along with the condition of nonfreezing was limited by the value of the excess pressure of 3–4 bars. Only two working fluids meet this requirement: toluene and heptane with saturation pressures of 2.18 and 3.0 bars, respectively, at a temperature of 140°C. An estimated calculation for them was made by Eq. (1) to find the value of the liquid column appearing at a 30-W heat load in the LTS loop with an inner diameter of lines of 3 mm. The calculation results are presented in Fig. 2 as a function of temperature. It is clear that at the same

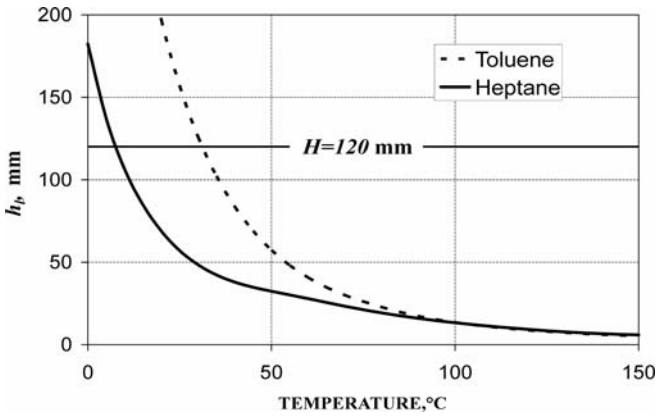

FIG. 2: Temperature dependence of the liquid column height in LTS for toluene and heptane

working temperature the height of the column for heptane is lower than for toluene up to 100°C. It is important for the LTS scheme under consideration because the liquid column blocks part of the condenser surface. Besides one can see that due to the height limitation in the maximal possible column of the LTS (H = 120 mm), the stationary circulation in the loop is possible not at all temperatures. For heptane it starts at lower temperatures of about 10°C than for toluene of about +30°C. The arguments listed acted as a reason to choose heptane as a working fluid.

3. LTS EXPERIMENTAL MODELS

Three prototypes with different types of condensers and evaporators were made and tested. Their designs are shown in Fig. 3 together with the radiators they were tested with.

Model #1 had a cylindrical evaporator supplied with a copper saddle. A porous insert of a copper highly porous cellular material (HPCM) was placed in the evaporator. In models #2 and #3, evaporators had the same disk shape but different capillary structures (CS). In model #2, a CS of 2.4-mm-thick copper HPCM was pressed mechanically to the inner heat-receiving surface of the evaporator. In model #3, the CS was made as a row of vertical grooves 0.1-mm wide and 0.25-mm deep. In all models, the condensers were of tubular type, in the tests they were mechanically pressed to the base of radiators. Noteworthy is a peculiarity of the condenser in model #2,

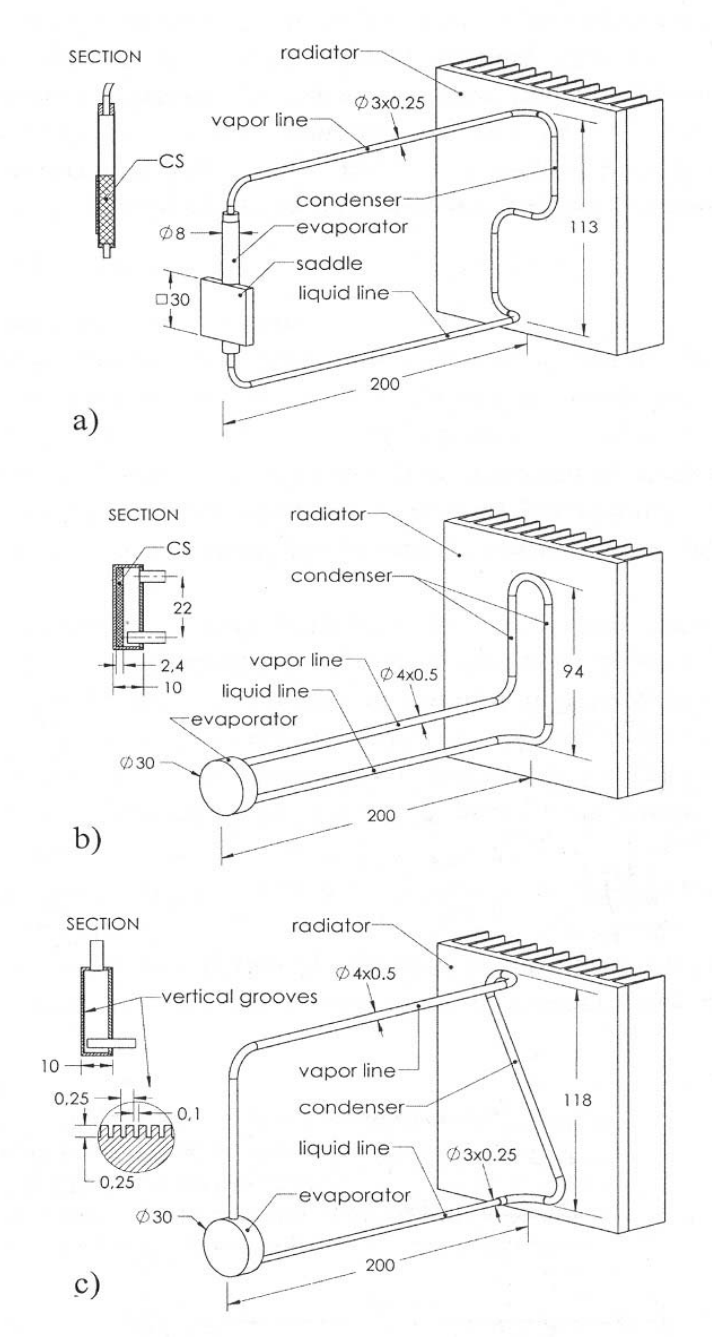

FIG. 3: Experimental LTS designs: a) model #1, b) model #2, c) model #3

which for greater compactness was made as a loop with two lines. One of them was ascending, i.e., the flow was directed against the gravity forces vector, the other line was descending.

All the models were made of copper. In models #1 and #2 water was used as a working fluid. Model #3 was filled with heptane. The mass of a filled model #2 was about 64 g, of models #2 and #3 – 54 ± 1 g.

A flat electric heater was used as a heat load simulator, which, through the thermal paste, was pressed to the heat-receiving side of the evaporator. The heat load range varied from 10 to 40 W. The radiator cooling was effected by free air convection at an indoor temperature of 22 ± 2^{o}C. The temperature was measured by T-type thermocouples placed on the heater contact surface, on the vapor and liquid lines and on the radiator base. In the tests the temperature field was measured in time, simultaneously the heat load was changed stepwise following the steady-state conditions. Tests were conducted with the devices oriented horizontally and at slopes of $\pm 20^{o}$.

4. TESTS RESULTS AND DISCUSSION

Typical temperature-time dependences of LTS operating regimes obtained in the experiments are shown in Fig. 4. It is clearly seen from Fig. 4a that a start-up of model #1 was accompanied with overheating of the liquid in the evaporator followed by sudden boiling and heating of the loop. Slight fluctuations of the temperatures of liquid and vapor lines are seen as well, they decreased with an increasing heat load. Hence it can be supposed that in the initial state the internal porous insert in the evaporator was fully saturated with the liquid. After boiling, and as liquid was removed from the large pores of the HPCM during the increase of the heat load, the evaporation regime started and the circulation flow stabilized.

The work of model #2 was accompanied by significant fluctuations of all the temperatures (Fig. 4b) and by a relatively higher temperature level under lower heat loads than in model #1. Such a behavior can be explained mainly by the geometry peculiarity of the loop-shaped condenser.

The formation of a continuous liquid plug in its lines led to the limitation of the maximal height of the driving liquid column to the value of 22 mm (the distance between the vapor and liquid lines in the transport section (see Fig. 3b). On the other hand, liquid was ejected from the evaporator in the loop pipes on explosive boiling up. At low temperatures this liquid column pressure was insufficient for overcoming the pressure losses in the loop. During the condenser blocking by the liquid, the temperatures grew to values when the mentioned height became sufficient to provide the

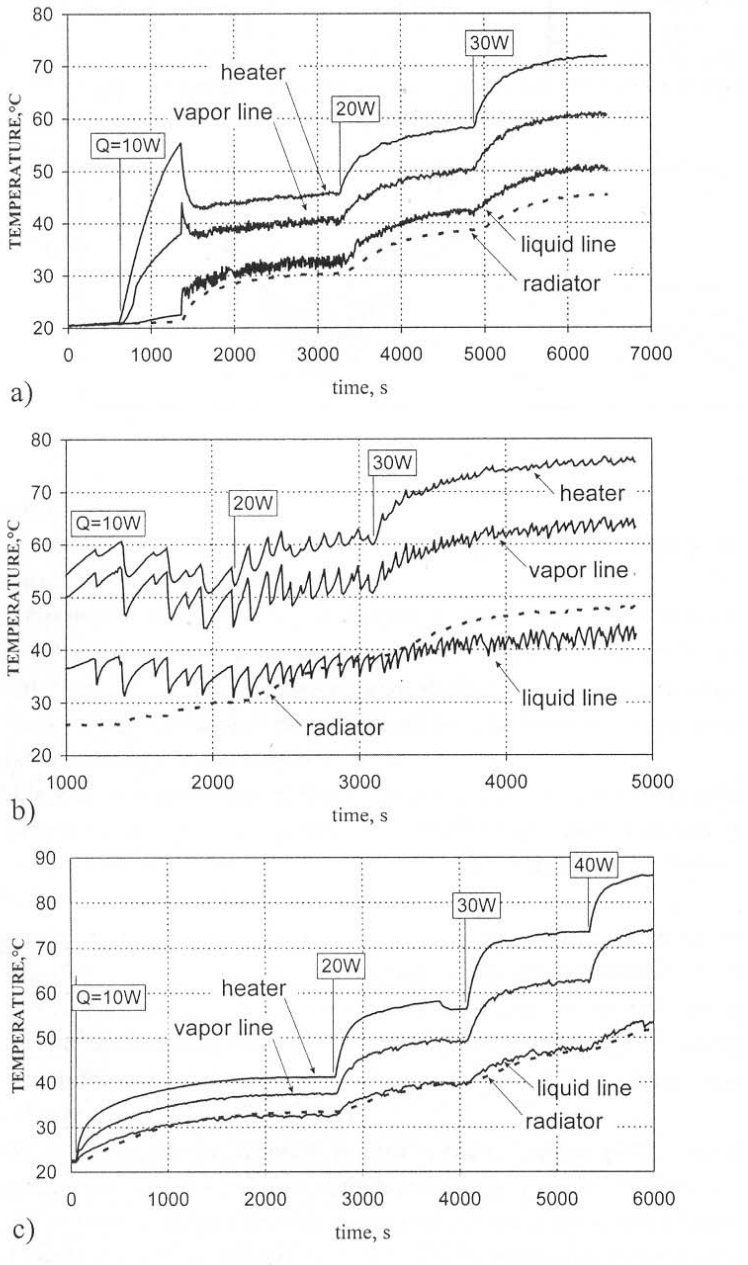

FIG. 4: Temperature-time dependences of the operating regimes at the orientation $\varphi = 0^{o}$: a) model #1, b) model #2, c) model #3

liquid access to the evaporator. Besides, the inflow of the subcooled liquid in the evaporator stimulated the initiation of pressure and temperature pulsations. It can be also seen that the amplitude of temperature oscillations decreased along with the heat load growth but did not disappear at all even on reaching its maximal value.

It is seen from the operating characteristics of model #3 (Fig. 4c) that its start-up was smooth without temperature pulsations and with progressive warming-up of the loop. It allows conclusion on the prevalence of the evaporative mechanism of the vaporization in the CS made as capillary grooves. The crisis was not observed up to a heat load of 40 W, which corresponded to a heat flux of 5.66 W/cm^2.

The comparison of total thermal resistances is shown in Fig. 5. This thermal resistance was determined as the relation of the temperature difference between the heater contact surface and the ambient to the supplied power. It means that it included all the contact resistances as well: LTS-heater and LTS-radiator.

A significant difference in the values of the total thermal resistance was observed only under low heat loads of 10–20 W, which can be explained by different operating regimes of the device described above. Under a nominal heat load of 30 W models #1 and #3 had the lowest resistance of about 1.66 ± 0.01^{o}C/W.

The tests on the influence of inclinations on the LTS operation were executed with models #1 and #3 at the nominal value of heat load 30 W (Fig. 6). It is seen that quantitative and qualitative characteristics were very close. The main influence of the slopes in the interval of $\pm 20^{o}$ on the characteristics can be related to the change of the flooding degree of the condenser. At negative inclinations the condenser was free from liquid while at positive ones – it was filled with liquid. Besides, at positive inclinations the degree of the evaporator filling with the liquid decreased. Hence it is

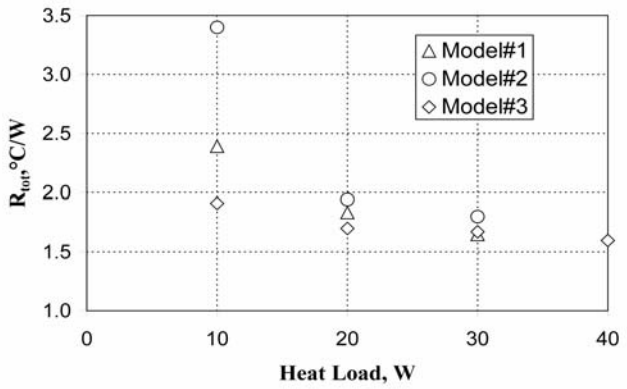

FIG. 5: Total thermal resistance vs heat load

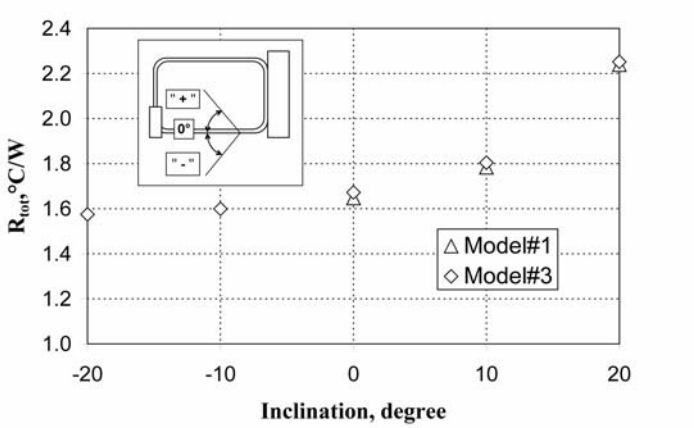

FIG. 6: Total thermal resistance vs LTS slopes. Heat load 30 W is constant

clear why the device was more sensitive to positive inclinations than to negative ones. It is obvious that greater positive inclinations are fraught with the violation of conditions of the working fluid circulation and as a result with full drying of the evaporator.

5. CONCLUSIONS

1. In solving the task of creating a compact and simple heat transfer device on the basis of a two-phase LTS, where the evaporator was supplied with a capillary structure, was proposed and tested. The tests of three experimental models have shown that at heat fluxes up to 5–6 W/cm^2, both HPCMs and constructive capillary grooves can be used as CS. It has been determined as well that the condenser in the form of a loop with an ascending line leads to the pulsation regime in the device operation.
2. The selection of heptane for a wide operating temperature range (from –40^{o}C to +140^{o}C) of the device is justified. Heptane as a working fluid was approved in LTS at vapor working temperatures from 37 to 74^{o}C. The total thermal resistance of the device in free-convection air cooling at a heat load of 30 W did not exceed 1.7^{o}C/W.
3. With the change of the inclinations to the horizon in the interval of $\pm 20^o$ the device remained workable. The corresponding range of the change in the total thermal resistance amounted to 1.58–2.25^{o}C/W.

4. For realization of the device practical application it seems actual to carry out an investigation of its working regimes in the whole temperature range from –40°C to +105°C prescribed by the specification. Of special interest are start-up regimes at low temperatures when a pronounced pulsation regime of operation is expected.

REFERENCES

1. Polasek, F. and Rossi, L., Thermal control of electronic equipment by heat pipe and two-phase thermosyphons, *Proc. 11th IHPC*, Tokyo, Japan, pp. 50–74, 1999.
2. Ramawamy, C., Joshi, Y., and Nakayama, W., Performance of a compact two-chamber two-phase thermosyphon: effect of evaporator inclination, liquid fill volume and contact resistance, *Proc 11th IHTC*, Kyongju, Korea, vol. 2, pp. 127–132, 1998.
3. Pal, A., Joshi, Y., Beitelmal, M., Patel, C., and Wenger, T., Design and performance evaluation of a compact thermosyphon, *IEEE Trans., Components Packag. Technol.*, 25(4):601–607, 2002.
4. Vasiliev, L. L., Zhuravlev, A. S., and Shapovalov, A., Comparative analysis of heat transfer efficiency in evaporators of loop thermosyphons and heat pipes, *Proc. 13th IHPC*, Shanghai, China, pp. 76–81, 2004.
5. Merilo, E. G., Sementic, T., and Catton, I., Experimental investigation of boiling heat transfer in bidispersed media, *Proc. 13th IHPC*, Shanghai, China, pp. 105–110, 2004.
6. Khrustalev, D., Loop thermosyphons for cooling of electronics, *18th IEEE SEMITHERM Symp.*, San-Diego, California, pp. 145–150, 2002.
7. Tsai, M. C., Hsieh, C. H., and Kang, S. W., Experimental study of a loop thermosyphon using methanol and water as a working fluid, *Proc. 14th IHPC*, Florianopolis, Brazil, pp. 348–352, 2004.
8. Lee, J. S., Rhi, S. H., Kim, C. N., and Lee, Y., Use of two-phase loop thermosyphon for thermoelectric refrigeration: experiment and analysis, *Proc. 12th IHPC*, Moscow, Russia, pp. 519–524, 2002.

Heat Pipe Science and Technology, *An International Journal* 1(1) 59–70 (2010)

DEVELOPMENT OF ADVANCED MINIATURE COPPER HEAT PIPES FOR A COOLING SYSTEM OF A MOBILE PC PLATFORM

Leonid L. Vasiliev, Jr.[*] *& Andrei G. Kulakov*

A. V. Luikov Heat and Mass Transfer Institute,
National Academy of Sciences of Belarus,
15 P. Brovka St., Minsk, 220072, Belarus

[*]Address all correspondence to L. L. Vasiliev, Jr.
E-mail: leonid.l.vasiliev.jr@gmail.com

At present, miniature heat pipes are widely used for cooling systems of mobile PCs. This paper presents an overview of the development of miniature heat pipes (MHP) with a sintered copper wick with emphasis to different ways of heat pipe wick optimization. Several designs of cylindrical heat pipes with 4-, 5-, and 6-mm outer diameter and 200-mm length, which are the most attractive for the CPU cooling system, have been tailored, tested, and compared to theoretical values in this study to evaluate its thermal performances. A new design of 4- and 5-mm-outer diameter miniature copper heat pipes with innovative wicks is suggested as a promising candidate for present and future cooling systems of high-power mobile PC platforms.

KEY WORDS: *electronics cooling, miniature heat pipe, evaporation, porous media*

1. INTRODUCTION

The modern trend in microelectronic and optoelectronic devices is to increase the level of integration by minimizing the device size (high-density packaging) and increasing the performance of the device (higher frequency). This results in an increase in both power dissipation and power density on the device with prediction to dissipate local heat flux by more than 300 W/cm^2. Such a high heat flux presents a serious challenge for existing thermal management techniques to ensure device performance

2151-7995/10/$35.00

NOMENCLATURE

A	cross section, m^2	σ	surface tension, N/m
D	diameter, m	**Subscripts**	
f	coefficient of friction	a	adiabatic
g	gravity force, m/s^2	c	capillary, condenser
h_{fg}	latent heat, J/kg	ch	channel
K	permeability, m^2	e	evaporator
L	MHP length, m	eff	effective
p	pressure, Pa	h	hydraulic
Q	heat load, W	l	liquid
r	radius, m	m	mean
Re	Reynolds number	*mod*	modified
Greek symbols		s	saturation, particle
θ	wetting angle, deg	v	vapor
μ	viscosity, $N \cdot s/m^2$	w	wick
ρ	density, kg/m^3		

and reliability while maintaining acceptable temperatures, especially for a computer processor [1].

One of the most promising candidates for the mobile PC platform is heat pipes, which offer a better alternative to liquid cooling provided they can handle the heat flux and power requirements [2–5]. The first implementation of a heat pipe in a notebook computer occurred in 1994 despite the fact that the first working heat pipe was built in 1963 [6]. Earlier notebook computers relied on simple metallic heat sinks, but by the late 1990s approximately 60% of notebook computers used heat pipes in thermal management solutions [7]. It is now common to find heat pipes in different configurations used in thermal solutions for portable computers. Almost every current notebook computer uses a heat pipe in its thermal management design. Most of these heat pipe-heat sinks use a heat pipe with outer diameters between 4 and 6 mm that carries the power from the CPU to a large aluminum plate. The heat is then conducted into the EMI shield of the keyboard, through the keyboard, and into the ambient air by natural convection and radiation. Most recent designs incorporate a heat sink/fan/vent with the use of a heat pipe. This concept permits the notebook designer

to locate the CPU independently of the heat sink. This allows the notebook designer to develop the most effective heat exchanger and an optimal airflow path. The optimal design helps to reduce airflow requirements and noise. Most applications use an aluminum evaporator block (heat input section), the heat pipe (heat transport section), and aluminum fins (heat sink section). Up to now, copper tubing, copper sintered powder and water, as a working fluid, is a brilliant combination of the materials used to manufacture heat pipes for application in the electronic components cooling system due to the materials chemical compatibility, high cooling capability, and manufacturability.

The main distinction of heat pipes, besides the working fluid and envelope material, is the wick structure. There are several types of wick structures: screen, grooves, felt, and sintered powder. Sintered powder metal wicks offer several advantages over other wick structures. An emerging advantage of the sintered powder wick is its ability to handle high heat fluxes with usually low thermal resistance. Since sintered powder wicks are generally more than 50% porous, there is, accordingly, a large surface area for evaporation. Another advantage of a heat pipe with a sintered powder wick, especially for the cooling system of a mobile PC platform, is that it can work in any orientation, that including against gravity (i.e., the heat source above the cooling source) while groove and screen mesh wicks have a very limited capillary force capability, they typically cannot overcome significant gravitational forces, and dry-out generally occurs. Additionally, since a sintered powder wick is integral with the heat pipe envelope, and there is enough fluid charge just to saturate the wick, the heat pipe can be subjected to freeze/thaw cycles without degradation in performance. It can also be bent and/or flattened in different shapes. The above attributes make the sintered powder wick the optimal structure for many thermal management solutions.

There are generally five physical phenomena that will limit a heat pipe ability to transfer heat, namely: sonic limit, the viscous limit, the entrainment limit, the boiling limit, and capillary limit. Latter two limits are usually the most restricting factors. The boiling limit occurs when the vapor generated at hot spots of the wick is trapped due to geometry limitation. The capillary limit occurs if the wick capillary pressure is lower than the sum of the pressure drops along the liquid circulation path. Therefore the cooling capability of the heat pipe strongly depends on the balance between capillary pressure and hydraulic resistance of the wick in both (longitudinal and cross) directions and an ideal heat pipe wick should have simultaneously the high wick permeability and high capillary pressure head accompanied by the high effective thermal conductivity. In turn, the capillary pressure head, effective thermal conductiv-

ity, and permeability of the HP wick are the function of the pore distribution inside the wick and finally the copper powder size and shapes.

One of the possible ways to improve HP thermal performance in practice is to apply the so-called irregular sintered wick structure [8]. Moreover it was found recently by Semenic et al. [9] that a sintered copper wick with an irregular biporous wick is able to dissipate up to 500 W/cm^2 using water as a working fluid.

This paper is devoted to development and testing of copper MHPs with 4-, 5-, and 6-mm outer diameter with regular and irregular wick structures. The results are presented in the form of transferred heat loads versus HP adiabatic temperature curves.

2. EXPERIMENTAL APPARATUS AND PROCEDURES

The experimental setup of the LHP is presented in Fig. 1. The general goal of this setup was to determine the heat pipe maximum power capacity and the temperature distribution along the LHP for different heat loads, condenser temperatures, and test-

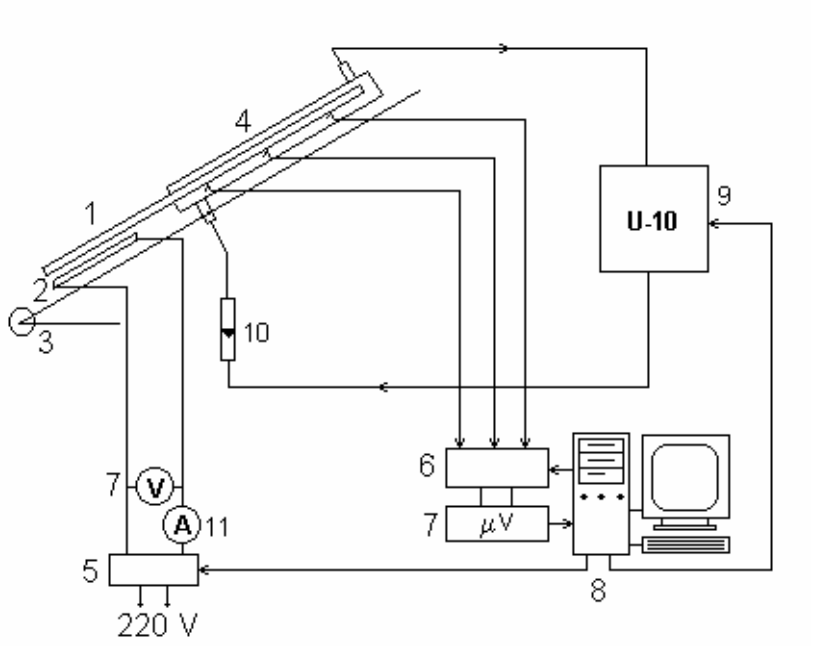

FIG. 1: Test setup: 1) heat pipe, 2) cartridge heater, 3) platform for heat pipe inclination, 4) liquid cooling jacket, 5) power supply, 6) electric switch unit with thermocouples, 7) electric voltmeter, 8) computer, 9) thermostat, 10) water rate recorder, 11) current meter

ing positions. To reproduce thermal activity of electronic components, an evaporator heating source is furnished with electric heaters, which are controlled by a DC power supply, while heat removal is performed by circulation of liquid through a co-axial liquid cooling jacket in the condenser.

The recirculating thermostat is used to provide continuous supply of cooling media at a constant temperature and flow rate where the temperature stability of the coolant tank can be controlled with an accuracy of +/–0.1°C. The heat load of the evaporator is applied through a PC controller. A heat pipe temperature has been monitored by T-type thermocouples. All measured temperatures were transmitted to a PC through a Data Acquisition Switch Unit (Agilent 34970A) in a real time mode. Heat pipe tilt measurements have been realized by a system for tilt regulation. To minimize the thermal losses from the HP to the environment by natural convection, the whole MHP surface was thermally insulated and installed inside the climatic chamber. During the experiment power was applied to heat pipes with a certain step. When steady-state conditions are established, the measured temperature distribution along heat pipes was used to obtain thermal resistance data. Maximum heat transfer was identified if sharp or nonproportional increase of evaporator temperatures was observed. Another approach, described earlier in [10], was also applied, when maximum heat transfer was obtained at constant power with a decrease of the evaporator temperature. Earlier this approach was found as very convenient for testing the miniature heat pipes, especially for heat pipes with mesh and wires, and recently it was also used for heat pipes with a sintered wick along with the general approach. The results obtained with both methods were identical.

Equation (1) was used to calculate maximum heat transfer capability for heat pipes which were under investigation in this study:

$$Q_c = \frac{\left(\frac{1}{r_c} - \frac{1}{r_v}\right) 2\sigma \cos\theta + \rho_l g L \sin\varphi}{\left(\frac{C(f_v \mathrm{Re}_v)\mu_v}{2(r_{h,v})^2 A_v \rho_v h_{fg}} + \frac{\mu_l}{K A_w h_{fg} \rho_l}\right)} \tag{1}$$

where the capillary force by action of the working fluid trapped in the HP condenser zone was taken into account:

$$\Delta p_\delta = \frac{2\sigma \cos\theta}{r_v} \tag{2}$$

3. RESULTS AND DISCUSSION

3.1 MHPs with Homogeneous and Isotropic Copper Sintered Powder

The first part of the present research program is devoted to determination of thermal performance of the copper heat pipes with homogeneous and isotropic wicks.

Both geometrical and structural parameters of HPs under investigation are presented in Table 1.

TABLE 1: Geometrical and physical parameters of MHPs with a homogeneous wick

	HP_1	**HP_2**	**HP_3**
HP diameter out./in. (mm)	6/5	4/3.4	5/4
L_e (mm)	50	50	50
L_a (mm)	93	84	87
L_c (mm)	60	60	60
D_{ch} (mm)	2.5	1.8	2
Size of raw copper particles (μm)	180–250	180–250	180–250
Mean pore diameter of a HP wick (μm)	70	70	70

Round shape copper particles are used as a raw material for HP_1, HP_2, and HP_3 wicks. This material is useful as a raw material for HPs due to high chemical purity, low cost, and availability on the metal powders market. Raw copper particles of size 180–250 μm were selected due to two reasons. On the one hand, the pressure loses in the liquid path, with the given HP geometrical parameters and working fluid properties, depend only on the wick permeability, which, in turn, relies on the size of raw copper particles. So, to increase the wick permeability and thus the HP cooling capability, the raw copper particles with a bigger size must be used. On the other hand, the size of raw copper particles is limited by the technological process of wick fabrication. Small-size copper particles penetrate easier into the HP copper container in the fabrication process. Thus, there is an optimum between the size of raw copper particles and final wick thickness. At the end, a particle size of 180–250 μm was selected.

In Fig. 2, the experimentally obtained thermal performances of HPs (solid lines) and the data calculated by Eq. (1) (dash lines) are shown. All the samples were tested in the horizontal orientation.

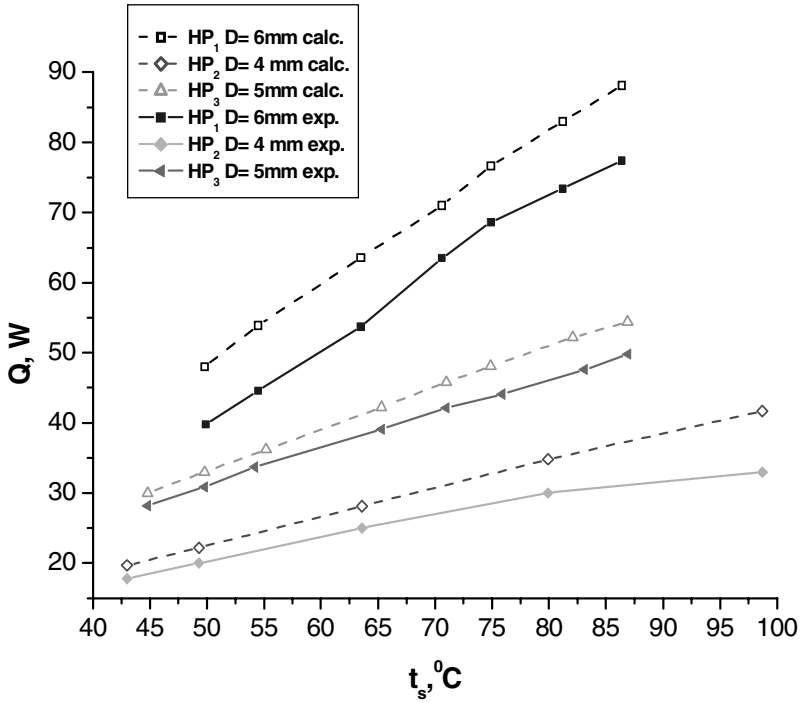

FIG. 2: Maximum heat transfer capability as a function of HP adiabatic temperature for HPs with 4-, 5-, and 6-mm outer diameter

As one can see from Fig. 2, the HP cooling capability increases with an increase in the operating temperature and HP diameter. Also it is important to note that the experimental data are in good correlation with those calculated and a capillary limit is the only one which should be taken into account in simulation of HP with sintered wick thermal performance.

3.2 Optimization of the MHP Wick

There are several possible ways to increase the wick permeability:

– to vary the porosity (permeability) along the HP with increasing from the evaporator to the condenser by applying copper particles of different size;

– to use a special kind of copper powder with the so-called dendritic form (Fig. 3) as a raw material and different wick thicknesses along the HP;

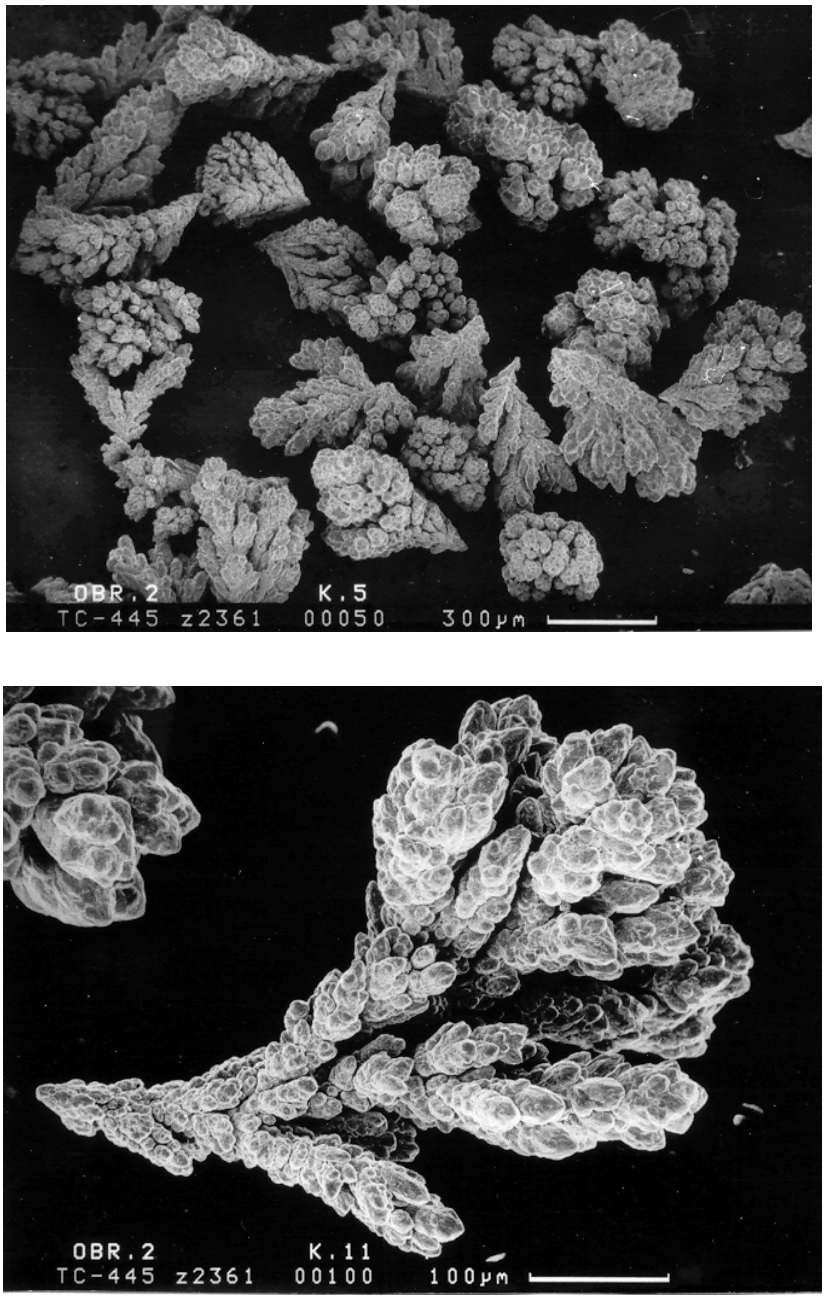

FIG. 3: Photos of copper powder with dendritic shape [11, 12]

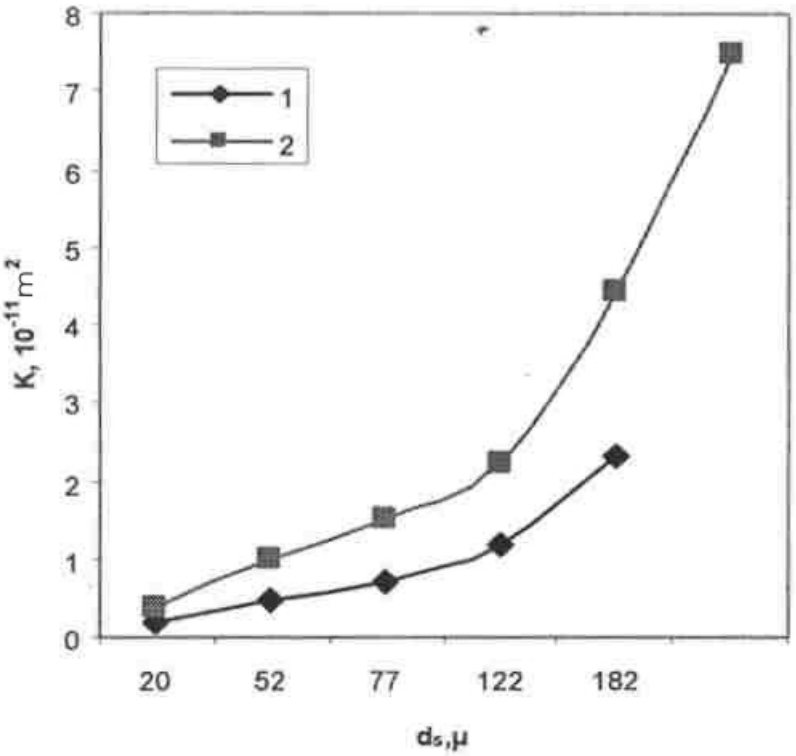

FIG. 4: Permeability of the HP wick with copper particles of round (curve 1) and dendritic (curve 2) shape

– to build the biporous wick structure where the macro- and micropores are present simultaneously — the combination of ways mentioned above.

From the practical point of view the first solution is not as attractive as other ones due to the complicity of finding an optimal temperature for sintering copper particles of different size simultaneously. Therefore, in this study two other solutions are adopted.

As can be seen from Fig. 4, the difference in the permeability of wicks made from copper particles of round and dendritic shape is very appreciable and for a size of 180–250 μm can exceed 2 times [11, 12].

In order to assess the role of an MHP wick, a set of HPs of a similar design, with wicks made from round and dendritic shape copper particles of the same size, were manufactured. Also, in MHPs with nonstandard copper particles the wick thickness is

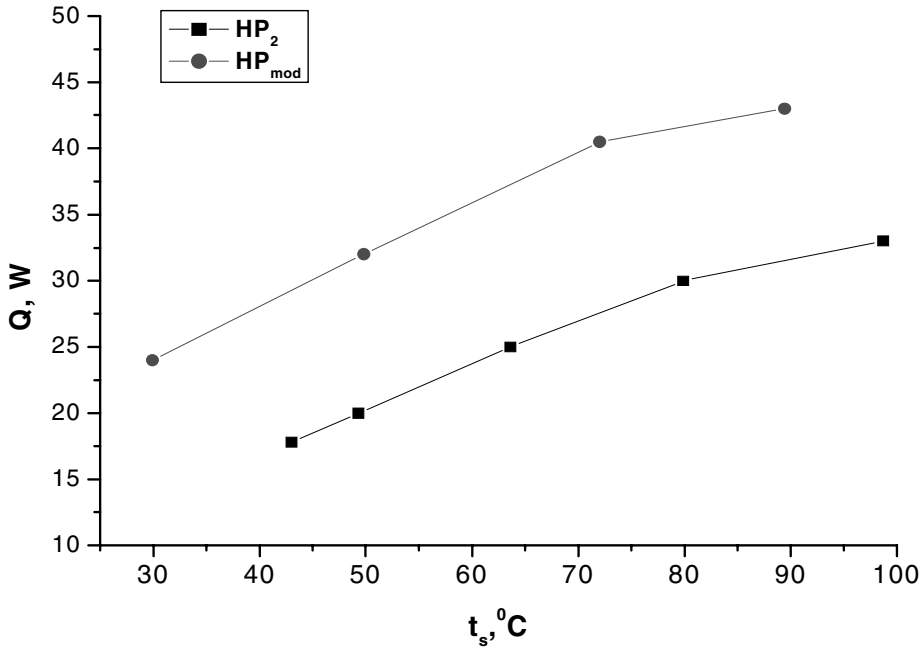

FIG. 5: Maximum heat transfer rate as a function of HP adiabatic temperature for HPs with a 4-mm outer diameter [round (HP_2) and dendritic shapes (HP_{mod}) of copper particles]

not constant along and across the HP. MHP thermal performance with a wick made from dendritic copper particles is better for all tested temperatures. The HP cooling capability was enhanced 1.4–1.6 times (Fig. 5).

Another possible way to increase the wick porosity and thus wick permeability is to add chemically inert particles to the wick, which volatilize in the initial phase of sintering.

This strategy was adopted for the last part of the present study and two HPs with a 5-mm outer diameter and similar design were fabricated.

The main difference between these samples is the wick. Actually, for both cases round standard copper particles of a size of 180–250 μm were used; however, only in one HP chemically neutral powder was also added (about 30% of the total wick volume). Then both HPs were fabricated and tested in the same manner. In Fig. 6, the experimental results of these tests are presented.

It is evident from Fig. 6 that using an additional "pore maker" we drastically changed the HP wick properties. By adding the chemicals to the wick we decreased

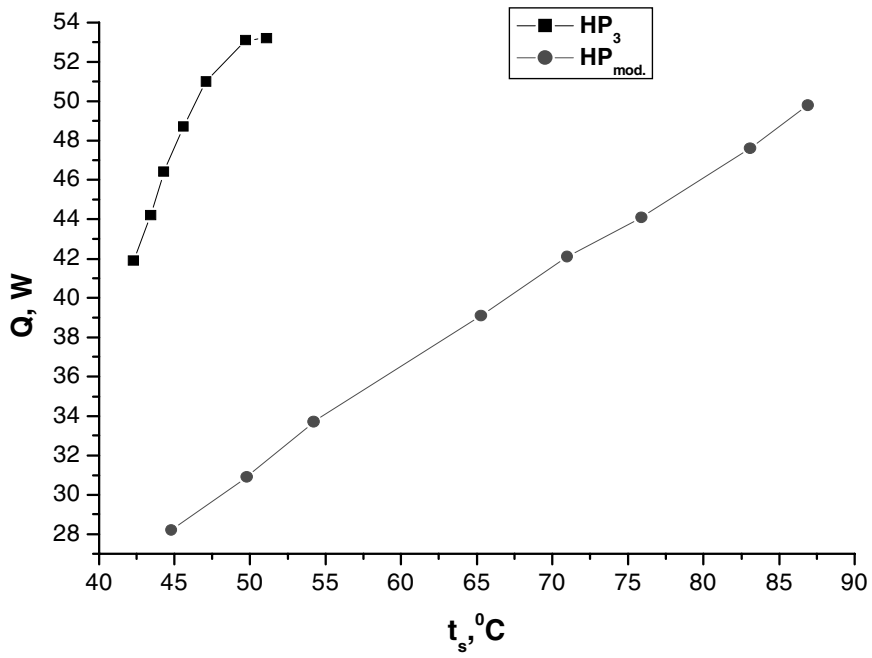

FIG. 6: Maximum heat transfer capability as a function of HP adiabatic temperature for HPs with a 5-mm outer diameter [homogeneous (HP_3) and biporous (HP_{mod}) approaches]

the wick hydraulic resistance. This resulted in an increase of heat transfer ability of miniature heat pipes.

4. CONCLUSIONS

1. It was found that sizes and shapes of raw copper particles played a great role in final structural characteristics of the wick. Due to an increase in the wick permeability, heat pipes with a 4-mm outer diameter with dendritic particles demonstrated better performance, with maximum heat transfer capability being enhanced 1.4–1.6 times compared with the wick made from copper particles of the same size but of round shape.
2. A biporous wick concept was suggested in this study as a promising method for improving the characteristics of miniature heat pipes. A pilot sample of the MHP with a 5-mm outer diameter was designed, fabricated, and tested. It was shown that MHP with a biporous wick has advantages in comparison with the homogeneous one. In particular, an approximately 1.5 fold increase of heat transfer capability was achieved.

ACKNOWLEDGMENT

The authors would like to acknowledge Dr. Viktor Maziuk from Scientific Production Amalgamation "Powder Metallurgy Institute", Minsk, Belarus for his great contribution to this paper.

REFERENCES

1. Ohadi, M. and Qi, J., Thermal management of harsh-environment electronics, in: S. Kakac, L. Vasiliev, Y. Bayazitoglu, and Y. Yener, Eds., *Microscale Heat Transfer, Fundamentals and Applications*, NATO Science Series, II–Vol. 193, Springer, 2005, pp. 479–498.
2. Faghri, A., *Heat Pipe Science and Technology*, London: Taylor and Francis, 1995.
3. Kulakov, A., Intensification of Heat and Mass Transfer in Two-Phase Thermal Control Systems, PhD Thesis, Minsk, 2005.
4. Maziuk, V., Kulakov, A., Rabetsky, M., Vasiliev, L., and Vukovic, M., Miniature heat-pipe thermal performance prediction tool — software development, *Appl. Thermal. Eng*., 21(5):559–571, 2001.
5. Nelson, J., Toth, J., and Hartenstine, J., 100 W/cm^2 and higher heat flux dissipation using heat pipes, in: *Proc. 13th Int. Heat Pipe Conf. "Heat Pipe Theory and Applications,"* September 21–25, 2004, Shanghai, China, pp. 460–465.
6. Ali, A., DeHoff, A., and Grabb, K., *Advanced Heat Pipe Thermal Solution for High Power Notebook Computers*, Technical Paper, Thermacore Inc., Lancaster, Pa, USA, 1999.
7. SeMin, O. and Vasiliev, L., Heat Pipe and Method of Manufacturing the Same, Patent US 20030141045 A1, July 31, 2003.
8. Semenic, T., Yu Lin, Y., and Catton, Y., Use of liquid film evaporation in biporous media to achieve high heat flux over large areas, in: *Proc. VI Minsk Int. Seminar "Heat Pipes, Heat Pumps, Refrigerators,"* September 10–15, 2003, Minsk, pp. 45–51.
9. Vasiliev, L., Jr., Rabetsky, M., Kulakov, A., Vasiliev, L., and Li, Z., An advanced miniature copper heat pipes development for cooling system of mobile PC platform, in: *Proc. VII Minsk Int. Seminar "Heat Pipes, Heat Pumps, Refrigerators,"* September 8–11, 2008, Minsk, pp. 336–244
10. Vasiliev, L., Maziuk, V., Kulakov, A., and Rabetsky, M., Heat pipes software development and experimental verification, in: *Proc. IV Minsk Int. Seminar "Heat Pipes, Heat Pumps, Refrigerators,"* September 4–7, 2000, Minsk, pp. 270–278.
11. Vasiliev, L., Micro and miniature heat pipes — electronic component coolers, *Appl. Thermal Eng*., 28(4):266–273, 2008.
12. Vasiliev, L., Kulakov, A., Vasiliev, L., Jr., Rabetsky, M., and Antukh, A., Heat Pipe, Patent 6708 BY, MPK F28 D15/00, 3.06.2003 (in Russian).

Heat Pipe Science and Technology, An International Journal 1(1) 71–87 (2010)

BACK TO EARTH AND REAL BIG BUSINESS: HEAT PIPES FROM SATELLITES AND MICROCHIPS TO INDUSTRY

Carlos Augusto Arentz Pereira

PETROBRAS S. A., Av. Almte Barroso 81 32th floor, Rio de Janeiro – RJ – Brazil; caarentz@petrobras.com.br

Heat pipe research and its applications seem to be much more attached to space exploration and microelectronics than other conventional uses. Evaluating this scenario, some actual and measurable opportunities for utilization of heat pipes in industry are listed, including selection of better spots and advantages for its usage. Potential achievable gains, barriers, and some suggestions to accomplish this goal are presented.

KEY WORDS: *heat pipe, thermosyphon, energy efficiency, energy conservation, industrial usage, heat recovery*

1. INTRODUCTION

Heat pipe and thermosyphon technologies share some basic operating principles but were developed in different times, with different basic purposes, at least in the beginning.

Thermosyphon was developed at the dawn of the nineteenth century during speeding up years of Industrial Revolution. It aimed at its birth, industrial usages like steam generation and steam machines. Later, a little by chance, it moved to baking apparatus like bread and food for the military during war period. Except for some proposed applications on patents required, this development rested for many years almost without further application. Heat pipe, on the other hand, was developed in the second half of the twentieth century, based on the same principles. But it aimed to solve a specific problem, cooling metal parts exposed to Sun during space exploration. The way to promote heating transfer in zero gravity by a simple and unmanned device at a reasonable cost was enhancing thermosyphon with a porous media and

2151-7995/10/$35.00

then you got heat pipe. Miniaturization era and higher density transistors – or better microchips – also began to demand heat transfer in a similar mood. With Earth gravity, of course, but with various geometrical shapes and positions, with lesser and lesser dimensions. And again heat pipe came, saw and conquered [1].

But this history left a legate on generations of researchers. Since heat pipe became a piece so important in spacecraft as the astronauts and so vital to microcomputing as the operating system, more and more money showered over research centers and universities from enterprises eager to have "the best" and "state of art" developments. No, no exaggeration. Without heat pipes many of the so fundamental "gizmos" needed to guarantee a safe space travel would not work and without these, what astronauts are needed for? On the same fashion, without heat pipes to assure the proper working temperature for your CPU, the basic tests in your computer will not allow it to run and again, who needs Windows? Well, all that money moved a lot of teachers, students, and researchers to work around these knowledge themes. Is that really so? To check this mere impression or feeling a little test was performed with internet assistance. An Internet search tool and successive matching queries were used to answer some questions like:

a) How many times heat pipe is referred?
b) How many times it is linked to one of these previously mentioned themes – space exploration and microcomputing?
c) How many times it occurs altogether with industrial devices?
d) Which language sites it occurs?
e) Where it occurs in the World? (These last questions came as a consequence of the search.)

First it is assumed that this is not a highly scientific and broadening method for a lot of reasons and a few are listed bellow:

- Not all scientific and technical production is available on the net.
- There is a good chance that many sites are repetitions of another one or basically tell the same story.
- Also there are many sites that deal with a fairly vast range of diverse subjects and by chance totally different topics may appear correlated.
- Using terms only in English all other occurrences in equivalent terms translated will be missed – this is specially significant considering ideographic languages like Japanese, Korean, Chinese and other Far East languages.
- Some selected terms may have different meaning depending on the context.

- Internet search tools may not be as exhaustive and accurate as we might wish them to be.

But please, be kind, this is not to prove a daring scientific hypothesis; it is just to support a point of view. In order to accomplish this test two approaches were made – positive and negative – that means:

- In the positive approach, it will be searched occurrences of "heat pipe" with another significant word like "satellite" – this is to devise how many documents or pages appear with these two terms.
- In the negative approach, it will be searched occurrences of "heat pipe" without the same other significant word – this to refuse documents where both words appear.

Considering the basic search accessed on July 23, 2008, "heatpipe" or "heat pipe" appeared 3,990,000 times. Whatever approach, when the search includes or excludes a term it will produce less occurrences because it is restricting the sample. This will be interpreted as follows – if heat pipe plus a term gives a number closer to the total occurrences of heat pipe alone, more likely, they are strongly related. Also, heat pipe less the same term resulting a quantity of occurrences much lower than the original plain search for heat pipe, will also mean a strong relation between them. On the contrary, heat pipe plus the term with a low number of matches or heat pipe minus the term with a high number of matches, will mean a weak link. Using these approaches and a sequence of successive searches, a comparison among the occurrence numbers will reveal some tendencies.

The following terms were selected to make the matches with "heat pipe" and they are related to some of our main topics:

- Microelectronics – chip; computer; cooler; CPU and electronics.
- Space exploration – Satellite and space.
- General industry – boiler; condenser; exchanger; furnace; heat exchanger; industry; oven; recovery; refinery and steam.

One may notice that the list for industry has more terms than others, but this is on purpose. Results of the searches are shown in Table 1.

With all possible flaws that this method may present it is clear to see, that at least on the internet, heat pipe is much more likely associated to subjects related to microelectronics and space exploration, because:

TABLE 1: Heat pipe plus/minus other terms

Negative	Heat pipe	Positive
1,750,000	chip	480,000
1,490,000	computer	749,000
1,150,000	cooler	1,510,000
1,100,000	CPU	232,000
1,870,000	electronics	212,000
1,970,000	satellite	125,000
1,910,000	space	207,000
2,130,000	boiler	15,200
2,130,000	condenser	27,400
2,130,000	exchanger	99,400
2,130,000	furnace	13,400
2,130,000	heat exchanger	43,600
1,980,000	industry	73,300
2,130,000	oven	11,100
1,740,000	recovery	62,800
2,120,000	refinery	1,720
2,030,000	steam	38,900
As accessed July 22, 2008		

1. Positive matching results in higher occurrences with terms related to microelectronics and space than industry related terms – twice to even ten times higher.
2. Negative matching of terms related to microelectronics and space reduces more the number of occurrences than industry terms.

Even though counting with a higher chance of coincidence than the other topics – simply because more terms were listed – correlation between heat pipe and industry seems to be very poor, compared with the universe of "heat pipe" occurrences. As a matter of fact the more specific, the lower the coincidence as in case of "refinery" that appears only 1720 times together with "heat pipe" merely 0.04% of this word internet appearances.

TABLE 2: Heat pipe occurrences concerning language sites

Language	Occurrences
English	886,000
German	421,000
Czech	348,000
French	256,000
Hebrew	168,000
Polish	158,000
Hungarian	131,000
Italian	88,300
Slovakian	60,000
Romanian	47,400
Spanish	44,100
Norwegian	37,600
Russian	33,700
Portuguese	25,800
Chinese simplified or traditional	23,000

And in which languages do these people that concern about heat pipe communicate? Again, just restricting some languages over that search that gave 3,990,000 matches, the results are expressed in Table 2, where the sum of this sample adds 2,727,900 occurrences (68.4% of 3,990,000).

And also the following question came easily, where in the World people discuss heat pipe? Again just restricting countries, results in Table 3.

This inevitably takes us to some inferences. For instance, it is most likely that a researcher or technician that is interested in heat pipe technology ought to be in North America or in Europe and communicates preferentially in a language from the European origin. But, somehow supporting that previous impression; it seems that most of them are more attached to heat pipe usages in outer space and in the micro world.

But there are a lot of opportunities for heat pipe utilization, back on Earth and with the big sized things especially in the industry. That is the goal of this text, reviewing in more detail some of these ideas.

TABLE 3: Heat pipe occurrences concerning countries

Country	Occurrences	% total heat pipe	% accum.
USA	436,000	10.9	10.9
Germany	419,000	10.5	21.4
Czech Republic	333,000	8.3	29.8
France	240,000	6.0	35.8
Israel	173,000	4.3	40.1
Poland	110,000	2.8	42.9
Hungary	93,500	2.3	45.2
Italy	87,200	2.2	47.4
United Kingdom	69,800	1.7	49.2
Ukraine	55,900	1.4	50.6
Slovakia	52,900	1.3	51.9
Romania	49,700	1.2	53.1
Turkey	49,500	1.2	54.4
Canada	45,200	1.1	55.5
Norway	38,900	1.0	56.5
Finland	36,500	0.9	57.4
Austria	31,600	0.8	58.2
Netherlands	29,800	0.7	58.9
Russia	28,800	0.7	59.7
Sweden	28,200	0.7	60.4
Spain	26,000	0.7	61.0
Australia	22,600	0.6	61.6
Switzerland	16,500	0.4	62.0
China	15,500	0.4	62.4
Brazil	14,800	0.4	62.8
South Korea	14,600	0.4	63.1

2. INDUSTRIAL ENERGY DEMAND IN A BROADENING VIEW

Industry in general is a heavy energy consumer. Like an immense Carnot engine, receives tremendous amounts of energy as input, uses it as work to transform materials

and outputs almost the same amount of energy exception for the quantity that was transferred to the main product during transformation process. One small detail. This enormous energy reject is somehow degraded in some qualities that make it useless for most processes that received the initial input. And basically this reject is HEAT in a temperature too low to allow its use back in the process, but on the other hand too high to be just returned to environment. And that is where all problems lie. There is a reasonable amount of energy available that has no use at that temperature, but if you simply throw it away, it will be too costly, because of energy costs and environmental issues. Also it is not only one process, there ought to be a lot of them, scattered around, rejecting energy at different temperatures and rates.

Is there a way to try to use this energy better? Yes, there is, it is called Process Integration, uses some specific methodologies like Pinch technology. It maybe used with a daring and innovative view providing an intense integration and dependency between very diverse processes and achieving an optimized energy efficiency operation point through higher investment and low operating costs. Or it might be applied in a more conservative view, promoting more independency between processes, obtaining reasonable energy efficiency with average investments and not so low operating costs. Whatever option, it will demand in the end of design two energy flow requirements, a hot and a cold utility. Both will have to comply with processes major and minor temperatures requirements and these two will work as a kind of exchange currency of energy through all the plant. The hot utility will be usually obtained from direct fuel burning or from steam and the cold, normally water. But why water and steam?

Water is considered to be a fairly available, low cost, and harmless fluid. And steam, water with high energy content, has two amazing characteristics concerning energy flow:

- Allows heat transfer at constant temperature – this quality reduces heat exchanger area and hence reduces investment costs and also.
- Allows energy conversion from heat to work – simply provides the actual way to manage energy use.

Not forgetting to mention the possibility to obtain a precise temperature by simple pressure control, thanks to thermodynamics qualities and Mollier curve. Also, possible reuse by condensation and return to boiler, either a fired or heat recovery one and some others good characteristics that are less significant at this point. Cooling with water is a fine option because by simple atmospheric evaporation you can restore the low temperature needed to the cold utility.

Pretty good, right? The perfect medium, nontoxic, with exceptional thermodynamic properties, who could ask for more? Sorry, nothing comes for free. The adoption of a steam system and a cooling water cycle demands a lot of companions and of course costs and some misfits.

Water either for hot or cold utility requires treatment. Previous, to provide quality that guarantees proper endurance of all steel equipment involved in the process like boilers, steam pipes, exchangers, valves etc. And effluent treatment in order to prevent discharging in environment harmful and toxic materials like oils, heavy metals etc. Both kinds of treatment will demand investments in equipment, operational costs due to chemicals, personnel, materials and more energy. And maintenance. Since the population of equipment has multiplied due to all these ancillary systems, so sorry again, you will have more things to take care of, break, fix, check, refill, lubricate, paint. In addition, more spare parts, that means stocks, including physical area to keep the parts properly, personnel to take care of it and money, yes money. Spare parts are actually money in form of potential assets, but in the end of the day, they are fixed money, or worse, financial costs. It is money that is not currency anymore, but must return the same interest otherwise, the company is loosing.

And let's not skip the losses! Thermodynamics 2nd Law provides us rules about unavoidable losses in energy conversion and distribution systems. With these we include heat to atmosphere thru insulation over pipes and boiler surfaces, fuel burning, stack gas heat etc. But there are other ones you have to get used to like steam leaks, fugitive steam thru steam traps, water leaks and so forth. More maintenance, personnel, materials, controls, more money! And to increase the mess, take all these aspects together bringing hazard to working environment. Steam leaks are noisy and potentially harmful. More equipment in the facility, more maintenance, more chances of an eventual accident. Handling chemicals, that many times are poisons or carcinogenic also does not help, either.

Quite a complicated world! But what are the numbers involved and where do heat pipes fit on this mess? One thing after the other. First the numbers.

Process heating accounts for about 36% of the total energy used in industrial manufacturing applications, while steam systems account for other 30%. These figures vary depending on the specific industry and process. Figure 1 shows a schematic view of U.S. Manufacturing Industry Energy Balance as a whole by 2004.

This picture shows that U.S. manufacturing industry uses 44% of its energy requirements in core process and 20% goes to steam, while a significant amount is recycled as heat and goes to losses that maybe reach 30% of total input. Taking a closer look at these losses in Figs. 2 and 3, it is clear to see that the share of usual

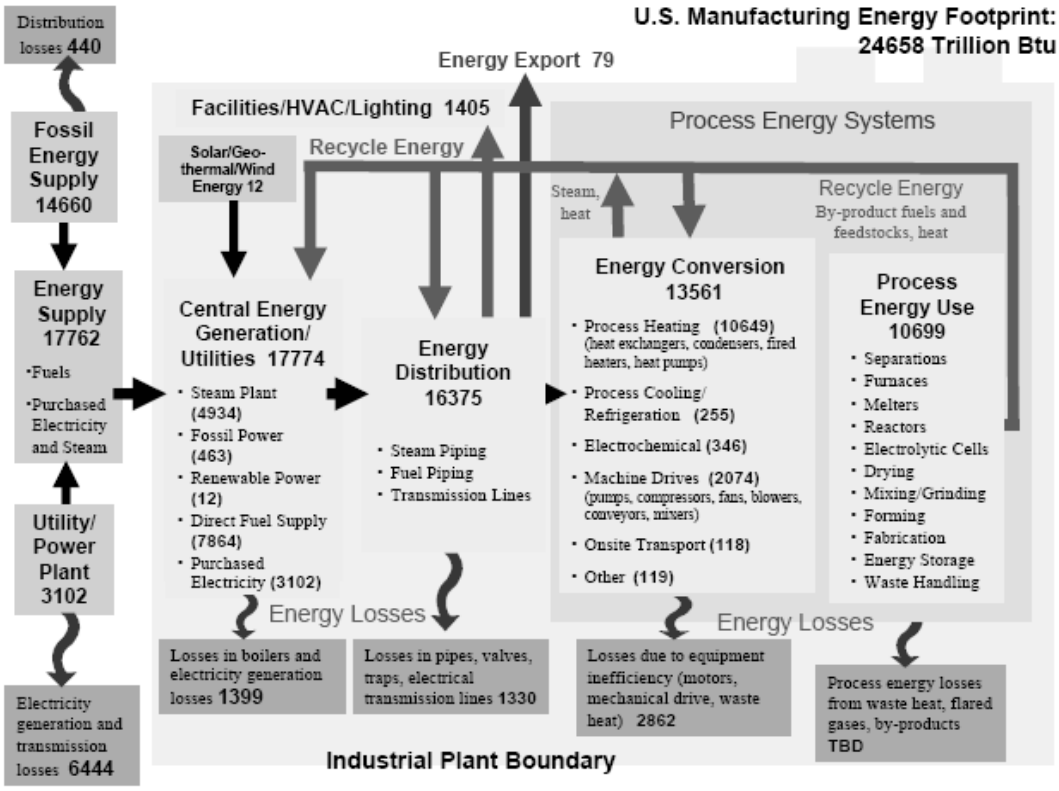

FIG. 1: U.S. manufacturing energy footprint [2]

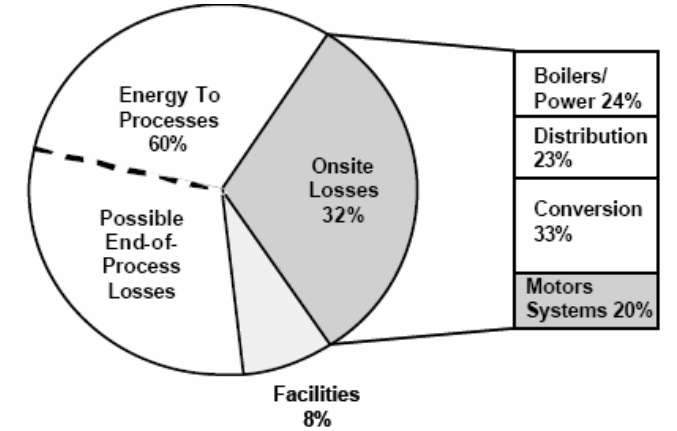

FIG. 2: Onsite energy loss profile for U.S. manufacturing and mining sector [2]

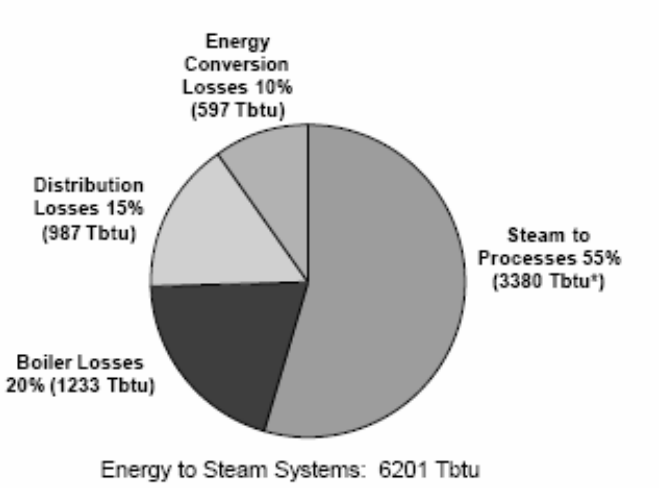

FIG. 3: Steam use and losses in manufacturing and mining [2]

losses over heat and steam is highly significant. On site losses with energy conversion and distribution may go up to 26% of total energy demand while losses due to steam system generation and distribution can add to 45% of the energy dedicated to this purpose.

So there are opportunities to make these systems more efficient throughout industry that could reduce annual plant energy costs by several billion dollars or euros. And since heat and consequently steam are produced by fuel burning correspondent environmental emissions of millions of metric tons of CO_2 could be avoided.

So much for the numbers, but what is there for heat pipe application?

3. POTENTIAL INDUSTRIAL HEAT PIPE APPLICATIONS

Back to basic design assumptions on heat pipes, they were a way to promote heating transfer by a simple and unmanned device at a reasonable cost. Heat pipes should be applied in the industry with this same approach. Well-designed heat pipes can provide heat transfer without many of the regular ancillary systems and misfits that energy distribution systems like steam bring together. For instance, since all necessary fluid to perform heat transferring process is confined inside the heat pipe itself, no previous treatment or effluent treatment will be demanded. Without that, you can count out some chemicals, personnel, materials, and energy, which means lower operational costs. In the specific case of steam, since there will be less steam circulat-

ing, it is likely that somewhere in the plant less fuel will be burned and again less atmospheric emissions. Less steam, fewer steam pipes, valves, steam traps, insulation, steam leaks, less losses, and less hazards. Therefore, less heat going in implies less heat out, so cooling systems maybe diminished. Fewer equipment, less maintenance, fewer spare parts. This leads to lower investments and even lower operational costs.

Figure 4 shows a generic process heating system and from that, it is concluded that main potential applications for heat pipe technology lie in heat transfer from combustion to process and waste heat recovery. Besides steam, there are some others.

Therefore, one great opportunity for heat pipe usage in the industry is to replace steam and water-cooling system. There are some advantages and disadvantages on this possibility:

Advantages:

- Reduced maintenance, labor, materials (chemicals and spare parts) costs.
- Reduced stock costs (spare parts and chemicals).
- Increased worker safety (reduced noise levels and hazard risks).

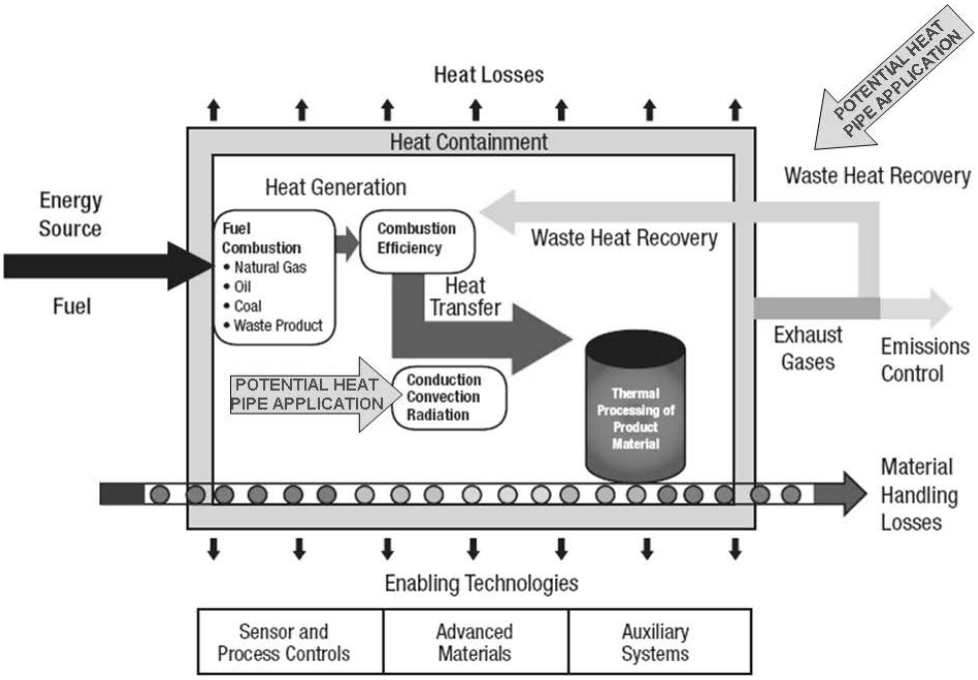

FIG. 4: Process heating system and opportunities for heat pipes. Adapted from [3]

- Reduced waste water output.
- Reduced CO, CO_2, NO_X, SO_X emissions.
- Increased energy efficiency (less conversion processes).

Disadvantages:

- Increased energy dependence between different processes.
- Usually heat pipe is not considered in basic projects design.
- Equipment usually not available ready to buy (tailor made).
- Lack of experience and reliability on heat pipe equipment in industrial operations.

It is important to remember that scarcely a basic design will totally disregard steam use, because it has many other general applications in industry [4]:

- Stripping.
- Fractionation.
- Power generation.
- Mechanical drive.
- Quenching.
- Dilution.
- Vacuum draw.

Only steam for process heating is subject of substitution by heat pipe, provide there is a heat source on the process itself, with adequate characteristics namely available and required temperatures. Among these, considering some specific equipment and processes, there are many different temperatures range available in industry only regarding wasted heat as Table 4.

There are many opportunities on heat recovery on the industry. Actually, the World still lacks an adequate technology for efficient use of excess energy, especially low-grade waste heat. And all achievable savings from improvements are available to be obtained by appropriate heat pipe usage even altogether with steam system. Some examples adapted from [3–6]:

- Blowdown heat recovery can reduce boiler fuel use by 2 to 5%.
- Every 25^{o}C reduction in net stack temperature is estimated to save 1 to 2% of boiler fuel use.
- Direct contact condensation heat recovery can save 8 to 20% of boiler fuel use, but costs may be relatively high.

TABLE 4: Typical waste heat at diverse temperature range from various sources

Types of device	Temperature, ^{o}C	
	Minimum	**Maximum**
Nickel refining furnace	1370	1650
Aluminum refining furnace	650	760
Zinc refining furnace	760	1100
Copper refining furnace	760	815
Steel heating furnaces	925	1050
Copper reverberatory furnace	900	1100
Open hearth furnace	650	700
Cement kiln (Dry process)	620	730
Glass melting furnace	1000	1550
Hydrogen plants	650	1000
Solid waste incinerators	650	1000
Process heaters	650	1450
Steam boiler exhausts	230	480
Gas turbine exhausts	370	540
Reciprocating engine exhausts	315	600
Heat treating furnaces	425	650
Drying and baking ovens	230	600
Catalytic crackers	425	650
Process steam condensate	55	88
Air compressors	27	50
Pumps	27	88
Internal combustion engines	66	120
Air conditioning/refrigeration condensers	32	43
Liquid still condensers	32	88
Drying, baking and curing ovens	93	230
Hot processed liquids	32	232
Hot processed solids	93	232
Adapted from reference [4]		

- For every 6^{o}C that the entering feed water temperature is increased, boiler fuel use is reduced by 1%.
- Reduce heat loss from condensate in a steam system can save over 1% of facility total energy use.
- Recovering waste heat through a recuperator can reduce kiln energy use by up to 30%; regenerators can save up to 50%.
- Recovering waste heat from furnaces, ovens, kilns, and other equipment can save 5% of typical facility total energy use.
- Recovering waste heat can reduce typical facility total energy use by about 5%.
- Preheating furnace combustion air with recovered waste heat can save up to 50% of furnace energy use.
- Recovering flue gas waste heat to preheat boiler feedwater can reduce boiler fuel use by up to 5%.
- Reusing heat in cascade within the diverse processes can reduce over 5% of facility total energy use.

More options can be considered also by combination with other technologies like heat pumps and organic fluids Rankine cycles:

- Recycle heat condensation energy from top of distillation columns to bottom reboiler.
- Use energy outlet from gas turbines to cool air input and obtain higher efficiencies.
- Use low heat outlet from processes to produce small-scale power to move pumps and compressors within the same plant.

Nowadays many industrial and commercial applications for heat pipe are already in course. Data from the Institute of Heat Pipe Technology, Nanjing University of Technology states that there were more than 370 different equipment by 2002, being used in industrial applications in China [7]. In that country also, even significant long distance closed loop thermosyphons are already in use to promote heat transfer between processes 50 meters away from each other. Other day-by-day larger size applications also begin to become more common like energy saving in air conditioning and dehumidification systems [8], industrial heat exchangers [9] and energy distribution uses [10].

Everything seems so shining bright! Isn't something missing? Yes, comparative investment costs. Just supposing that investment costs on the main equipment of a steam system match in cost all needed investment on an equivalent heat pipe network to do the same task is a too big simplification. It must be taken in account that this

move from micro to macro heat pipes will demand a big step for heat pipe technology. Changing from micro to meters will imply in bigger flow rates, distances and pressure drops. Nevertheless, some technical and non-technical barriers must be taken in equation as:

- Distance from heat source to heat sink related to entrainment and capillary limits inside heat pipe.
- Heat transfer rates related to sonic and boiling limits in heat pipe.
- Lack of technical and commercial reputation to be considered as a project option.
- Prejudice on investors and operators side to be considered actually applicable and reliable.

4. CONCLUSIONS

Enhancing heat recovery ought to be an important part of any company strategy for accomplishing lower costs, higher overall efficiency and environmental goals. Heat recovery is in fact a renewable and pollution-free energy. It can be used for heating, cooling, humidity control and power. This is where much room for heat pipe application in the industry lies.

This technology most be presented as more efficient, reliable and capable of using a variety of energy sources than other options. Including integration with low-temperature waste heat, cogeneration and conventional heating and cooling systems, some points must be addressed as key advantages on using heat pipes:

- Attach to existing investments – it can be adapted to existing assets and improve their efficiency.
- Add shareholder value – it can be measured in terms of avoided operational and investment costs reduction obtained by its application, altogether with a sustainability image.
- Improve worker comfort and safety – since it reduces or avoids usage of more equipment, chemicals, fuels and demands less maintenance it can reduce working hazards.
- Environmental friendly – again less chemicals and fuels, it can reduce direct and indirect impacts to environment.
- Improved reliability and capacity utilization – it can reduce downtimes through reduced maintenance frequency, improve productivity and be easily and quickly, scaled and designed to fit processes demands.

How to accomplish these aspects? Attracting and working together with the industry seems to be a decisive approach. Some other steps are suggested:

- Access and conduct technical audits of energy recovery opportunities, related costs and losses over the industry, especially potential sources, uses and costs of waste heat.
- Create partnership with industries that have bigger potential return over heat pipe advantages, to access data and investments opportunities for research and application.
- Create demonstration sites in various industrial applications to measure and quantify energy, comfort, productivity, health, safety and environmental benefits of heat pipe usage.
- Promote educational programs and communication about heat pipe technologies common applications for architects, engineers, the public, service technicians and investors in order to spread its potential use.

Nowadays, energy conservation and energy efficiency have gained a greater importance concerning environment and specially greenhouse gases emissions reduction. However, economics is still a major issue. Heat pipe can be an alternative weapon on this battle, providing all energy savings and same by products other technologies produce. But since it proves its availability, reliability and compared cost effectiveness, it can occupy a significant share of heat transfer and waste heat recovery in general industry.

REFERENCES

1. Pereira, C. A. A., Heat pipe – A brief history and a future application view, *Proc. 14th Int. Heat Pipe Conf. (14th IHPC)*, Florianópolis, Brazil, pp. 13–21, 2007.
2. U.S. Department of Energy, Office of Energy, Efficiency and Renewable Energy. Industrial Technologies Program *Energy Use, Loss and Opportunities Analysis: U.S. Manufacturing & Mining,* prepared by Energetics, Incorporated and E3M, Incorporated, December 2004.
3. U.S. Department of Energy, Office of Energy, Efficiency and Renewable Energy. *Improving Process Heating System Performance: A Sourcebook for Industry*, prepared by Lawrence Berkeley National Laboratory, Washington, DC, 2nd ed., 2007.
4. http://www.em-ea.org/Guide%20Books/book-2/2.8 Waste Heat Recovery.pdf Accessed Jul 23, 2008.
5. U.S. Environmental Protection Agency, *Climate Wise: Wise Rules for Industrial Efficiency*, EPA 231-R-98-014, July 1998.
6. U.S. Department of Energy, Office of Energy, Efficiency and Renewable Energy. *Steam System Opportunity Assessment for the Pulp and Paper, Chemical Manufacturing, and Petroleum Refining Industries*, prepared by Research Dynamics Corporation, October 2002.

7. Zhang, H. and Zhuang, J., Research, development and industrial application of heat pipe technology in China, *Appl. Thermal Eng*., 23:1067–1083, 2003.
8. Firouzfar, E. and Attaran, M., A review of heat pipe heat exchangers activity in Asia, *Proc. World Acad. Sci. Eng. Technol.*, 30, July 2008.
9. Noie, S. H., Lofti, M., and Sghatoleslami, N., Energy conservation by waste heat recovery in industry using thermosyphon heat exchangers, *Iranian J. Sci. Technol., Trans. B,* 28(B6):707–712.
10. Angelo, W., Mantelli, M. H., and Milanez, F. H., Design of a heater for natural gas stations assisted by two-phase loop thermosyphon, *Proc. 14th Int. Heat Pipe Conf. (14th IHPC)*, Florianópolis, Brazil, pp. 386–391, 2007.

Heat Pipe Science and Technology, *An International Journal* 1(1) 89–98 (2010)

REVIEW OF THE CURRENT CONDITIONS FOR THE APPLICATION OF HEAT PIPES (THERMOSYPHONS) TO STABILIZE THE TEMPERATURE OF SOIL BASES UNDER FACILITIES IN THE FAR NORTH

A. P. Popov, S. L. Vaaz, & A. A. Usachev[*]

Public Corporation "VNIPIgazdobycha", Saratov, Russia

[*]Address all correspondence to A. A. Usachev
E-mail: UsachevAA@vnipigaz.gazprom.ru

The article provides a review of the current state of application of seasonal cooling devices for the Northern facilities' construction. Layout diagrams of the devices in the structures of bases and foundations of buildings and constructions are provided. Comparison of thermal fields of soil bases is given by an example of design modeling. Description of the main types and structures of cooling devices is also given in the article.

KEY WORDS: *termosyphons, seasonal cooling devices, permafrost, soil base*

The permafrost zone covers a considerable part of the Russian territory, mainly its northern and eastern regions. The larger part of gas and oil fields are located in this territory. Construction and development of the fields is going on under permafrost conditions. The experience in the construction and operation of engineering structures shows that their reliability can be provided only in the case of proper account for the thermal and mechanical interface between the structure foundations and soil bases. One of the methods to provide for the reliability of buildings is the maintenance of soil bases in frozen conditions. The reliability of buildings and structures in permafrost areas depends primarily on the strength and stability of soil bases. The mechanical and strain properties of soil bases are greatly dependent on the temperature and liquid limit of soil. Under the influence of "dangerous" geological processes of natu-

2151-7995/10/$35.00

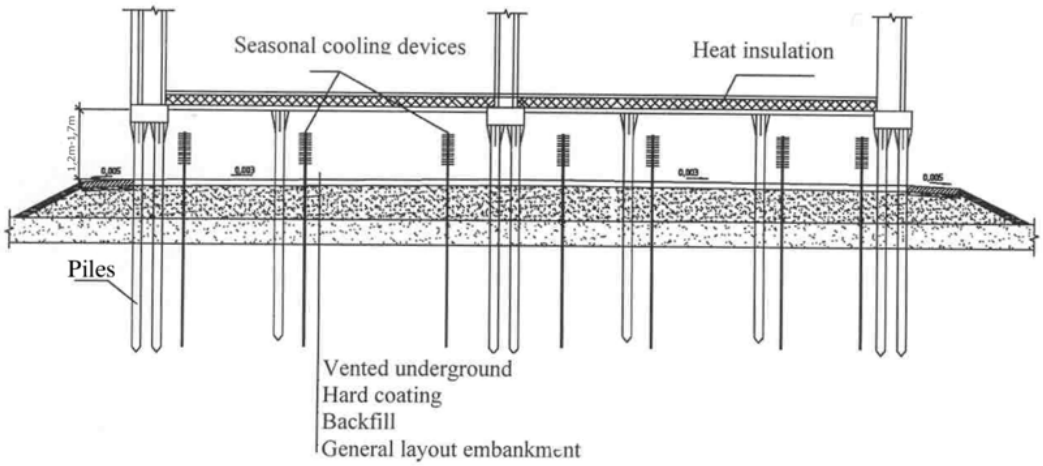

FIG. 1: Schematic diagram of vented underground construction with vertical seasonal cooling devices

ral and technogenic kind, the temperature and liquid limit of bottom soil may vary significantly. Beginning from the end of 1990s, seasonal cooling devices came to be commonly used for maintaining frozen conditions in the soil bases of buildings and structures. The construction of the Yubileinoye field facilities marked the beginning of mass introduction of these devices. By now seasonal cooling devices are widely used in construction of gas industry facilities in permafrost areas.

The use of cooling devices ensures the reliability of facilities in subsiding (while thawing) and low bearing capacity of permafrost soils. Cooling by seasonal cooling devices forms icy soil mass that ensures the bearing capacity of foundations in one or more cycles of winter cooling. The temperature of the soil mass continues to decrease further. Modern designing of bases and foundations is associated with optimization of the construction of foundation (depth, diameters of piles) and with the measures taken to strengthen soils "thermally". Artificial freezing (cooling) of soil makes it possible to raise the bearing capacity of soil bases and therefore simplify the construction and "zero-cycle" construction process. And in a number of cases it allows one to reduce the construction period, consumption of materials, as well as cost of construction. The main technical solution for the construction of foundations in permafrost is application of vented underground, where seasonal cooling devices are installed (Fig. 1).

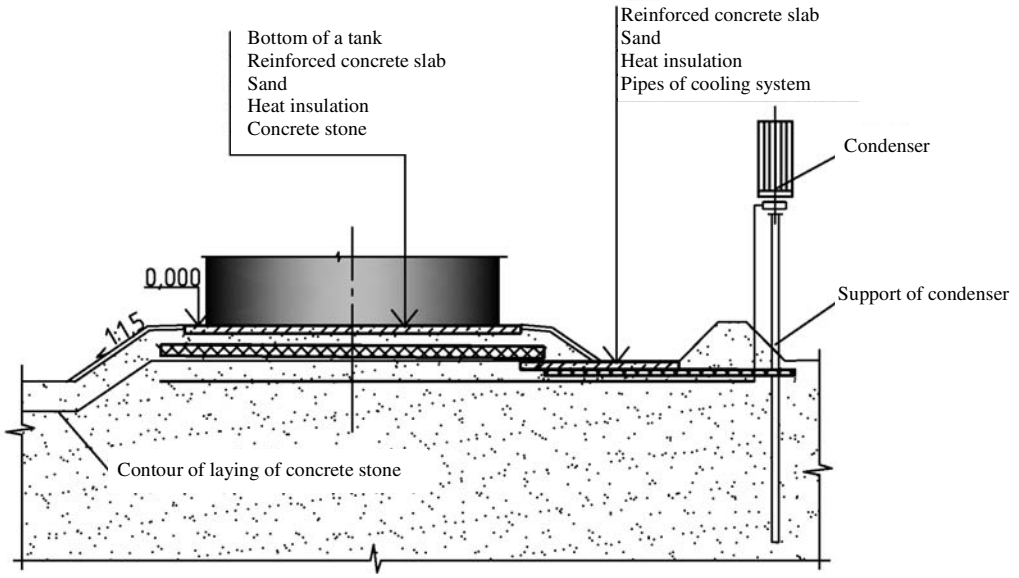

FIG. 2: Schematic diagram of construction of a structure with flooring at the ground level using heat insulation and horizontal seasonal cooling devices

In the cases where it is reasonable to construct a foundation of "flooring at the ground level" type, a combination of cooling systems with heat-insulating screens is used (Fig. 2).

A comparison of the results of modeling of the thermal field of soil bases of foundations with seasonal cooling devices and without them is given below in Figs. 3 and 4, respectively.

Cooling devices are used for construction of northern facilities with the aim to:

- preconstruct the freezing of soilbases of buildings and structures;
- freeze soil bases in the process of construction and operation;
- decrease the thermal effect of buildings and structures on soil bases in the process of operation;
- restore frozen conditions of soil in the bases of buildings and structures that were built according to the first principle;
- create cutoff curtains;
- create frozen (thermal) curtains.

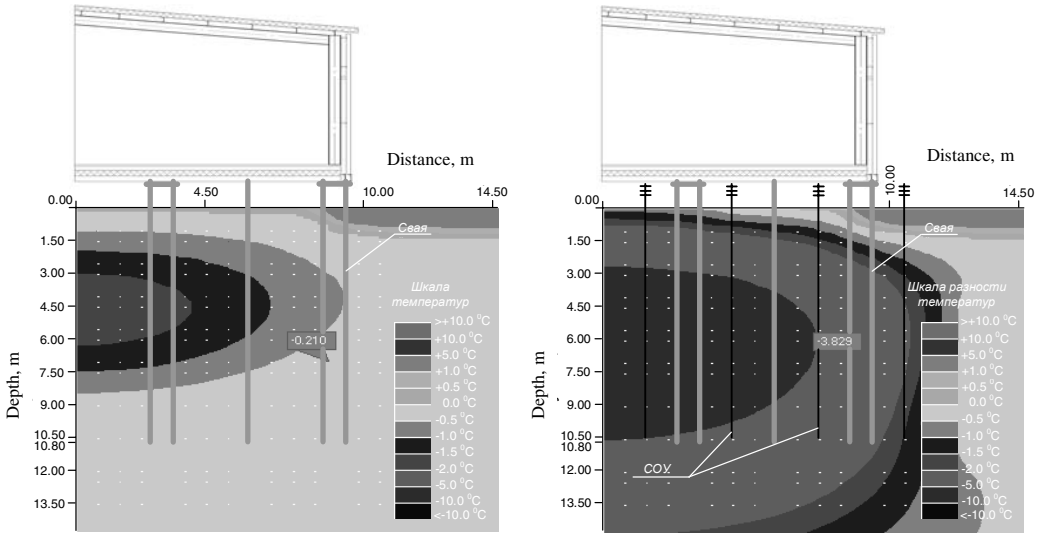

FIG. 3: Results of modeling a thermal field in the base of a building with vented underground without seasonal cooling devices (a) and with installed seasonal cooling devices (b)

Cooling devices with a heat carrier moving within the field of gravity, i.e., thermosyphons, are used in the construction of facilities in the north. From the point of view of their functionality, seasonal cooling devices are "thermal diodes" that conduct "cold" during a cold period and do not conduct "heat" during a warm period. Differences in practical application and specific features of seasonal cooling devices led to a variety of structures, as well as type and size of stabilizers according to the above-mentioned variants of application. The following categories of devices can be pointed out:

- seasonally acting vertical cooling devices;
- seasonally acting horizontal (low-inclined) cooling devices;
- year-round acting cooling devices;
- seasonally/year-round acting cooling systems.

Vertical cooling devices are used for cooling the soil under buildings with vented undergrounds (Fig. 5), or along the contour of a structure, or at supports of pipeline racks. The model of a seasonal cooling device with a double V-type condenser (Fig. 6) is used for structures with vented underground that are less than 1 meter in height

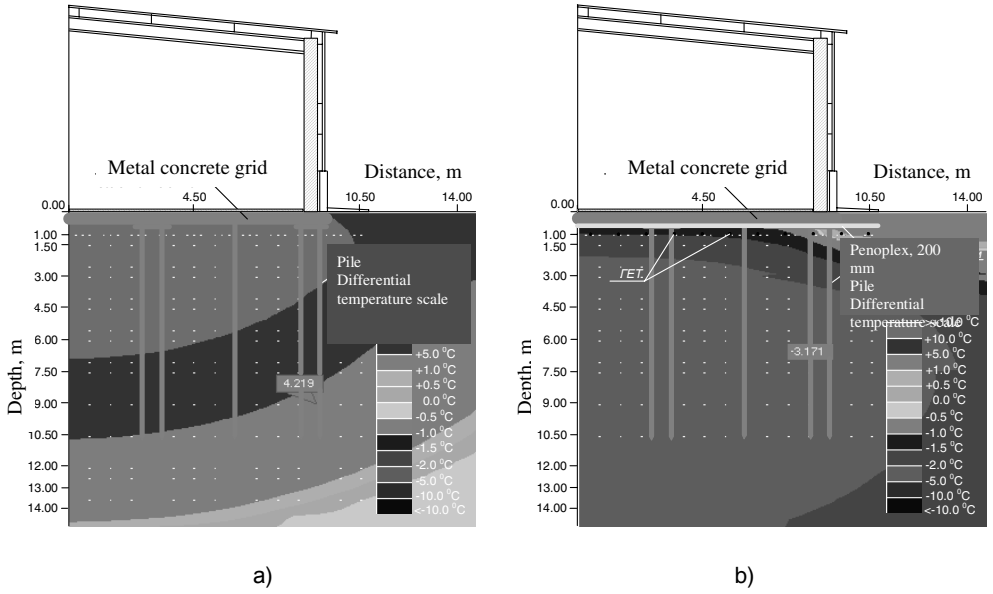

FIG. 4: Results of modeling a thermal field in the base of a building with flooring at the ground level without seasonal cooling devices (a) and with installed seasonal cooling devices (b)

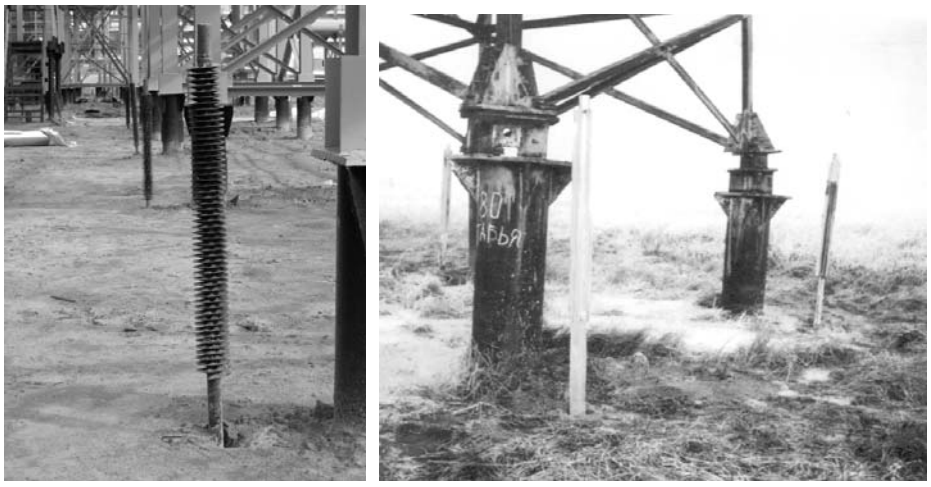

FIG. 5: Seasonal cooling devices with one vertical condenser

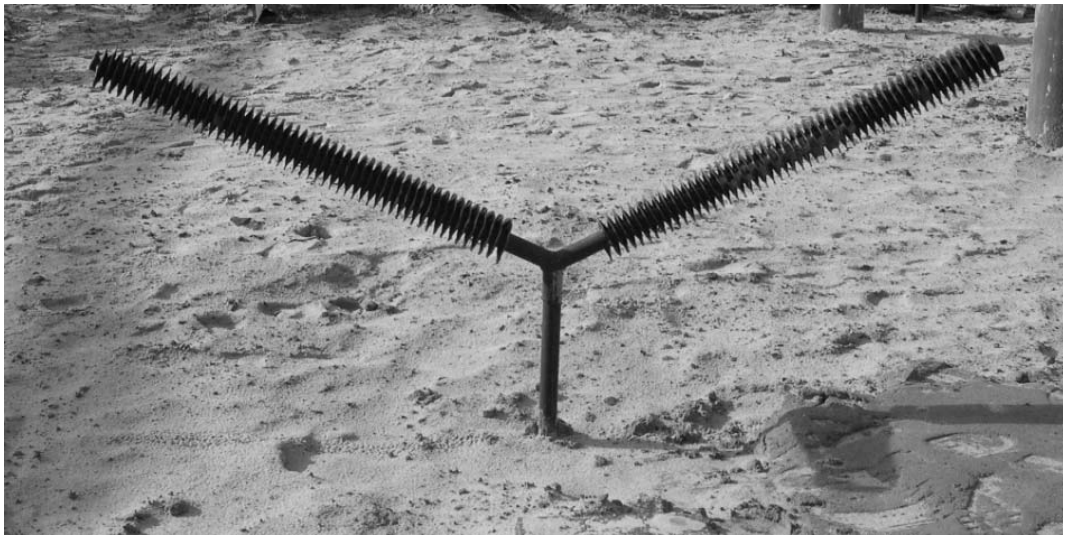

FIG. 6: Seasonal cooling device with a double V-type condenser

and increase the cooling efficiency. The structure of a number of cooling devices implies flexible connections, which, due to metal hoses, allow for their installation in vented underground, under site structures, etc., as well as carryover of a thermal stabilizer beyond the facility boundaries (Fig. 7).

Thermal stabilizers with an evaporator having a bend angle of 3–5^{o} in the direction og the vertical surface were developed for thermal stabilization of soil under structures with no vented underground, for example, under tanks. Thus, it is possible to locate an evaporator under a structure, leaving a condenser beyond the contour (Fig. 8).

The structures of year-round acting cooling devices are used in those cases where it is necessary to generate cooling or freezing of soils in a warm period according to construction conditions or facilities operation. Year-round acting cooling devices are equipped with different types of refrigerating machines (refrigerating units, thermoelectric coolers) and condensers with ribbed part for device operation as seasonal cooling at air temperatures below zero. Different structures of year-round acting cooling devices are shown in Fig. 9.

Cooling systems with natural cooling agent circulation are used for developing the structures. Pressure and direct flow of a cooling agent is organized in the under-

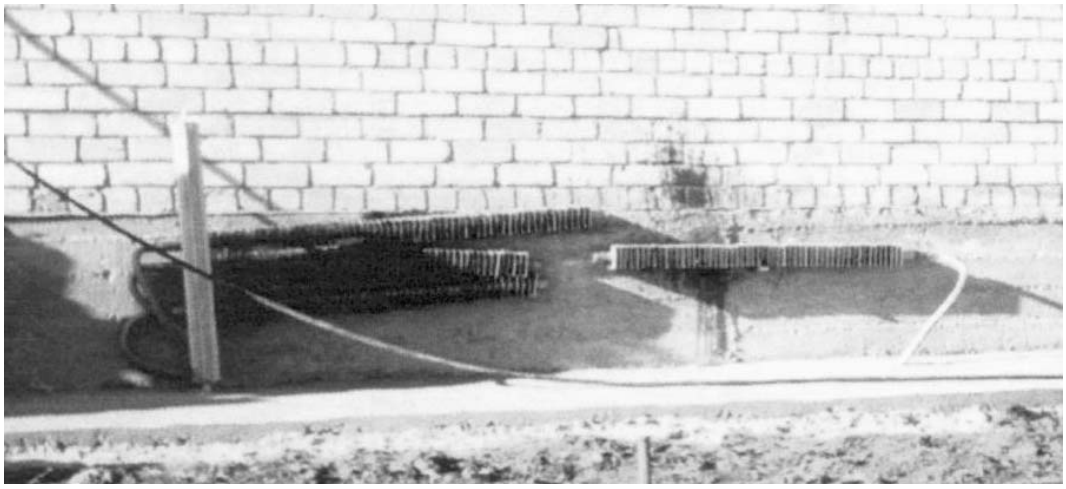

FIG. 7: Seasonal cooling device with flexible connection

FIG. 8: Seasonal cooling devices of horizontal type

a) b) c)

FIG. 9: Structures of year-round acting cooling devices: a) with thermoelectric cooler; b) with replaceable condensate part; c) with refrigerating units

ground profile. Such a structure allows for increasing the length of underground heat exchanger up to several hundred meters. These systems (Fig. 10) consist of cooling pipes, connection pipes, condensate block, and a hydraulic lock. The condensate block is an air-cooling device, the hydraulic lock is meant for providing unit-direction motion of a heat carrying agent in the system. The cooling and connection pipes are used for cooling the agent in circulation. Horizontal cooling pipes are made of steel or polyethylene pipes. Cooling systems operate in a cold period, and it is also possible to connect mobile compressor–condenser units to them with the purpose of forcing cooling agent circulation, if required.

Subsurface seasonal cooling devices are used for freezing and thermal stabilization of the soils of dams, gas producing wellheads, and other structures (Fig. 11). A subsurface cooling device is a waterproof one-piece welded structure, filled with a cooling agent, and having the depth of an underground part of up to 100 m.

Apparently, the existing structures of seasonal cooling devices solve the main part of the problems connected with the construction of bases and foundations, but still

a) b)

FIG. 10: Cooling systems: a) condensers; b) laying of horizontal cooling profile

FIG. 11: Application of subsurface seasonal cooling devices for creating cutoff curtains

there is a number of requirements to be observed while creating new perspective structures, that is:

- increase of the efficiency of seasonal cooling devices;
- application of a safe heat carrier;
- increase in the performance of seasonal cooling devices during the period of facility construction.

Vapor–liquid cooling devices are the most effective seasonal cooling devices, since they provide higher intensity of inner heat exchange processes. However, in the complicated process of heat exchange from soil to atmosphere, the processes of heat transfer to air and heat conduction in soil mass are the limiting ones. The intensity of inner heat transfer of a vapor–liquid device is not determinative, and different types of vapor–liquid heat carriers become competitive. Extension of the period of operation of seasonal cooling devices is associated with the terms of starting the operation of seasonal cooling devices. It should be set up that seasonal cooling devices start to operate while thawing in winter, as well as in autumn and spring months during night hours when air temperature is below zero.

Different process liquids can be used as heat carriers of cooling devices; in practice, freons are usually used, such as R22 (difluorochloromethane), R717 (ammonia), and R744 (hydrocarbon). A proper process liquid is selected mainly on the basis of the range of steam space operation temperatures. There are several acceptable process liquids for a certain temperature range.

Designing requirements testify to the fact that an efficient operation of seasonal cooling devices is necessary for preconstruction preparation of soils and for the first years of facility operation. Small number of cooling devices is necessary for maintaining the required temperature during further operation of the structure. It defines application of cooling devices of year-round acting type or development of the methods of seasonal cooling devices extraction from soil, as well as their reuse.

Heat Pipe Science and Technology, An International Journal 1(1) 99–112 (2010)

MODELING OF TRANSFER IN THE MICROREGION IN AXIALLY GROOVED HEAT PIPES. COMPARISON OF FLUID PERFORMANCES

R. Bertossi,[1*] V. Ayel,[1] C. Romestant,[1] Y. Bertin,[1] & Z. Lataoui[2]

[1]*CNRS – Institut Prime-Université de Poitiers – ENSMA UPR 3346, Département Fluides, Thermique, Combustion, 1, avenue Clément Ader BP 40109, 86961 FUTUROSCOPE CHASSENEUIL Cedex*
[2]*Laboratoire d'Etudes des Systémes Thermiques et Energétiques, 5019 Monastir, Tunisie*

[*]Address all correspondence to R. Bertossi
E-mail: remi.bertossi@let.ensma.fr

Axially grooved heat pipes are the devices mainly used to dissipate the heat flow arising due to latent heat of fluid phase change at the state of saturation. Part of the heat injected at the evaporator flows through a microregion where a meniscus remains hung at the top of each groove. This paper presents a 1D steady-state model constructed to study the heat and mass transfers in this zone. It allows one to show an important result concerning the respective behavior of the meniscus in the microregion and in the macroscopic one. Then, the paper compares the performances of various metal/fluid couples relative to the flux evacuated through the microregion and contact angle. Thus, the present study completes the characterization of the microregion and will directly participate in the heat pipe design improvement.

KEY WORDS: *microregion, evaporation, meniscus, fluid performances, heat pipe*

NOMENCLATURE

A	dispersion constant, J	$\hat{\sigma}$	accommodation coefficient, –
b	groove width, m	χ	nondimensioned abscissa, m
h	latent heat enthalpy, $J \cdot kg^{-1}$	**Subscripts**	
P	pressure, Pa	c	capillary
$\dot{q}_e$	heat-flux density, $W \cdot m^{-2}$	d	disjunction
Q	heat flux, $W \cdot m^{-1}$	in	input
R	curvature radius at the liquid/vapor interface, m	l	liquid
r_g	gas constant, $J \cdot kg^{-1} \cdot K^{-1}$	lv	liquid–vapor
T	temperature, K	max	maximal
x, y	coordinate, m	min	minimal
z	longitudinal coordinate, m	mic	microscopic
Greek symbols		sat	saturation
δ	liquid film thickness, m	v	vapor
λ	thermal conductivity, $W \cdot m^{-1} \cdot K^{-1}$	w	wall
μ	dynamic viscosity, Pa·s	0	initial conditions
ρ	density, $kg \cdot m^{-3}$	^	nondimensional quantities
σ	liquid/vapor surface tension, $N \cdot m^{-1}$	′	derivative with respect to

1. INTRODUCTION

Grooved heat pipes are the closed devices permitting the transfer of heat from hot sources to cold ones by using the liquid–vapor change-of-phase at the state of saturation of a fluid. At the hot source, heat is removed by evaporation of the working fluid, thus increasing the pressure of vapor; this increase leads to the vapor flow from the evaporator to the condenser where the vapor undergoes condensation. The liquid formed can return into the evaporator by capillary pumping generated by the surface tension forces at the liquid/vapor interface. According to the Young–Laplace formula, the capillary pressure between the liquid and vapor phases can be written in the case of grooved heat pipe as: $\Delta P_c = \sigma / R_c$. All along the heat pipe, the curvature of the meniscus adjusts itself to counterbalance the pressure losses in the liquid and vapor phases. Thus, on each z coordinate along the groove (Fig. 1) one has:

$$\Delta P_c(z) = P_v(z) - P_l(z)$$

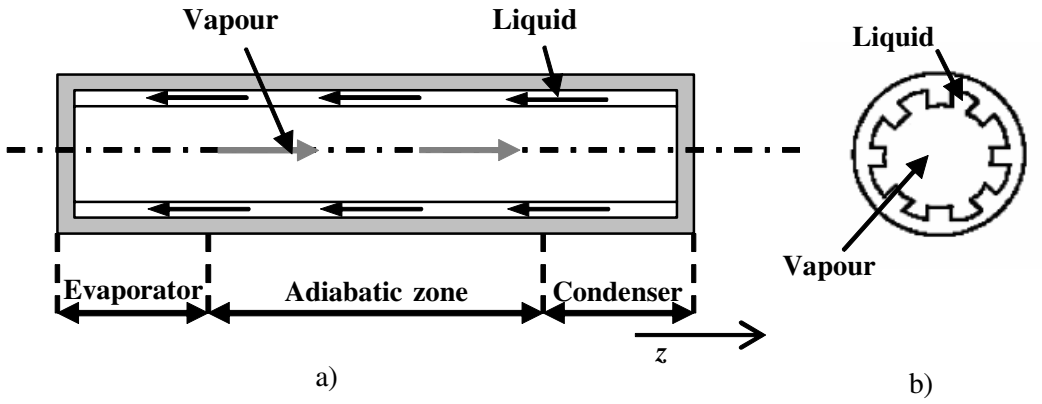

FIG. 1: Axial grooved heat pipe: a) longitudinal section; b) transversal section

The present paper, focused on the evaporation zone, studies more precisely the zone where the meniscus remains attached at the top of the grooves as shown in Fig. 2a. Stephan and Busse [1] showed that evaporation mainly takes place in this zone called a microregion for the systems characterized by a strong contrast between the wall and liquid thermal conductivities. Indeed, as the latter is low compared to the former, the heat flux will be mostly evacuated into the microregion where the liquid thickness is the lowest. While the modeling of the microregion by Stephan and Busse [2] was already used in [3, 4], the present paper focuses on original physical interpretations of the main results obtained by different parametric studies still nonexisting. The results are linked to specific applications, restricted here to aluminum/ammonia heat pipes.

First, the microregion and different physical mechanisms which interfere in transfer will be precisely described; then the model will be presented, and the influence of the value of the macroscopic radius of the meniscus on the transfers occurring in the microregion will be discussed after the validation of the calculations presented here by comparing them with the results obtained by Stephan and Busse [1, 2]. Finally, the performances of three metal/fluid couples, in terms of the flux transferred Q_{mic} and contact angle θ, will be compared. The analysis of these results will serve as a basis for better understanding of the microregion characterization.

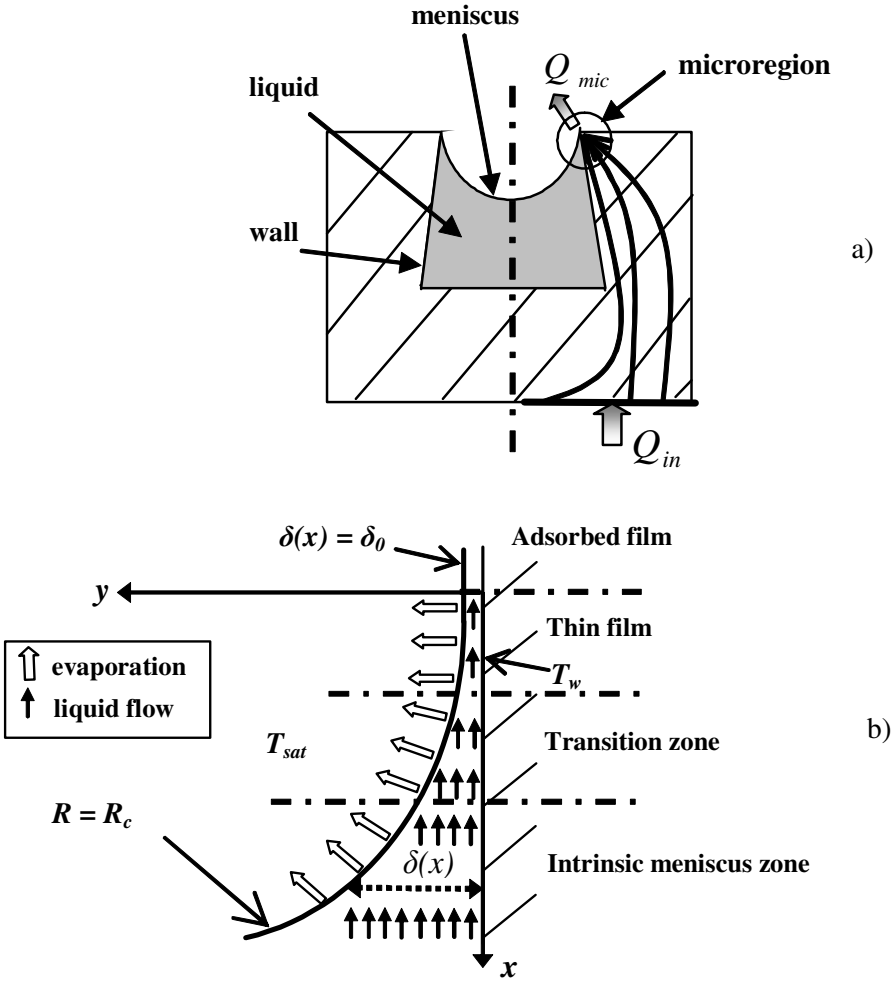

FIG. 2: Heat transfer in a trapezoidal groove section: (a) heat conduction through the solid wall; (b) heat and mass transfer in the microregion

2. THE MICROREGION

As shown in Fig. 2b, in the section of a groove, the microregion is a very little part of the global meniscus. Indeed, it is located between the adsorbed film, where the liquid thickness is very low and remains constant, due to the absence of heat flow inside, and the intrinsic meniscus zone corresponding to a constant radius of curvature.

On the one hand, in the adsorbed film, where there is no transfer, intermolecular interactions between the wall and the liquid/vapor interface dominate. They correspond to the disjunction pressure. Typically, for nonpolar molecules, one has the relation

$$P_d = -\frac{A}{\delta^3} \tag{1}$$

where P_d is the disjunction pressure and A is the dispersion constant.

On the other hand, intermolecular forces are negligible in the intrinsic meniscus zone where the curvature becomes constant. In this zone, the liquid is too thick to be influenced by the liquid-solid interactions. It is mainly governed by the capillary forces (the Young–Laplace formula). Between these two zones, in the microregion, one has to take into account both the intermolecular and capillary forces [2, 5]:

$$\Delta P_c = \frac{A}{\delta^3} + \frac{\sigma}{R_c} = -P_d + \frac{\sigma}{R_c} \tag{2}$$

One can also notice that, in the very first part of the microregion (thin film), the capillary forces are negligible compared to the intermolecular forces due to the very low curvature at the beginning of the increasing liquid thickness.

3. DESCRIPTION OF THE MODEL

The steady-state model developed here was previously studied by Wayner et al. [6, 7] and particularly used by Stephan and Busse [1, 2]. This model permits one to study the main physical phenomena in the very little zone located between the adsorbed film and intrinsic meniscus zone.

3.1 Hypotheses

The hypotheses for the liquid phase are:

- a constant liquid pressure P_l across a groove;
- a laminar, incompressible and two-dimensional liquid flow parallel to the wall (Fig. 2b);
- neglected gravity effects;

- thea liquid velocity equal to zero at the wall and viscous stresses equal to zero at the liquid/vapor interface.

The hypotheses for the vapor phase are:

- a constant vapor pressure P_v;
- an isothermal saturated vapor (($T_v = T_{sat}(P_v)$);
- negligible inertial effects of the vapor dynamic pressure term $1/2\rho_v u_v^2$, perpendicular to the liquid/vapor interface, compared to $\Delta P_c(x)$: for example, for T_{sat} = 303.15 K, T_w = 304.15 K and for x = 1 μm (a typical abscissa of the microregion), one has: $1/2\rho_v u_v^2 = 9.9 \times 10^{-2}$ Pa, whereas $\Delta P_c(x = 1\ \mu m) = 128$ Pa.

Concerning heat transfer through the microregion, several hypotheses have to be taken into account:

- a constant wall temperature T_w [5, 8];
- a temperature of the liquid/vapor interface T_{lv} given by Eq. (3) [6]:

$$T_{lv} = T_{sat}\left(1 + \frac{\Delta P_c}{\rho_l h_{lv}}\right). \tag{3}$$

- 1D heat conduction in the liquid film along the y axis and evaporation at the liquid/vapor interface, perpendicular to the liquid flow;
- evaporation heat coefficient calculated according to the Maxwell–Boltzmann statistics [9].

Thus, the heat-flux density in the microregion is given by Eq. (4):

$$\dot{q}_e(x) = \frac{T_w - T_{lv}}{\dfrac{\delta(x)}{\lambda_l} + \dfrac{2-\hat{\sigma}}{2\hat{\sigma}}\dfrac{\sqrt{2\pi r_g T_{sat}}}{\rho_v h_{lv}^2}T_{sat}} \quad . \tag{4}$$

3.2 Equations

Thanks to the previous hypotheses, one obtains the following system [10] of four differential equations (here nondimensionalized for numerical reasons):

$$\frac{d\hat{\delta}}{d\chi} = \hat{\delta}' \ , \tag{5}$$

$$\frac{d\hat{\delta}'}{d\chi} = \frac{\delta_0 \Delta P_{c,0}}{\sigma}\left(1 + \hat{\delta}'^2\right)^{3/2}\left(\Delta\hat{P}_c - \frac{1}{\hat{\delta}^3}\right) \ , \tag{6}$$

$$\frac{d(\Delta\hat{P}_c)}{d\chi} = \left(-\frac{3\mu_l}{\rho_l h_{lv}} \frac{\lambda_l (T_w - T_{sat})}{\delta_0^2 \Delta P_{c,0}} \right) \frac{\hat{Q}_{mic}}{\hat{\delta}^3} \quad , \tag{7}$$

$$\frac{d\hat{Q}_{mic}}{d\chi} = \frac{1 - \Delta\hat{P}_c}{\hat{\delta} + \dfrac{\lambda_l}{\delta_0} \left(\dfrac{2 - \hat{\sigma}}{2\hat{\sigma}} \right) \dfrac{\sqrt{2\pi r_g T_{sat}}}{\rho_v h_{lv}^2} T_{sat}} \quad , \tag{8}$$

with $\chi = x/\delta_0$; $\hat{\delta} = \delta/\delta_0$; $\Delta\hat{P}_c = \Delta P_c/\Delta P_{c,0}$ and $\hat{Q}_{\text{mic}} = Q_{\text{mic}}/\lambda_1(T_w - T_{sat})$, where δ_0 and $\Delta P_{c,0}$ are respectively the values of the capillary pressure and of the film thickness for $x = 0$ (i.e., at the end of the adsorbed film, Fig. 2b).

3.3 Boundary Conditions

It is assumed that there is no heat transfer in the adsorbed film. In this case, Eq. (4) yields that $T_{lv} = T_w$. Further, the initial value of the capillary pressure is equal to the constant capillary pressure of the adsorbed film $\Delta P_{c,0}$. With the aid of Eq. (3), one finds

$$\Delta P_{c,0} = \rho_l h_{lv} \left(\frac{T_w}{T_{sat}} - 1 \right) , \tag{9}$$

Due to the continuity of the liquid film, the initial thickness δ_0 corresponds to that of the adsorbed film. Thus, Eqs. (2) and (9) give

$$\delta_0 = \left(\frac{T_{sat}}{T_w - T_{sat}} \frac{A}{\rho_l h_{lv}} \right)^{1/3} , \tag{10}$$

In other words, the above equations (9) and (10) yield the values of nondimensionalized boundary conditions $\hat{\delta}_0$ and $\hat{P}_{c,0}$ equal to 1.

Concerning $\hat{\delta}'$ and $\hat{Q}_{\text{mic}}$, the boundary conditions are less obvious. Indeed, these values should be equal to 0 at $x = 0$; but, if it was the case, one would always obtain a trivial solution of the numerical problem: a liquid film thickness that stays constant for every abscissa, not allowing any heat transfer between the wall and the interface. As one wants a solution physically acceptable ($R_c \neq \infty$), very little perturba-

tions ε_1 and ε_2 have been chosen for the initial values of $\hat{\delta}$ and $\hat{Q}_{\text{mic}}$, respectively: $\hat{\delta}_0 = \varepsilon_1$, $\hat{Q}_{\text{mic},0} = \varepsilon_2$. The values of these little perturbations do not have a notable influence on the results. The system of equations (5)–(8), associated with the above boundary conditions (9)–(10), is solved using the fourth-order Runge–Kutta method, as was already done by Romestant et al. [4] in 2006. Additionally, in the algorithm, one imposes an interval of values for R_c, this latter being a result of the differential equations (5)–(8). The algorithm loop continues to solve the problem, changing partially, until the calculated value of the radius R_c of the intrinsic meniscus is included inside the previously fixed interval.

4. RESULTS AND DISCUSSION

4.1 Results for Aluminum/Ammonia Couple

The results presented in this part have been obtained for a typical aluminum/ammonia heat pipe used for spatial applications. Numerous calculations have already shown the influence of various parameters on the calculated quantities (Q_{mic}, θ, ...) [10]. Here, an important result is particularly recalled concerning the behavior of the macroscopic meniscus relative the transfer occurring in the microregion. However, before performing any analysis, a direct comparison between the results obtained with the aid of the present model and those obtained by Stephan and Busse [2] has been made using the same thermophysical properties. The curves given in Fig. 3 show very similar results concerning the evolutions of the calculated quantities: δ, T_{lv}, $\dot{q}_e$, and Q_{mic}.

Let us recall that in our study the abscissa $x = 0$ m refers to the end of the adsorbed film. As already explained in [2], one can notice that the liquid thickness remains very low (less than 1×10^{-9} m) for very little abscissas and begins to increase regularly starting from $x = 2 \times 10^{8}$ m. In the same way, $\dot{q}_e$ increases sharply and attains its maximal value (5.27×10^{7} W·m^{-2} for $x = 3.2 \times 10^{-8}$ m) before decreasing in correspondence with the increasing thickness of the liquid layer. Similarly, T_{lv}, set equal to T_w just after the end of the adsorbed film, decreases rapidly to become very close to T_{sat}, corresponding to the quick increase of $\dot{q}_e$ as δ remains nearly constant in the same abscissa interval ($x < 2 \times 10^{-8}$ m). Stephan and Busse also added that according to Eq. (3) the quick decrease in T_{lv} is due to the strong decrease in ΔP_c, this latter being required to drive the transverse flow of liquid in the microregion. The quantity Q_{mic}, being the integrated value of $\dot{q}_e(x)$ between 0 and x, rises rapidly until $x = 0.1$ μm and then continues to increase regularly. Additionally, considering

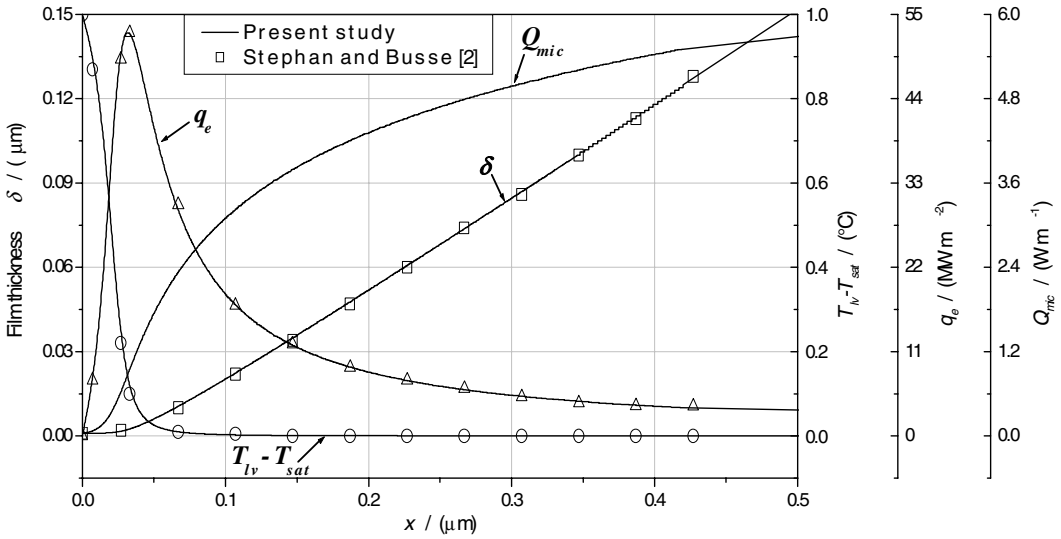

FIG. 3: Evolutions of δ, (T_{lv} – T_v), $\dot{q}_e$, and Q_{mic} in the microregion: comparison between the present study and Stephan and Busse [2]

the quasi-linear evolution of δ after x = 0.2 μm, one can have a precise evaluation of θ, the contact angle of the interface at the connection between the microregion and the intrinsic meniscus zone, calculated thanks to. As Stephan and Busse [2] have done, the microregion length is chosen equal to 1 μm as θ remains quasi-constant at the end of this domain.

Figure 4 shows that still using the data from Stephan and Busse [2], here for T_{sat} = 300 K and x = 1 μm Q_{mic} and θ remain nearly constant whatever the values of R_c (the relative error between the two extreme values of Q_{mic} is of about 0.04% and for θ it does not exceed 0.4%). These results demonstrate that, in such conditions, the transfer occurring in the microregion is completely independent of the intrinsic meniscus zone. Particularly, there is no direct link between the contact angle θ and R_c: the macroscopic radius of the meniscus is not influenced by the hanging phenomena occurring near the contact line. However, θ still permits determining the minimal value of R_c, $R_{c,\text{min}}$, thanks to relation (11), obtained using geometrical considerations:

$$R_{c,\text{min}} = \frac{b/2}{\cos\theta} \tag{11}$$

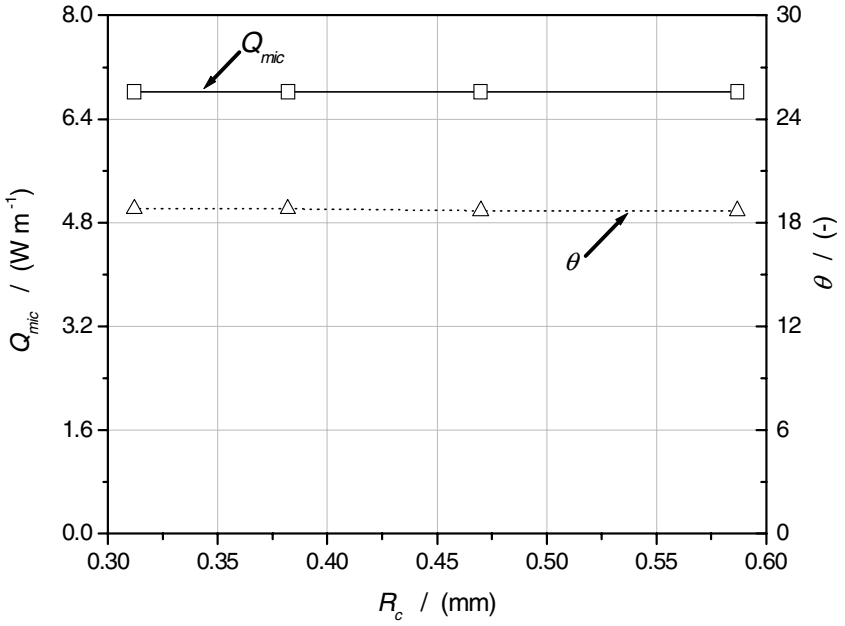

FIG. 4: Q_{mic} and contact angle θ as functions of the meniscus radius (T_{sat} = 300 K, x = 1 μm).

θ can be considered as the minimal macroscopic contact angle under which the meniscus can stay no longer attached to the wall. Besides, particularly for rectangular grooves, the maximal capillary pressure that can be reached in such a heat pipe is given by

$$\Delta P_{c,\max} = \frac{\sigma}{R_{c,\min}} \tag{12}$$

4.2 Comparison of the Performances of Three Metal/Fluid Couples

In this section, performances of aluminum/ammonia, copper/methanol, and silicium/heptane couples are compared, for T_{sat} = 303.15 K, in terms of the heat flux and contact angle. The results are gathered in Fig. 5. The knowledge of the dispersion constant A is not obvious and the literature can supply very different values for a given couple. The values of A used here are given by Ha [11] for copper/methanol and by Dasgupta [12] for silicium/heptane.

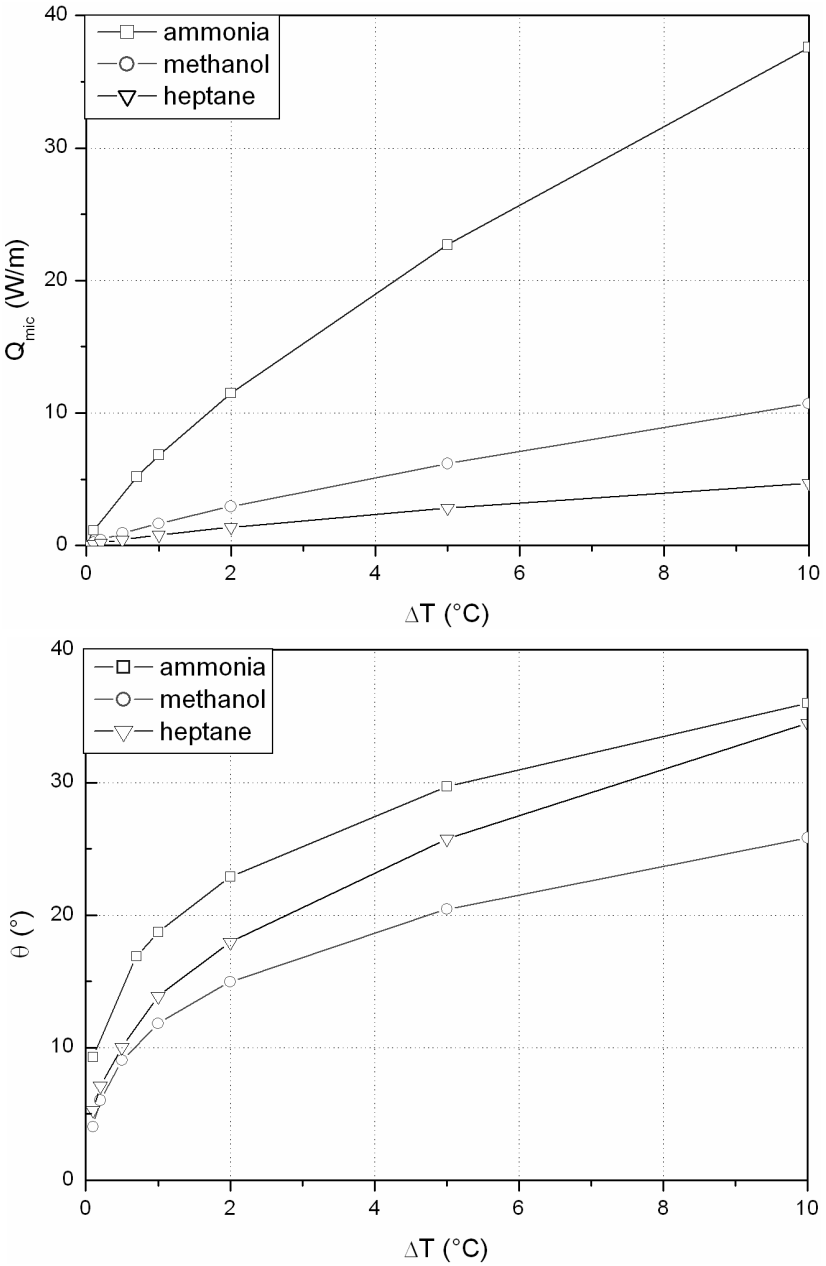

FIG. 5: Comparison of Q_{mic} and θ in the microregion for 3 fluids (T_{sat} = 303.15 K, x = 1 μm)

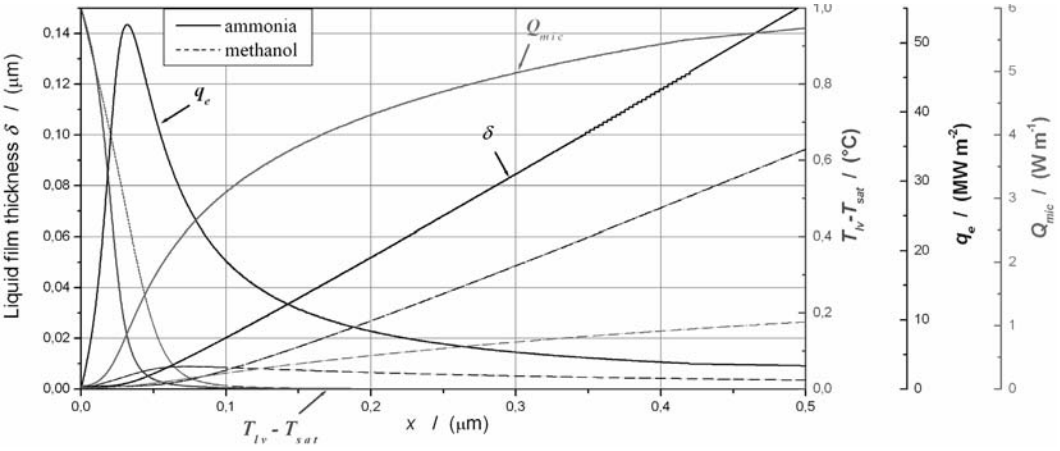

FIG. 6: Evolution of δ, Q_{mic}, $\dot{q}_e$, and $T_{lv} - T_{sat}$ through the microregion for methanol and ammonia

In Fig. 5a, it is shown that Q_{mic} is greater for ammonia than for methanol and heptane, whereas in Fig. 5b, one can see that $\theta_{ammonia} > \theta_{heptane} > \theta_{methanol}$. Consequently, for rectangular grooves, the maximal capillary pressure is more important for methanol than for the two other fluids, while a maximal heat flux is more important for ammonia.

In Fig. 6, the evolutions of $\dot{q}_e$, δ, Q_{mic}, and $(T_{lv} - T_{sat})$ are compared for ammonia and methanol, using the same conditions as in Fig. 3, trying to explain the differences between the values of Q_{mic} bserved in Fig. 5a. Particularly, the heat flux density $\dot{q}_e$ is one order of magnitude greater for ammonia than for methanol (quite 20 times) for the same conditions. At the very beginning of the microregions, the liquid film thicknesses are so small that the only thermal resistances that have to be taken into account are the evaporative ones. One has: $R_{evap,methanol}/R_{evap,ammonia} \approx 20$. This ratio directly explains the values of observed in Fig. 6. Identically, $R_{evap,heptane}/R_{evap,ammonia} \approx 25$, which explains the same tendency observed in Fig. 5a.

However, the resistances of evaporation are very close for methanol and heptane: the differences between the values of Q_{mic} can be explained by the values of the conductive resistances. Indeed, for T_{sat} = 303.15 K, $\lambda_{l,methanol} = 0.203$ W·m^{-1}·K^{-1} and $\lambda_{l,heptane} = 0.11$ W·m^{-1}·K^{-1}. Besides, given the results gathered in Fig. 5b,

$\theta_{heptane} > \theta_{methanol}$, so one can consider that $\tilde{\delta}_{heptane} > \tilde{\delta}_{methanol}$ and, consequently, $R_{cond,heptane} > R_{cond,methanol}$, which explains that for methanol the flux in the microregion is almost two times greater than for heptane.

5. CONCLUSIONS

The phenomena occurring during heat transfer by evaporation in a grooved heat pipe are to be compared to the description of the transfer near the contact line. A model has been constructed to make an exhaustive study of the heat and mass transfers in the microregion. First, an original and important result has been obtained: the contact angle and the radius of the intrinsic meniscus are totally independent of one to another. However, the contact angle permits one to determine the minimal value of the intrinsic meniscus radius physically hung at the top of the groove. Then, performances of three metal/fluid couples have been compared and it appears that a compromise has to be found, in terms of the heat flux exchanged and maximal heat transport capacity of the heat pipe. The latter study makes it possible to complete the characterization of the microregion and should directly participate in the heat pipe design improvement.

REFERENCES

1. Stephan, P. C. and Busse, C. A., Assessment of an improved model for the heat transfer coefficient of grooved heat pipes evaporators, in: *Proc. 4th European Symp. on Space Environmental and Control Systems, Florence*, 1991, pp. 587–592.
2. Stephan, P. C. and Busse, C. A., Analysis of the heat transfer coefficient of grooved heat pipes evaporators wall, *Int. J. Heat Mass Transfer*, 35(2):383–391, 1992.
3. Sartre, V., Chaker Zaghdoudi, M., and Lallemand, M., Effect of interfacial phenomena on evaporative heat transfer in micro heat-pipes, *Int. J. Thermal Sci.*, 39:498–504, 2000.
4. Romestant, C., Alexandre, A., and Lataoui, Z., Evaporation en film mince dans un caloduc rainuré, *La Houille Blanche*, 5:21–27, 2006.
5. Faghri, A., *Heat Pipe Science and Technology*, New York: Taylor and Francis, 1995, pp. 61–111.
6. Wayner, Jr., P. C., Adsorption and capillary condensation at the contact line in change of phase heat transfer, *Int. J. Heat Mass Transfer*, 25(5):707–713, 1982.
7. Wayner, Jr., P. C., Kao, Y. K., and Lacroix, L. V., The interline heat transfer coefficient of an evaporating wetting film, *Int. J. Heat Mass Transfer*, 19:487–492, 1976.
8. Mathieu, B., Lebaigue, O., and Tadrist, L., Modélisation physique et numérique déune ligne de contact dynamique avec changement de phase, *La Houille Blanche*, 5:1–8, 2003.
9. Carey Van, P., *Liquid–Vapor Phase-Change Phenomena, An Introduction of the Thermophysics of Vaporization and Condensation Processes in Heat Transfer Equipement*, Herbon, Ky, USA: Taylor and Francis, Ch. 4–8, 1992.

10. Bertossi, R., Lataoui, Z., Ayel, V., Romestant, C., and Bertin, Y., Modeling of thin liquid film in grooved heat pipes, *Numer. Heat Transfer, Part A*, 55:1075–1095, 2009.
11. Ha, J. M. and Peterson, G. P., The interline heat transfer of evaporating thin films along a micro grooved surface, *J. Heat Transfer*, 118:747–754, 1996.
12. Dasgupta, S., Schonberg, J. A., and Wayner, P. C., Investigation of an evaporating extended meniscus based on the augmented Young–Laplace equation, *J. Heat Transfer*, 73:212–223, 1980.